

Response: We thank the reviewers for thoughtful suggestions and constructive criticism that have helped us improve our manuscript. Below we provide responses to reviewer concerns and suggestions in blue font. All changes to the manuscript can be identified in the version submitted using Track Changes.

Anonymous Referee #1:

General Comments: The paper presents aerosol composition data results in Manila during an 18-month sampling period including 2 monsoon seasons. Overall, the results provide a detailed connection between aerosol composition, pollution source and source region. Many related analyses are performed and provide for a complete picture of the measured organic acids and MSA. The authors did a very good job of weaving together such detailed analysis into one manuscript. However, minor revisions are needed to help with the readability of the paper.

Specific Comments:

1) The fact that the PMF did not include sea salt as a contributor for MSA is alarming and needs to be addressed more (first described in lines 401-405). While it is possible that there are other sources as seen in the Beijing and California studies, the fact that there is absolutely no link between sea salt and MSA needs further analysis. Could it be that local sources of sea salt were not aged enough to allow for MSA formation (the sea salt air masses were too fresh)? What was the height of the roof where the sampler was placed? Does this possibly suggest an error in the PMF?

Response: The fact that MSA is not a contributor to sea salt can be initially alarming, however, there are at least two possible explanations for this. First of all, as you pointed to the sea salt in the region is relatively fresh and likely not very aged, thus yielding low MSA concentrations. The second explanation is that Manila is not like any other coastal site because it is a mega-center for urban and burning emissions and is also a receptor for transported plumes of aerosol types such as smoke. Consequently, concentrations of MSA from these other non-marine sources could be much higher. Because of these reasons it is understandable how the model does not assign MSA concentrations to sea salt, but to other sources. We believe our text in Section 5.6 about MSA is sufficient and requires no revision.

2) In the paper, the individual sources are linked to a source and to a season but I don't think there is a clear link between which sources dominate on whole for each season. ie: during the monsoon, biomass is strongest with a source region from the southwest. . . (made up results)

Response: Our goal was to show what organic acids are associated with what sources, not what sources dominate each season. Our current analyses does not determine what sources dominate each season. We don't believe this comment requires any revision.

3) Section 2.2: include information on filter extraction

Response: A detailed version of the extraction method can be seen in Stahl et al. (2020), however, we added a brief summary of the extraction for convenience, which reads:

Lines 166-172: “Substrates were stored in a freezer at -20 °C after samples were collected from the MOUDI until extractions could be carried out. The stored substrates were then extracted by sonication in Milli-Q water (18.2 MΩ-cm) for 30 minutes. After sonication, solutions were immediately analyzed to prevent degradation while the remaining extracts were stored in a refrigerator for additional analyses.”

4) Line 230-231: include a reference for PMF

Response: Done.

Line 237: “... concentration budgets of the species discussed in this work (Paatero and Tapper, 1994).”

5) Line 253-283: this should not be shown in results. Move to new section in methods section – such as new section 2.3

Response: We created a new Section 3 between Methods and Results called “3. Background on Measured Acids”.

6) Line 291-293: are these accumulated rain over the entire period or rain per day. If per day this should be noted. If accumulated rain, how is there variability?

Response: We are referring to accumulated rain over the sampling period for any given set and then averaged per season. There is variability between sets where some sets might not have any rain, while others can have substantial amounts. We don’t believe this comment requires any revision.

7) Discussion: Many related analyses are performed and are summarized in the first paragraph of each subsection. This should be a numbered, indented list so they stand out more allowing for comparison between the different species. Currently this good discussion is presented as a long run-on sentence at the beginning of each subsection.

Response: Done.

72

73 8) Discussion: a long list of measurements in other locations are included for each compound (ie:
74 Line 4750-479; 519-524; 556-561. . .). This is not needed as this is not a review. I would suggest
75 including 1 or 2 relevant measurements for comparison and including the rest in the
76 supplemental information if needed.

77 Response: The reason for a large list of measurements is to show how our measurements
78 compare to other regions around the world as there is variability for different species. We feel
79 this helps readers gain an appreciation for how Manila compares to other sites.

80

81 9) Line 630 and following: this is not a clear bi-modal distribution. Rather 2-3 modes that run
82 together possibly showing a similar secondary source for all sizes

83 Response: It is hard to determine for sure whether or not there are 3 modes where 2 modes are
84 overlapping. We can tell for sure there are at least 2 notable modes, which is why we say
85 “appeared”. But we still added this line to address this concern:

86

87 Lines 656-657: “Note that the modes discussed here represent the most pronounced ones but
88 others could have been present too reflecting other sources.”

89

90 10) Throughout: the use of “Trans” as an abbreviation is unneeded and a little distracting.
91 Replace with “Transition”

92 Response: Done.

93

94 11) Table 3: I think switch Table 3 and Table S6 so only the correlation for all size distributions
95 is in the main text.

96 Response: We thought that it would be more impactful to show correlations of both sub- and
97 super-micrometer ranges. Additionally, since there is a lot of mass in the submicrometer range
98 the correlations for the entire size range and submicrometer size range are near identical. As a
99 result we would like to push for keeping it the way it was.

100

101 12) Figure 1: include clearer labels for each season above each panel

102 Response: Done.

103

104 Technical Corrections:

105 1) Line 32 and throughout: 148.59 +/- 94.26 has too many significant figures. Your variability
106 should be trimmed to 1 or 2 significant figures and then your average adjusted to match the
107 decimal place. That is it should be 149 +/- 94. Other places noted (not a complete list): lines 289-
108 290; line 337-338

109 Response: Done.

110

111 2) Line 33: define PMF

112 Response: Done. The line now reads:

113 Lines 33-35: "Both positive matrix factorization (PMF) and correlation analysis is conducted
114 with tracer species to investigate the possible sources for organic acids and MSA."

115

116 3) Line 35 & 38: line 35 remove "(SWM18)" and line 38 replace "SWM" with "monsoon"

117 Response: Done.

118

119 4) Line 37: "linked to burning" should be "linked to biomass burning"

120 Response: Done, the line now reads:

121 Lines 37-38: "Peculiarly, MSA had negligible contributions from marine sources but instead was
122 linked to biomass burning and combustion."

123

124 5) Line 44-48: run-on sentence. Split into two easier to understand sentences

125 Response: Done and now reads:

126 Lines 45-48: "Oxalate's strong association with sulfate in the submicrometer mode supports an
127 aqueous-phase formation pathway for the study region. However, high concentration during
128 periods of low rain and high solar radiation indicates photo-oxidation is an important formation
129 pathway."

130

131 6) Line 67: new paragraph

132 Response: Done.

133

134

135 7) Line 132: 12.9 million

136 Response: Done.

137

138 8) Line 136: word choice for quintessential – maybe use “fitting”

139 Response: Done, the line now reads:

140 Lines 137: “Because of these reasons, Metro Manila is a fitting location for examining
141 locally...”

142

143 9) Line 181: “a subset of species were listed here, which were used for analyses.” should be
144 replaced with “a subset of species used for analyses are listed here.”

145 Response: Done, the line now reads:

146 Lines 188-189: “It should also be noted that only a subset of species used for analyses were
147 listed here.”

148

149 10) Line 199: Replace “the roof of MO. Measured” with “the roof. Measured”

150 Response: Done, the line now reads:

151 Lines 205-206: “...Davis Vantage Pro2™ Plus automatic weather station, which was located on
152 the roof.”

153

154 11) Line 227: should use CWT and not WCWT

155 Response: Done.

156

157 12) Line 320: replace “(0.80 ± 0.66 %), ranging from 0.23 – 1.49 % across” with “(0.80 ± 0.66
158 %) across” – this was redundant with later in the paragraph

159 Response: Done, the line now reads:

160 Lines 329-330: “Combined, the measured organic acids and MSA accounted for only a small
161 part of the total cumulative mass (0.80 ± 0.66 %) across the 11 individual gravimetric sets.”

162

163 13) Line 364-380: suggest making these a numbered list so they stand out more

164 Response: Done, the sources are now numerically listed.

165

166

167

Anonymous Referee #2

168 This manuscript reports the analytical results of five organic acids and MSA in the size-resolved
169 aerosols from Manila and discusses their sources and characteristics based on the correlation
170 analyses with a 16-month dataset of inorganic ions and trace metals. Because of no studies on
171 organic acids in the aerosols from Manila areas, authors' dataset may be of interest for the
172 community of atmospheric chemistry. However, this manuscript is very descriptive and
173 sometimes redundant. As authors pointed, the concentration levels of organic acids are
174 surprisingly low compared with other polluted areas (lines 22-23, 704-706) although authors did
175 not provide a reasonable explanation. My major concern is that the concentrations of organic
176 acids and MSA could be seriously underestimated due to biodegradation because there is no
177 description in the text to avoid possible decomposition of organic acids and other chemical
178 species during sample storage and analytical procedure. Another concern is that, although
179 authors mentioned "Little is reported in terms of the size-resolved nature of organic acids and
180 MSA .." (line 92-93), there are several studies that reported size distributions of organic acids
181 (see below for details). The above points should be clarified in the revision before the
182 consideration for the decision on a possible acceptance to ACP. More specific comments are
183 followed:

184 1. Lines 31-33. Oxalate was approximately an order of magnitude more abundant...

185 Which size fraction are you talking about? Total (<0.056 to $>18\ \mu\text{m}$)?

186 **Response:** This refers to the total size range (0.056 - $18\ \mu\text{m}$). Additional information was added to
187 clarify the size range. It now reads:

188 **Lines 31-33:** "Oxalate was approximately an order of magnitude more abundant than the other
189 five species ($149 \pm 94\ \text{ng m}^{-3}$ versus others being $< 10\ \text{ng m}^{-3}$) across the $0.056 - 18\ \mu\text{m}$ size
190 range."

191

192 2. Line 51 and others. Some of the references are not properly cited. For example, in line 51,
193 authors cited Kondo et al. (2011) in the discussion of organic acids. However, Kondo et al.
194 (2011) focused on black carbon but not for organic acids. Please check the possible mistakes in
195 referring previous citations.

196 **Response:** The Kondo et al. (2011) reference discusses black carbon as well as organic aerosols,
197 which was determined to be relevant to our narrative. We confirm this was not a mistake.

198

199 3. Lines 92-93. There are several studies on the size-segregated dicarboxylic acids from different
200 regions in the world. For example:

201 Mochida, M., N. Umemoto, K. Kawamura, H. Lim, and B. J. Turpin (2007), Bimodal size
202 distributions of various organic acids and fatty acids in the marine atmosphere: Influence of

anthropogenic aerosols, Asian dusts, and sea spray off the coast of East Asia, *J. Geophys. Res.*, 112, D15209, doi:10.1029/2006JD007773.

Kawamura K., M. Narukawa, S.-M. Li and L. A. Barrie, Size distributions of dicarboxylic acids and inorganic ions in atmospheric aerosols collected during polar sunrise in the Canadian High Arctic. *J. Geophys. Res.*, 112, D10307, doi:10.1029/2006JD008244, 2007.

Gehui Wang, Kimitaka Kawamura, Mingjie Xie, Shuyuan Hu, Junji Cao, Zhisheng An, John G. Waston and Judith C. Chow, Organic Molecular Compositions and Size Distributions of Chinese Summer and Autumn Aerosols from Nanjing: Characteristic Haze Event Caused by Wheat Straw Burning, *Environ. Sci. Technol.*, 43 (17), 6493–6499, 2009.

Gehui Wang, Kimitaka Kawamura, Mingjie Xie, Shuyuan Hu, and Zifa Wang, Water-soluble organic compounds in PM_{2.5} and size-segregated aerosols over Mt. Tai in North China Plain, *J. Geophys. Res.*, 114, D19208, doi:10.1029/2008JD011390, 2009.

Smita Agarwal, Shankar Gopala Aggarwal, Kazuhiro Okuzawa, and Kimitaka Kawamura, Size Distributions of Dicarboxylic Acids, Ketoacids, α -Dicarbonyls, Sugars, WSOC, OC, EC and Inorganic Ions in Atmospheric Particles Over Northern Japan: Implication for Long-Range Transport of Siberian Biomass Burning and East Asian Polluted Aerosols, *Atmos. Chem. Phys.*, 10, 5839-5858, 2010.

Gehui Wang, Kimitaka Kawamura, Mingjie Xie, Shuyuan Hu, Jianjun Li, Bianhong Zhou, Junji Cao, Zhisheng An, Selected water-soluble organic compounds found in sized-resolved aerosols collected from urban, mountain, and marine atmospheres over East Asia, *Tellus*, 63B, 371-381, 2011.

Miyazaki, Y., K. Kawamura, and M. Sawano (2010), Size distributions and chemical characterization of water-soluble organic aerosols over the western North Pacific in summer, *J. Geophys. Res.*, 115, D23210, doi:10.1029/2010JD014439.

Dhananjay Kumar Deshmukh, Kimitaka Kawamura and Manas Kanti Deb, Dicarboxylic acids, ω -oxocarboxylic acids, α -dicarbonyls, WSOC, OC, EC, and inorganic ions in wintertime size-segregated aerosols from central India: Sources and formation processes, *Chemosphere*, 161, 27-42, 2016.

Those references should be cited.

Response: We are not stating that there have not been size-segregated studies of dicarboxylic acids, we are saying there are not that many size-segregated studies of dicarboxylic acids that are long term (> 6 months) with high sampling frequency (at least weekly), and with temporal resolution around \leq 48-hours. The references that were shared here do not meet most if not all of those criteria, therefore, we do not think it is necessary to add in those references. The manuscript already has 215 references.

4. Method section. There is no description on the sample storage from sampling to chemical analysis. Did you store the samples at room temperature or at -20°C in a freezer? After the water extraction of the sample, how long did you store the water extracts at room temperature? Storage of filter samples and water extracts at room temperature may be subject to biodegradation of organic acids. In Manila, high humidity conditions may provide more moistures to the aerosols. Please provide the information of storage of samples and extracts.

Response: Once samples were collected they were sealed in a Petrislide and wrapped with Parafilm before being stored in a freezer at – 20 °C. After water extractions the samples were immediately analyzed using ion chromatography, limiting the amount of biodegradation. Storage and extraction methods have been described in great detail for these samples in Stahl et al. (2020), however, a brief description of these methods was added for clarification:

Lines 166-172: “Details of the sample sets are shown in Table S2 can be found in more detail in Stahl et al. (2020), but a brief summary of the storage and extraction methods will be described here. Substrates were stored in a freezer at -20 °C after samples were collected from the MOUDI until extractions could be carried out. The stored substrates were then extracted by sonication in Milli-Q water (18.2 MΩ-cm) for 30 minutes. After sonication, solutions were immediately analyzed to prevent degradation while the remaining extracts were stored in a refrigerator for additional analyses.”

5. Results section. Some paragraphs are too long and redundant (e.g., 31 lines in the paragraph starting at line 253). By reorganizing the paragraphs and rephrasing the sentences, authors could improve them to become more readable.

Response: The paragraph was broken into 3 separate paragraphs (MSA, saturated organic acids, and unsaturated organic acids).

6. Lines 340-344. Authors mentioned lower concentrations of oxalate and MSA than expected for a megacity Manila. This point should be critically verified including the discussion of methods used; potential biodegradation of organic acids and MSA during sample storage and analytical protocol.

Response: As stated previously a section has been added to address the methods used. Biodegradation of the organic acids and MSA is very possible in the environment, however, measures were taken to ensure samples were properly stored to minimize the potential of biodegradation of the samples. Sample filters were stored in a freezer after they were collected and were extracted once they were going to be analyzed. Therefore, we do not believe this comments warrants additional revision.

276 7. Discussion. What is the reason to start the discussion with phthalate that is not the major
277 organic acid? Why do you discuss oxalate at the end that is the most abundant organic acid? I
278 wondered if you could improve the discussion section by reorganizing the order of the
279 compounds.

280 Response: The reasoning was to start with the largest chain organic (phthalate) and end with the
281 smallest (oxalate), followed by MSA. This is because the large chain organics will decompose to
282 the smaller chain organics and we thought it was necessary to discuss the larger species first to
283 properly relay the narrative of where the smaller chain organic acids come from. For example, it
284 helps in the discussion of oxalate to have first covered the larger acids that can break down to
285 form oxalate. We revised this line:

286

287 Lines 475-477: “Subsequent sections discuss each organic acid and MSA in more detail,
288 beginning with larger acids since knowledge of their behavior is important to better understand
289 the smaller acids.”

290

291 8. Lines 514-515. How do you explain the crustal sources (35.9%) for adipate? In other places in
292 the text, authors discuss the combustion sources of adipic acid (lines 261-262).

293 Response: The crustal sources for adipate are likely due to adsorption onto larger dust particles.
294 We are not saying that adipate comes from crustal sources, rather we are saying it is added on
295 through aging. There are no plausible explanations of direct emissions for supermicrometer
296 adipate to our knowledge, so the only explanation is that adipate (and other organic acids for that
297 matter) adsorbs onto larger particles. Work by Sullivian and Prather (2007) further implies that
298 dicarboxylic acids have an affinity towards adsorption onto dust particles over sea salt. This
299 reinforces our stance that adipate is adsorbing onto these larger dust particles, which is why
300 adipate is associated strongly with crustal sources.

301

302 9. Lines 621-622 and 704-706. Again how do you explain the “surprisingly low concentrations
303 of oxalate” ? This reviewer is skeptical about data quality; i.e., a potential loss of organic acids
304 and MSA due to biodegradation during the sample storage and analytical procedure used in this
305 study.

306 Response: As stated multiple time above, once the samples were removed from the MOUDI they
307 were sealed and stored in a freezer until they were ready to be analyzed. Then they were
308 extracted and immediately analyzed with little to no storage time.

309

310 10. Lines 695-698. Is it possible to discuss the fraction of organic acids and MSA on a carbon
311 basis? Did you measure TOC or WSOC?

Response: Unfortunately, TOC and WSOC were not measured so we are not able to discuss the fraction of organic acids and MSA on a carbon basis.

References

Stahl, C., Cruz, M. T., Banaga, P. A., Betito, G., Braun, R. A., Aghdam, M. A., Cambaliza, M. O., Lorenzo, G. R., MacDonald, A. B., Pabroa, P. C., Yee, J. R., Simpas, J. B., and Sorooshian, A.: An annual time series of weekly size-resolved aerosol properties in the megacity of Metro Manila, Philippines, Sci Data, 7, 128, 10.1038/s41597-020-0466-y, 2020.

Sources and characteristics of size-resolved particulate organic acids and methanesulfonate in a coastal megacity: Manila, Philippines

Connor Stahl¹, Melliza Templonuevo Cruz^{2,3}, Paola Angela Bañaga^{2,4}, Grace Betito^{2,4}, Rachel A. Braun¹, Mojtaba Azadi Aghdam¹, Maria Obiminda Cambaliza^{2,4}, Genevieve Rose Lorenzo^{2,5}, Alexander B. MacDonald¹, Miguel Ricardo A. Hilario², Preciosa Corazon Pabroa⁶, John Robin Yee⁶, James Bernard Simpas^{2,4}, Armin Sorooshian^{1,5}

¹Department of Chemical and Environmental Engineering, University of Arizona, Tucson, Arizona, 85721, USA

²Manila Observatory, Quezon City, 1108, Philippines

³Institute of Environmental Science and Meteorology, University of the Philippines, Diliman, Quezon City, 1101, Philippines

⁴Department of Physics, School of Science and Engineering, Ateneo de Manila University, Quezon City, 1108, Philippines

⁵Department of Hydrology and Atmospheric Sciences, University of Arizona, Tucson, Arizona, 85721, USA

⁶Philippine Nuclear Research Institute - Department of Science and Technology, Commonwealth Avenue, Diliman, Quezon City, 1101, Philippines

Correspondence to: armin@email.arizona.edu

Abstract

A 16-month (July 2018 – October 2019) dataset of size-resolved aerosol composition is used to examine the sources and characteristics of five organic acids (oxalate, succinate, adipate, maleate, phthalate) and methanesulfonate (MSA) in Metro Manila, Philippines. As one of the most polluted megacities globally, Metro Manila offers a view of how diverse sources and meteorology impact the relative amounts and size distributions of these species. A total of 66 sample sets were collected with a Micro-Orifice Uniform Deposit Impactor (MOUDI), of which 54 sets were analyzed for composition. Organic acids and MSA surprisingly were less abundant than in other global regions that are also densely populated. The combined species accounted for an average of 0.80 ± 0.66 % of total gravimetric mass between 0.056 and 18 μm , leaving still 33.74 % of mass unaccounted for after considering black carbon and water-soluble ions and elements. The unresolved mass is suggested to consist of non-water-soluble metals as well as both water-soluble and non-water-soluble organics. Oxalate was approximately an order of magnitude more abundant than the other five species (1498.59 ± 94.26 ng m^{-3} versus others being < 10 ng m^{-3}) across the 0.056 – 18 μm size range. Both positive matrix factorization (PMF) and correlation analysis is conducted with tracer species to investigate the possible sources for organic acids and MSA. Enhanced biomass burning influence in the 2018 southwest monsoon (SWM18) resulted in especially high levels of submicrometer succinate, MSA, oxalate, and phthalate. Peculiarly, MSA had negligible contributions from marine sources but instead was linked to biomass burning and combustion. Enhanced precipitation during the two monsoonSWM seasons (8 June – 4 October 2018 and 14 June – 7 October 2019) coincided with stronger influence from local emissions rather than long-range transport, leading to notable concentration enhancements in both the sub- and supermicrometer ranges for some species (e.g., maleate and phthalate). While secondary formation via gas-to-particle conversion largely explained submicrometer peaks for all species, several species (i.e., phthalate, adipate, succinate, oxalate) exhibited a prominent peak in the coarse mode, largely owing to their association with crustal emissions (i.e., more alkaline aerosol type) rather than sea salt. Oxalate's strong association with sulfate in the submicrometer mode supports an aqueous-phase formation pathway for the study region, but also However, high concentration during periods of low rain and high solar radiation indicates photo-oxidation is an important formation pathway.

1. Introduction

Organic acids are ubiquitous components of ambient particulate matter and can contribute appreciably to total mass concentrations in diverse regions ranging from the Arctic to deserts (e.g. Barbaro et al., 2017; Ding et al., 2013; Duarte et al., 2017; Gao et al., 2003; Kondo et al., 2011; Skyllakou et al., 2017; Sun et al., 2012; Youn et al., 2013). Furthermore, another class of species contributing to ambient aerosol mass is organosulfur compounds, with methanesulfonate (MSA) being an example species (Bardouki et al., 2003b; Ding et al., 2017; Falkovich et al., 2005; Kerminen et al., 1999; Maudlin et al., 2015; Ziemba et al., 2011). The spatiotemporal and size-resolved mass concentration profiles of organic and sulfonic acids are difficult to characterize and can significantly vary depending on the time of day, season, region, and meteorological profile (Adam et al., 2020; Bagtasa et al., 2019; Kobayashi et al., 2004; Maudlin et al., 2015; Mochida et al., 2003; Reid et al., 2013). It is necessary to quantify their relative abundances, and to understand factors affecting their production and eventual removal to be able to quantify their influence on aerosol hygroscopic and optical properties (Beaver et al., 2008; Cai et al., 2017; Freedman et al., 2009; Marsh et al., 2017; Marsh et al., 2019; Myhre and Nielsen, 2004; Peng et al., 2016; Xue et al., 2009). Low molecular weight organic acids are water-soluble and can range widely in hygroscopicity when in their pure salt form depending on factors such as carbon number (Prenni et al., 2001; Saxena and Hildemann, 1996; Sorooshian et al., 2008) and interactions with other components in multi-component aerosol particles (Drozd et al., 2014).

Organic acids are generally believed to effectively scatter light and have a cooling effect on climate (McGinty et al., 2009; Myhre and Nielsen, 2004), although their overall impact on properties such as refractive index in multicomponent aerosols is poorly characterized. Refractive indices for species investigated in this work range widely from 1.43 (MSA) to 1.62 (phthalic acid). MSA is assumed to be purely scattering similar to sulfate (Hodshire et al., 2019) and to have hygroscopic properties close to those of ammonium sulfate (Asmi et al., 2010; Fossum et al., 2018). However, its hygroscopic and optical behavior is not fully understood, and is still an active area of research (Liu et al., 2011; Peng and Chan, 2001; Tang et al., 2019; Tang et al., 2015; Zeng et al., 2014).

Decades of research into atmospheric organic acids and MSA have yielded rich insights into their sources, production mechanisms, and fate in the atmosphere (Baboukas et al., 2000; Bardouki et al., 2003a; Gondwe et al., 2004; Kawamura and Bikkina, 2016; Limbeck et al., 2001; Norton et al., 1983; Ovadnevaite et al., 2014; Sorooshian et al., 2009; van Pinxteren et al., 2015). MSA is produced predominantly from the oxidation of dimethylsulfide (DMS) emitted from oceans (Bates et al., 2004; Davis et al., 1998; Kerminen et al., 2017), but it also can be linked to biomass burning, urban, and agricultural emissions (Sorooshian et al., 2015). Sources of organic acids include primary emissions from biomass burning, biogenic activity, and the combustion of fossil fuels (Kawamura and Kaplan, 1987) and secondary formation via gas-to-particle conversion processes stemming from both biogenic (Carlton et al., 2006) and anthropogenic emissions (Sorooshian et al., 2007b). Secondary processing can include both aqueous phase chemistry in clouds (Blando and Turpin, 2000; Ervens, 2018; Ervens et al., 2014; Hoffmann et al., 2019; Rose et al., 2018; Sareen et al., 2016; Warneck, 2005) and photo-

oxidation of volatile organic compounds (VOCs) in cloud-free air (Andreae and Crutzen, 1997; Gelencsér and Varga, 2005). These various sources and production pathways result in mono- and dicarboxylic acids being prevalent across a range of aerosol sizes (Bardouki et al., 2003b; Kavouras and Stephanou, 2002; Neusüss et al., 2000; Yao et al., 2002). Little is reported in terms of the size-resolved nature of organic acids and MSA over long periods (> 6 months) of time with high sampling frequency (weekly or better). Although insights have already been gathered from size-resolved measurement studies (Table S1), most measurement reports are based on bulk mass concentration measurements (Chebbi and Carlier, 1996; Kawamura and Bikkina, 2016). Studying the seasonal variations of size-resolved organic acid and MSA aerosols could prove vital in improved understanding of their formation and removal mechanisms, and associated sensitivity to seasonally dependent sources and meteorological factors.

The Philippines is an important region to study aerosols due to the wide range in both meteorological conditions and diverse local and regional emissions sources (Alas et al., 2018; Bagtasa and Yuan, 2020; Braun et al., 2020; Hilario et al., 2020a; Kecorius et al., 2017). In addition to aerosol sources from nearby regions (Hilario et al., 2020b), the Philippines also has a significant source of local pollution largely consisting of vehicular emissions due to high population density (Madueño et al., 2019), the use of outdated vehicles (Biona et al., 2017), ship exhaust from high density shipping lanes (Streets et al., 1997; Streets et al., 2000), and more lenient air regulations leading to significant air pollution due to rapid growth and urbanization (Alas et al., 2018; Kecorius et al., 2017). This leads to Metro Manila containing some of the highest black carbon (BC) concentrations in Southeast Asia, and quite possibly the world (Alas et al., 2018; Hopke et al., 2011; Kecorius et al., 2017; Kim Oanh et al., 2006). Past aerosol characterization work for that region has focused mainly on gravimetric analysis for total bulk mass (e.g., PM_{2.5}, PM₁₀) (Bagtasa et al., 2018; Bagtasa et al., 2019; Cohen et al., 2009; Kim Oanh et al., 2006), water-soluble inorganic and organic ion speciation (AzadiAghdam et al., 2019; Braun et al., 2020; Cruz et al., 2019; Kim Oanh et al., 2006; Simpas et al., 2014; Stahl et al., 2020a), and BC analysis (Alas et al., 2018; Bautista et al., 2014; Kecorius et al., 2017; Takahashi et al., 2014). In an analysis of two size-resolved aerosol sets in Manila, a significant portion of the total mass unaccounted for by the water-soluble inorganic, water-soluble organic, and BC components was attributed to (but not limited to) organics and non-water soluble metals (Cruz et al., 2019). However, a concentrated effort to characterize the contributions of the water-soluble organic acids to the total aerosol mass in Manila over the course of a full year has not been undertaken.

The aim of this study is to use a 16 month-long dataset of size-resolved composition in Quezon City in Metro Manila to address the following questions: (i) how much do organic acids and MSA contribute to the region's aerosol mass concentrations?; (ii) what are the seasonal differences in the mass size distribution profile of organic acids and MSA, and what drives the changes?; and (iii) what are the sources and predominant formation mechanisms of these species in the sub- and super-micrometer diameter ranges? The results of this study are put in broad context by comparing findings to those in other regions.

2. Methods

2.1 Study site description

Metro Manila is comprised of 16 cities and a municipality totaling to a population of about 12.889 million people and a collective population density of 20,800 km⁻² (Alas et al., 2018; PSA, 2016). Quezon City is the most populated city in Metro Manila containing 2.94 million people with a population density of 18,000 km⁻² (PSA, 2016), which is amidst the highest in the world. Because of these reasons, Metro Manila is a quintessential fitting location for examining locally produced anthropogenic aerosols superimposed on a variety of other marine and continentally influenced air masses transported from upwind regions (Kim Oanh et al., 2006).

Measurements were conducted over a 16-month period between July 2018 and October 2019 at Manila Observatory (MO; 14.64° N, 121.08° E) on the third floor (~85 m a.s.l.) of an office building, which is on the Ateneo de Manila University campus in Quezon City, Philippines (Fig. 1). Sampling was conducted approximately 100 m away from the nearest road on campus and therefore campus emissions do not impact sampling to a large degree, qualifying the monitoring site as an urban mixed background site (Hilario et al., 2020a) capturing local, regional, and long-range transported emissions. The following four seasons were the focus of the sampling period: the 2018 southwest monsoon (SWM18, 8 June – 4 October 2018) (PAGASA, 2018a, b), a transitional period (Transitional, 5 – 25 October 2018), the northeast monsoon (NEM, 26 October 2018 – 13 June 2019) (PAGASA, 2018c), and the 2019 southwest monsoon (SWM19, 14 June – 7 October 2019) (PAGASA, 2019b, a). These seasons have also been defined in other works (i.e., Akasaka et al., 2007; Cruz et al., 2013; Matsumoto et al., 2020) and can predominately be separated into two general seasons, wet (SWM) and dry (NEM). Generally, there is a second transitional period in May that transitions between the NEM and SWM (Bagtasa and Yuan, 2020), however, recent studies suggest that the transition is abrupt (Matsumoto et al., 2020). Consequently, the second transitional period was combined with the NEM season.

2.2 Instrument description

Ambient aerosol was collected with a Micro-Orifice Uniform Deposit Impactor II (MOUDI II 120R, MSP Corporation, Marple et al. (2014)) using Teflon substrates (PTFE membrane, 2 µm pores, 46.2 mm diameter, Whatman). The MOUDI-II is a 10-stage impactor with aerodynamic cutpoint diameters (D_p) of 10, 5.6, 3.2, 1.8, 1.0, 0.56, 0.32, 0.18, 0.10, and 0.056 µm with a nominal flow rate of ~30 L min⁻¹. A total of 66 MOUDI sets were collected on a weekly basis usually over a 48-hour period; however, only 54 sets were analyzed for ions and 47 of those sets were also analyzed for elements. A 48-hour period was chosen because it offered an optimal compromise between gathering samples with fine temporal resolution and samples with a sufficiently large chemical signal to exceed analytical limits of detection. Details of the sample sets are shown in Table S2 can be found in more detail in Stahl et al. (2020a), but a brief summary of the storage and extraction methods will be described here. Substrates were stored in a freezer at -20 °C after samples were collected from the MOUDI until extractions could be carried out. The stored substrates were then extracted by sonication in Milli-Q water (18.2 MΩ-

cm) for 30 minutes. After sonication, solutions were immediately analyzed to prevent degradation while the remaining extracts were stored in a refrigerator for additional analyses.

Water-soluble organic acids, MSA, and inorganic ions were speciated and quantified using ion chromatography (IC; Thermo Scientific Dionex ICS-2100 system) with a flowrate of 0.4 mL min⁻¹. The anionic species of relevance to this study were MSA, chloride (Cl⁻), nitrate (NO₃⁻), sulfate (SO₄²⁻), adipate, succinate, maleate, oxalate, and phthalate. These anions were resolved using potassium hydroxide (KOH) eluent, an AS11-HC 250 mm column, and an AERS 500e suppressor. The cationic species of relevance to this study was sodium (Na⁺), which was detected using methanesulfonic acid eluent, a CS12A 250 mm column, and a CERS 500e suppressor. The IC instrument methods for anion and cation analysis can be found in Stahl et al. (2020a). Water-soluble elements were measured using a triple quadrupole inductively coupled plasma mass spectrometry (ICP-QQQ; Agilent 8800 Series). The quantified elements of relevance to this study include Al, As, Cd, K, Ni, Pb, Rb, Ti, and V. Limits of detection (LOD) and recoveries were calculated for all ionic and elemental species and provided in Table S3. Aside from the species that are the focus of this study (organic acids and MSA), the other elements and ions were included as they are useful tracers for different aerosol sources to aid in source apportionment. Although pyruvate was speciated with IC, it is not considered with the other organic acids because it was below the LOD for 48 of the 54 sets. It should also be noted that only a subset of species ~~were listed here, which were used for analyses~~ were listed here. The full suite of species can be seen in Stahl et al. (2020a).

Eleven of the 66 MOUDI sets included simultaneously operated MOUDIs next to each other to complement the chemical speciation analysis with gravimetric analysis. A Sartorius ME5-F microbalance (sensitivity of ± 1 µg) was used in an air-buffered room with controlled temperature (20 – 23 °C) and relative humidity (RH: 30 – 40 %). Each substrate was passed near an antistatic tip for approximately 30 seconds to minimize bias due to electrostatic charge. Multiple weight measurements were conducted before and after sampling, with the difference between weighings being less than 10 µg for each condition, respectively. The difference between substrate weights before and after sampling was equated to total gravimetric mass.

Black carbon was measured using a Multi-wavelength Absorption Black Carbon Instrument (MABI; Australian Nuclear Science and Technology Organisation). The MABI optically quantifies black carbon concentrations by detecting the absorption at seven wavelengths (405, 465, 525, 639, 870, 940, and 1050 nm); however, the wavelength at 870 nm is used here as black carbon is the primary absorber at that wavelength (Cruz et al., 2019; Ramachandran and Rajesh, 2007; Ran et al., 2016).

Meteorological parameters were measured at MO during the study period using a Davis Vantage Pro2™ Plus automatic weather station, which was located on the roof of MO. Measured parameters of relevance included temperature, accumulated rain, RH, and solar radiation. Data were collected in five-minute increments and were cleaned based on the method of Bañares et al. (2018) to verify values were in acceptable ranges. The meteorological parameters, except for rain, were averaged over each sampling period while rain was summed over time to obtain the accumulated precipitation for a sampling period. There were two periods where the automatic

weather station located at MO had missing values, 6 November – 27 November 2018 and 7 August – 3 September 2019. In these cases, missing values were substituted with values from a secondary automatic weather station located approximately 2 km away (14.63° N, 121.06° E), and if missing data still persisted, a tertiary station located 5 km away (14.67° N, 121.11° E) was used. Identical data cleaning procedures were implemented for the secondary and tertiary sites.

2.3 Concentration weighted trajectories (CWT)

A CWT analysis was conducted to identify sources of detected species. The method assigns a weighted concentration to a grid that is calculated by finding the mean of sample concentrations that have trajectories crossing a particular cell in the grid (e.g., Dimitriou, 2015; Dimitriou et al., 2015; Hilario et al., 2020a; Hsu et al., 2003). The software TrajStat (Wang et al., 2009) determines CWT profiles by using back-trajectories from the NOAA Hybrid Single-Particle Lagrangian Integrated Trajectory (HYSPLIT) model (Rolph et al., 2017; Stein et al., 2015). Three-day back-trajectories were obtained with an ending altitude of 500 m above ground level using the Global Data Assimilation System (GDAS) and the “Model vertical velocity” method. The choice of 500 m is based on representativeness of the mixed layer and having been widely used in other studies (e.g., Crosbie et al., 2014; Mora et al., 2017; Sorooshian et al., 2011). Trajectories were obtained every 6 hours after MOUDI sampling began for each sample set, yielding approximately nine trajectories per set. A grid domain of 95° to 150° E longitude and -5° to 45° N latitude was used with a grid cell resolution of 0.5° × 0.5°. The analysis was performed for each measured organic acid and MSA for the full diameter range of MOUDI sets (0.056 – 18 µm). A weighting function was applied to the CWT plots to minimize uncertainty; hereafter CWT plots will be referred as WCWT plots.

2.4 Positive matrix factorization (PMF)

PMF analysis was applied to identify sources and their relative importance for the mass concentration budgets of the species discussed in this work (Paatero and Tapper, 1994). Model simulations were conducted based on MOUDI data for the diameter range of 0.056 – 18 µm. Nineteen species (Al, Ti, K, Rb, V, Ni, As, Cd, Pb, Na⁺, Cl⁻, NO₃⁻, SO₄²⁻, MSA, adipate, succinate, maleate, oxalate, and phthalate) were included in the analysis and categorized as “strong”. Each individual stage of MOUDI sets was considered an independent variable for the analysis. Missing values or values below detection limit were replaced with zeros with the exception of sets where ICP-QQQ analysis was not performed (57, 59, 60, 61, 62, 64, 65). Those missing values were replaced with the geometric mean for each respective stage. The uncertainty for each stage and species was calculated as follows:

$$Uncertainty = 0.05 * [x] + LOD \quad (Eq. 1)$$

where [x] is the concentration of the species (Reff et al., 2007). No additional uncertainty was added to account for any unconsidered errors for all species. The uncertainty of the model output was evaluated using displacement (DISP), bootstrapping (BS), and bootstrapping with

displacement (BS-DISP). For BS, 100 resamples were used and a value of 0.6 was used as a threshold for the correlation coefficient (r) to pass as successful mapping for each simulation.

To qualify as a valid result, reported PMF results had to meet the following criteria: (i) factors mapped with BS runs, (ii) no factor swaps in DISP, (iii) dQ values being close or equal to 0%, and (iv) no factor swaps in BS-DISP where Al, Ti, K, Rb, V, Ni, As, Cd, Pb, Na⁺, Cl⁻, NO₃⁻, and SO₄²⁻ were displaced. PMF diagnostics can be seen in Table S4 based on the method of Brown et al. (2015).

3. Background on Measured Acids

A brief overview of the species being examined is first provided before reviewing concentration statistics. MSA is an oxidation product of dimethylsulfide (DMS) emitted primarily from the ocean (Berresheim, 1987; Saltzman et al., 1983), but it can also be formed from dimethyl sulphoxide (DMSO) emitted from anthropogenic sources such as industrial waste (Yuan et al., 2004). Gaseous MSA can become associated with particulate matter via new particle formation (Dawson et al., 2012), and through heterogeneous reactions or condensation onto existing particles (De Bruyn et al., 1994; Hanson, 2005).

Of the three saturated dicarboxylic acids, succinate (C₄) and adipate (C₆) are larger chain dicarboxylic acids linked to ozonolysis of cyclic alkenes, which is common in areas with extensive vehicular emissions (Grosjean et al., 1978; Hatakeyama et al., 1987). They can also be emitted via processes such as meat cooking (Rogge et al., 1993) and biomass burning (Kawamura et al., 2013; Pereira et al., 1982) and can be secondarily formed by the photo-oxidation of higher chain organic acids, such as azelaic acid (Bikkina et al., 2014; Ervens et al., 2004). Oxalate (C₂) is the smallest of those three acids and is usually the most abundant on a mass basis of all dicarboxylic acids in tropospheric aerosols as it represents an end-product in the oxidation of both larger-chain carboxylic acids and also glyoxylic acid (Ervens et al., 2004). It can be emitted via direct emissions such as from biomass burning (Graham et al., 2002; Narukawa et al., 1999; Xu et al., 2020), combustion exhaust (Kawamura and Kaplan, 1987; Kawamura and Yasui, 2005; Wang et al., 2010), and from various biogenic sources (Kawamura and Kaplan, 1987).

Maleate (C₄) is an unsaturated dicarboxylic acid originating from combustion engines, including via direct emissions (Kawamura and Kaplan, 1987) and secondarily produced from the photo-oxidation of benzene (Rogge et al., 1993). Lastly, phthalate (C₈) represents an aromatic dicarboxylic acid associated with incomplete combustion of vehicular emissions (Kawamura and Kaplan, 1987) and oxidation of naphthalene or other polycyclic aromatic hydrocarbons (Fine et al., 2004; Kawamura and Ikushima, 2002; Kawamura and Yasui, 2005). However, it has also been linked to biomass burning (Kumar et al., 2015) and burning of plastic material such as polyvinyl chloride (PVC) products, garbage, and plastic bags (Agarwal et al., 2020; Claeys et al., 2012; Fu et al., 2012; Li et al., 2019; Nguyen et al., 2016; Simoneit et al., 2005). Secondary formation via aqueous-phase chemistry has been documented for these organic acids (Kunwar et

al., 2019; Sorooshian et al., 2007a; Sorooshian et al., 2010; Sorooshian et al., 2006; Wonaschuetz et al., 2012) and MSA (Hoffmann et al., 2016).

4. Results

4.1 Meteorology and Transport Patterns

Meteorological data are ~~next~~ summarized based on average values temporally coincident with each MOUDI sample set period for each of the seasons. The exception to this was the accumulated rainfall, which was summed for the MOUDI set duration. Temperatures were stable during the different seasons: 28.0 ± 1.04 °C (SWM18), 28.9 ± 0.8 °C (Transitional), 28.3 ± 1.9 °C (NEM), and 28.4 ± 1.5 °C (SWM19). Solar radiation was the highest during the Transitional (279.61 ± 19.68 W m⁻²) and NEM (304.01 ± 67.54 W m⁻²) seasons, and lowest during the SWM18 (225.32 ± 56.26 W m⁻²) and SWM19 (256.05 ± 86.88 W m⁻²) seasons owing largely to more cloud cover. Accumulated rain was highest for both SWM seasons (SWM18: 29.78 ± 27.28 mm; SWM19: 16.66 ± 23.98 mm) and much lower during the Transitional (1.00 ± 1.11 mm) and NEM (2.20 ± 6.70 mm) seasons. Relative humidity was relatively consistent across seasons: SWM18 (69.6 ± 5.0 %), Transitional (69.2 ± 2.2 %), NEM season (62.4 ± 8.0 %), SWM19 (72.6 ± 11.7 %). Finally, Fig. 1 summarizes predominant wind patterns for each season based on HYSPLIT back-trajectories collected every 6 hours during sampling periods. The SWM18 and SWM19 seasons were characterized by predominantly southwesterly winds, while the NEM and Transitional seasons experienced mostly northeasterly winds. In conclusion, there was much higher potential for wet scavenging during the SWM seasons, with the potential for more photochemical reactivity in the NEM and Transitional seasons owing to enhanced incident solar radiation. As humidity was generally enhanced year-round, there was the likelihood of aqueous-phase processing to occur in all seasons. The combination of sustained RH, low boundary layer height, and high surface-level particle concentrations have been suggested to counteract the effects of wet deposition on total particle concentration in Metro Manila (Hilario et al., 2020a).

4.2 Bulk aerosol measurements

The range, mean, and standard deviation of concentrations integrated across the MOUDI diameter range (0.056 – 18 µm) are shown in Table 1 for each organic acid and MSA for all seasons. In order of decreasing concentration, the following was the order of abundance based on the cumulative dataset: oxalate (1498.59 ± 94.26 ng m⁻³) > succinate (109.53 ± 22.25 ng m⁻³) > maleate (109.52 ± 2019.66 ng m⁻³) > phthalate (98.68 ± 143.77 ng m⁻³) > adipate (7.60 ± 9.438 ng m⁻³) > MSA (5.40 ± 5.23 ng m⁻³). The relative order of abundance varies for the sub- and super-micrometer ranges with the only consistent feature being that oxalate was the most abundant species. This result was consistent with past works showing oxalate to be the most abundant organic acid in different global regions (e.g., Decesari et al. (2006); Kerminen et al. (1999); Sorooshian et al. (2007b); Ziemba et al. (2011)).

Figure 2 shows the combined contribution of the organic acids and MSA to total gravimetric mass, while Table S5 summarizes percent contributions of individual species to total mass for different size bins. Combined, the measured organic acids and MSA accounted for only a small part of the total cumulative mass ($0.80 \pm 0.66 \%$), ~~ranging from 0.23 – 1.49 %~~ across the 11 individual gravimetric sets. When the combined contribution of organic acids and MSA to total gravimetric mass were separated by season, results are generally the same (Fig. S1), with differences in the percent range being as follows: SWM18 = 0.64 %; Transitional = 0.95 %; NEM = 0.50 – 1.49 %; and SWM19 = 0.23 – 0.83 %. The highest contribution of these organic acids and MSA occurred for MOUDI sets collected 12 – 14 March 2019 during the NEM season, which accounted for 1.49 % ($0.50 \mu\text{g m}^{-3}$) of the total mass. The lowest contribution of these organic acids and MSA occurred for MOUDI sets collected 11 – 13 September 2019 during the SWM19 season, which accounted for 0.23 % ($0.06 \mu\text{g m}^{-3}$) of the total mass. The summed contributions of the six species were nearly the same in the sub- and supermicrometer ranges ($0.78 \pm 0.74 \%$ and $0.84 \pm 0.58 \%$, respectively). Their contributions peaked in the two sizes bins covering the range between 0.56 and $1.8 \mu\text{m}$ ($0.56 - 1 \mu\text{m}$: $1.06 \pm 1.01 \%$; $1 - 1.8 \mu\text{m}$: $1.01 \pm 0.78 \%$). After accounting for all measured species (BC, water-soluble species), there still remained $33.74 \pm 19.89 \%$ (range: 23.86 – 50.88 %) of unresolved mass. Therefore, the six species of interest in this work only explain a small amount of the region's mass concentrations and further work is still needed to resolve the remaining components, which presumably is dominated by water-insoluble organics and elements. Of most need is to resolve those missing components in the supermicrometer range, where Table S5 shows that the unresolved fraction is $69.10 \pm 25.91 \%$, in contrast to $17.78 \pm 17.25 \%$ for the submicrometer range.

Although there are fairly wide ranges in concentration for the individual species, a few features are noteworthy based on the cumulative dataset. First, the oxalate concentrations are lower than expected for such a highly polluted area, as will be expanded upon in Sect. ~~45.65~~. Second, there is a significant decrease in concentration after oxalate for the remaining five species, which had similar mean concentrations. Lastly, although the sampling site is on an island and close to marine sources, MSA is surprisingly the least abundant among the six species of interest.

Mean mass concentrations of these species varied greatly by season as visually shown in Fig. 3a and summarized numerically in Table 1. In contrast, Fig. 3b shows that the mass fractions of the six species did not change much seasonally owing to the dominance of oxalate ($37.67 - 472.82 \text{ ng m}^{-3}$), which accounted for between 69.1-87.3 % of the cumulative concentration of the six species across the four seasons. Important features with regard to seasonal mass concentration differences include the following: (i) maleate concentrations were much higher in the SWM18 and SWM19 seasons; (ii) the lowest overall concentrations of most species, besides oxalate and succinate (lowest in SWM19), were observed in the NEM season; (iii) oxalate and phthalate were the only species that peaked in the Transitional period, whereas the rest of the species peaked in either SWM18 or SWM19; and (iv) succinate and phthalate were peculiarly much more enhanced in SWM18 than SWM19, pointing to significant variability between consecutive years.

4.3 Source apportionment

To help elucidate how different emissions sources impact the six species, PMF analysis was conducted and yielded a solution with five source factors using year-round data (Fig. 4). The five sources are as follows in decreasing order of their contribution to the total mass based on the sum of species used in the PMF analysis (Fig. 4): combustion (32.1 %), biomass burning (20.9 %), sea salt (20.9 %), crustal (14.2 %), and waste processing (11.9 %). The contribution of each source to the total concentration of organic acids and MSA was as follows: combustion (33.5 %), biomass burning (29.0 %), crustal (27.0 %), waste processing (9.8 %), and sea salt (0.6 %). The source factor names were determined based on the enhancement of the following species (Fig. 4): (i) crustal (Al, Ti) (Harrison et al., 2011; Malm et al., 1994; Singh et al., 2002), (ii) biomass burning (K, Rb) (Andreae, 1983; Artaxo et al., 1994; Braun et al., 2020; Chow et al., 2004; Echalar et al., 1995; Ma et al., 2019; Schlosser et al., 2017; Thepnuan et al., 2019; Yamasoe et al., 2000), (iii) sea salt (Na, Cl) (Seinfeld and Pandis, 2016), (iv) combustion (V, Ni, As) (Allen et al., 2001; Linak et al., 2000; Mahowald et al., 2008; Mooibroek et al., 2011; Prabhakar et al., 2014; Wasson et al., 2005), and (v) waste processing (Cd, Pb) (Cruz et al., 2019; Gullett et al., 2007; Iijima et al., 2007; Pabroa et al., 2011). While both SO_4^{2-} and NO_3^- are secondarily produced, the latter is more commonly linked to supermicrometer particles (Allen et al., 1996; Dasgupta et al., 2007; Fitzgerald, 1991; Maudlin et al., 2015), including in the study region (Cruz et al., 2019). Additionally, Al, K, and Cl are linked to biomass burning (Reid et al., 1998; Reid et al., 2005; Schlosser et al., 2017; Wonaschütz et al., 2011). The source factor names should be interpreted with caution, as a single profile may consist of a mix of sources (e.g., waste processing). It should be noted that Cruz et al. (2019) performed PMF analysis for only the SWM18 season, which yielded similar and additional sources for only the SWM18 season, whereas this study used year-round data.

To provide size-resolved context for the five aerosol sources, Fig. 5 shows their respective reconstructed mass size distributions based on PMF output. Distributions for combustion, biomass burning, and waste processing primarily peaked in the submicrometer range, while crustal and sea salt sources primarily peaked in the supermicrometer range. Combustion and biomass burning factors showed a dominant peak between 0.32 – 0.56 μm , whereas waste processing had a peak between 0.56 – 1 μm . The crustal and sea salt factors exhibited their peak concentrations between 1.8 – 5.6 μm . Both crustal and biomass burning sources showed signs of bimodal size distributions with a minor peak in the sub- and supermicrometer ranges, respectively.

As reported in Table 2, combustion was the largest contributor to the cumulative mass concentrations of organic acids and MSA, with the largest influence being for maleate (69.7 %) and MSA (57.4 %). Biomass burning was marked by its significant contribution to succinate (90.3 %). The sea salt source showed minor contributions to phthalate (9.9 %) and adipate (4.7 %). The crustal source contributed appreciably to adipate (35.9 %) and oxalate (31.2 %), with the rest of the organic acid or MSA species being less influenced (0.1 – 13.3 %). Organic acids have been shown in past work to be associated with mineral dust (Russell et al., 2002), including both oxalic and adipic acids (Falkovich et al., 2004; Kawamura et al., 2013; Sullivan and Prather,

2007; Tsai et al., 2014), although less has been documented for adipate. Wang et al. (2017) and Yao et al. (2003) both report that gaseous acids are likely to adsorb onto supermicrometer particles that are highly alkaline, such as dust. The waste processing factor contributed to maleate (30.1 %), oxalate (10.5 %), and MSA (1.4 %). An unexpected result was that the sea salt factor did not contribute to MSA even though the latter is derived from ocean-emitted DMS; the results of Table 2 suggest that other sources such as biomass burning and industrial activities are more influential in the study region similar to other regions like Beijing (Yuan et al., 2004) and coastal and inland areas of California (Sorooshian et al., 2015).

4.4 Species interrelationships

Correlation analysis was conducted for the same species used in the PMF analysis to quantify interrelationships and to gain additional insight into common production pathways. Correlation coefficients (r) values are reported in Table 3 for the sub- and supermicrometer ranges, whereas results for full size range are shown in Table S6. Values are only shown and discussed subsequently for correlations with p -values below 0.05. Unless otherwise stated, correlations discussed below correspond to the full size range for simplicity, whereas notable results when contrasting the two size ranges ($< 1 \mu\text{m}$ and $> 1 \mu\text{m}$) are explicitly mentioned.

MSA exhibited a statistically significant correlation with Rb ($r = 0.37$), suggestive of its link with biomass burning as Rb has been shown in the study region to be a biomass burning marker (Braun et al., 2020). Additionally, MSA was correlated with Na, NO_3^- , and SO_4^{2-} ($r: 0.35 - 0.59$), which are associated with marine aerosol (e.g., sea salt, DMS, shipping) but also biomass burning. The supermicrometer results indicate MSA was correlated only with Na ($r = 0.32$), due presumably to co-emission from both crustal and sea salt sources, with the former commonly linked to biomass burning (Schlosser et al., 2017). For the submicrometer range, MSA was correlated with Rb and SO_4^{2-} ($r: 0.39 - 0.60$), which are derived from biomass burning and other forms of combustion, consistent with smaller particles formed secondarily from gas-to-particle conversion processes. That is also why MSA was well correlated with succinate, oxalate, and phthalate ($r: 0.53 - 0.67$), which were also prominent species in either (or both of) the biomass burning and combustion factors.

Adipate only exhibited significant correlations with maleate and phthalate for the full diameter range ($r: 0.43 - 0.45$), while maleate was correlated only with adipate. In contrast, succinate, oxalate, and phthalate were correlated with a wide suite of species, indicating that maleate and adipate exhibited more unique behavior in terms of their production routes. Succinate, oxalate, and phthalate similarly exhibited significant correlations with each other, and species linked to crustal sources (Al, Ti, Na), sea salt (Na), and biomass burning (Rb). Succinate and oxalate in particular were better correlated with tracer species related to either dust or sea salt (Al, Na) in the supermicrometer range, and were correlated with each other also in that size range.

4.5 Cumulative size distribution variations

Mass size distributions for each individual organic acid and MSA are shown for the full study period in Fig. S2 and seasonal mass size distributions can be seen in Figs. 6-11. General information for the cumulative dataset will be described here before examining seasonal results in Sect. 4.5. While significant variability exists between individual sets for the cumulative dataset, a few general features are evident: (i) mass size distributions all appear multi-modal with the exception of maleate, which on average exhibited a uni-modal profile; (ii) all species show a larger peak in the submicrometer range versus supermicrometer sizes; (iii) phthalate and adipate show more comparable peaks in the sub- and supermicrometer range; and (iv) the size bin where the peaks occur vary between species. These results point to differences in the species with regard to their source, formation mechanism, and eventual fate.

One factor relevant to the mass size distribution plots is the source origin of sampled air masses. The ~~WC~~WCT plots in Fig. 12 reveal the bulk of the concentration of a few species (e.g., phthalate, succinate, and MSA) was explained by southwesterly flow. Consistent with the PMF results showing that the biomass burning factor contributed the most to these three species, the predominant fire sources were to the southwest of Luzon. Past work has linked these areas to significant biomass burning influence over Luzon and the South China Sea during the SWM season (Atwood et al., 2017; Ge et al., 2017; Hilario et al., 2020b; Reid et al., 2016; Song et al., 2018; Wang et al., 2013; Xian et al., 2013). Noteworthy is that the ~~WC~~WCT maps for SWM18 reveal more influence from the biomass burning hotspots to the southwest (e.g., Borneo and Sumatra), in contrast to SWM19, pointing to more biomass burning influence in the former season. Oxalate's ~~WC~~WCT profile shows the most spatial heterogeneity in terms of source regions; this is consistent with it being an end-product in the oxidation of other carboxylic acids that can originate from numerous sources. Finally, adipate and maleate similarly showed a localized hotspot in terms of where their greatest influence originated, approximately 290 km to the north-northwest of MO. This could be partly linked to the Sual coal-fired power station located near that area where an ash disposal site is also in close proximity. The uniquely similar ~~WC~~WCT maps between adipate and maleate is consistent with them having few correlations, if any, with species aside from each other (Table S6). Subsequent sections discuss each organic acid and MSA in more detail ~~including seasonal behavior, beginning with larger acids since knowledge of their behavior is important to better understand the smaller acids.~~

5. Discussion

5.1 Phthalate

Results from Sect. 3.4 show that phthalate has the following characteristics:

- (i) influenced most by biomass burning (49.5 %), followed by combustion (27.4 %), crustal sources (13.3 %), and then sea salt (9.9 %);
- (ii) significant correlations with more species in Table S6 than any other organic acid or MSA;
- (iii) comparable mass size distribution modes in the sub- and supermicrometer size ranges;

(iv) highest mass concentration in the Transitional period, but also exhibited significantly different concentrations between the two SWM seasons; ~~and~~
(v) had concentrations dominated by sources to the southwest.

Previous studies measuring phthalate in other regions have found concentrations of 40.1 – 105 ng m⁻³ (Hong Kong; PM_{2.5}; Ho et al. (2006)), <0.01 – 7.6 ng m⁻³ (remote marine; total suspended particles (TSP); Kawamura and Sakaguchi (1999)), 0.16 – 3.25 ng m⁻³ (Arctic; TSP; Kawamura et al. (2010)), and 0 – 57.3 ng m⁻³ (Rondônia, Brazil; PM_{2.5}; Decesari et al. (2006)). The latter was more consistent with concentrations in this study (0 – 67.02 ng m⁻³), albeit the size ranges examined vary. A more detailed examination based on seasonally resolved mass size distributions and WCWT maps follows to try to gain more insights into this species. Although not referenced hereafter, Table S7 provides numerical details about mass concentration mode sizes and associated concentrations for each season and the cumulative dataset for each species.

The average size distributions for phthalate appeared bi-modal for each individual season (Fig. 6). Depending on the season, concentration peaks occurred in three separate MOUDI stages for the submicrometer range, and between 1.8 – 3.2 or 3.2 – 5.6 µm in the supermicrometer range. The NEM season was unique in that the supermicrometer peak was considerably more pronounced than in the submicrometer range, which was a rare occurrence in this study for all species except adipate. Phthalate appears in the submicrometer range due to secondary formation by photo-oxidation (i.e., Kautzman et al., 2010; Kawamura and Ikushima, 2002; Kawamura and Yasui, 2005; Kleindienst et al., 2012) and from primary emissions (i.e., combustion, biomass/waste burning) (i.e., Deshmukh et al., 2016; Kawamura and Kaplan, 1987; Kumar et al., 2015; Kundu et al., 2010). Its general presence in the supermicrometer range, especially during the NEM season, can be explained by possible adsorption onto larger particles such as dust and sea salt (i.e., Wang et al., 2012; Wang et al., 2017). Others have observed an enhancement in phthalate in the supermicrometer mode, specifically in Xi'an, China, due to suspected adsorption of its vapor form (Wang et al., 2012) derived from photo-oxidation of naphthalene (Ho et al., 2006; Wang et al., 2011; Wang et al., 2012; Wang et al., 2017).

WCWT results for phthalate (Fig. S3) showed high concentrations across all seasons coming from the southwest, most notably in the SWM18 and SWM19 seasons. The significant reduction in phthalate levels from SWM18 (176.75 ± 254.80 ng m⁻³) to SWM19 (5.72 ± 7.41 ng m⁻³) is coincident with stronger influence from biomass burning from the southwest in 2018. Figure 3 showed that the highest concentration of phthalate occurred in the Transitional period, assumed to be largely due to local emissions (e.g., vehicular traffic) based on the WCWT results with significant influence in the immediate vicinity of Luzon unlike the other seasons. The peculiar size distribution results for the NEM season can be explained by the WCWT map showing strong influence from the northeast, which likely includes supermicrometer aerosol influences from sea salt and dust from East Asia. The reduced influence of upwind anthropogenic and biomass burning emissions during the NEM season can explain the lower seasonal concentrations, especially in the submicrometer size range (Hsu et al., 2009).

5.2 Adipate

Adipate was shown in Sect. 3.4 to have the following features:

- (i) influenced most by crustal sources (35.9 %), followed by combustion (32.9 %), biomass burning (26.4 %), and finally sea salt (4.7 %);
- (ii) only correlated with maleate and phthalate;
- (iii) comparable concentrations in the sub- and supermicrometer size ranges, with a mode between 5.6 and 10 μm ;
- (iv) highest mass concentration in the SWM seasons, but especially the SWM19 season; ~~and~~
- (v) concentrations dominated by sources from the southwest as well as from the northwest.

Concentrations for adipate measured in other regions include 3.78 – 32.1 ng m^{-3} (Hong Kong; $\text{PM}_{2.5}$; Ho et al. (2006)), 3.8 – 16.8 ng m^{-3} (Rondônia, Brazil; $\text{PM}_{2.5}$; Decesari et al. (2006)), 0.60 – 13 ng m^{-3} (remote marine; TSP; Kawamura and Sakaguchi (1999)) and 0.21 – 2.94 ng m^{-3} (Arctic; TSP; Kawamura et al. (2010)). The range in this study was 0 – 43.83 ng m^{-3} , with an upper bound that exceeded those in the previous works.

Mass size distributions for adipate were the most variable in structure compared to the other five species with multiple peaks present at different sizes (Fig. S2). In general, its distributions appeared uniquely and consistently tri-modal with the exception of the SWM18 season where it was bi-modal (Fig. 7). Modes appeared between 0.10 – 0.18 μm and 0.32 – 0.56 μm for the submicrometer range, and between 1.0 – 1.8 μm and 3.2 – 5.6 μm in the supermicrometer range. The SWM19 season was unique for adipate as the highest peak was in the supermicrometer range and it was higher than any other peak across the other seasons. Submicrometer adipate is likely derived from a photo-oxidation of higher chain organic acids (i.e., van Drooge and Grimalt, 2015), ozonolysis of vehicular emissions (i.e., Grosjean et al., 1978), and from the primary emissions of biomass burning (i.e., Graham et al., 2002). The appearance in the supermicrometer range likely due to adsorption onto larger particles such as dust and sea salt (e.g., Wang et al., 2012; Wang et al., 2017). As the PMF results suggest crustal sources were more influential for adipate in contrast to sea salt, dust was more likely the supermicrometer particle type that adipate preferentially partitioned to. The source of the dust was likely a combination of long-range transport from (i) the southwest especially during biomass burning periods, (ii) East Asia, and (iii) locally generated dust via anthropogenic activities (Fig. S4).

Past work in the study region showed that broad mass size distributions with comparable concentrations in the sub- and supermicrometer ranges were coincident with wet scavenging (Braun et al., 2020) and appreciable primary emissions of sea salt and dust (AzadiAghdam et al., 2019; Cruz et al., 2019). Scavenging was suggested to remove transported pollution while allowing for more pronounced contributions from more localized emissions, which could include vehicular traffic, sea salt, and anthropogenic forms of dust (e.g., road dust, construction), all of which are consistent with adipate's mass size distribution data and ~~W~~CWT maps (Fig. S4) showing high concentrations predominately around Luzon for all seasons.

5.3 Succinate

Succinate exhibited the following characteristics:

- (i) influenced primarily by biomass burning (90.3 %) followed by crustal sources (9.7 %);
- (ii) exhibited high correlation coefficients (0.67 – 0.76) with oxalate, phthalate, and MSA (Table S6);
- (iii) mass was focused in the submicrometer range;
- (iv) highest mass concentrations were in the SWM18 season, and, similar to phthalate, showed a significant reduction in the SWM19 season; ~~and~~
- (v) had concentrations dominated by sources from the southwest.

The range of concentrations in this study ($0 - 166.28 \text{ ng m}^{-3}$) is somewhat consistent with those from other regions: $61.8 - 261 \text{ ng m}^{-3}$ (Rondônia, Brazil; $\text{PM}_{2.5}$; Decesari et al. (2006)), $13.1 - 121 \text{ ng m}^{-3}$ (Hong Kong; $\text{PM}_{2.5}$; Ho et al. (2006)), $9.2 - 31.7 \text{ ng m}^{-3}$ (New England, USA; $0.4 - 10 \mu\text{m}$; Ziemba et al. (2011)), $0.29 - 16 \text{ ng m}^{-3}$ (Remote Marine; TSP; Kawamura and Sakaguchi (1999)), and $1.35 - 12.9 \text{ ng m}^{-3}$ (Arctic; TSP; Kawamura et al. (2010)).

The average size distributions for succinate varied in the number of peaks present (2 – 4), but on average were bi-modal with a submicrometer mode usually between $0.32 - 0.56 \mu\text{m}$ or $0.56 - 1.0 \mu\text{m}$, and a smaller supermicrometer mode between either $1.8 - 3.2 \mu\text{m}$ or $3.2 - 5.6 \mu\text{m}$ (Fig. 8). The chief source of succinate, which is concentrated in the submicrometer peak, is biomass burning (Pratt et al., 2011; Vasconcellos et al., 2010), which is reinforced by the PMF results (Table 2), its high correlation with the biomass burning tracer Rb ($r = 0.67$; Table S6) (Braun et al., 2020) and ~~W~~CWT maps showing its most pronounced influence from biomass burning hotspots to the southwest during the SWM18 season (Fig. S5). There likely was also local biomass burning during the NEM season contributing to succinate concentrations. Hilario et al. (2020a) showed based on satellite data that local fire activity peaks between March and May. There was less influence from biomass burning in the SWM19 season, which is why succinate's levels were lower ($4.73 \pm 7.43 \text{ ng m}^{-3}$) than in the SWM18 season ($221.61 \pm 43.10 \text{ ng m}^{-3}$). Similar to phthalate and adipate, there were more local hotspots of concentration in seasonal ~~W~~CWT maps pointing to local anthropogenic sources such as vehicular traffic and the presence of supermicrometer particles like dust and sea salt that succinate can partition to (e.g., Wang et al., 2012; Wang et al., 2017).

5.4 Maleate

The results of Sect. ~~3-4~~ showed that maleate had the following attributes:

- (i) influenced most by combustion (69.7 %), followed by waste processing (30.1 %), and then barely by crustal sources (0.2 %);

- (ii) only correlated with adipate of all species shown in Table S6;
- (iii) showed a uni-modal mass size distribution, with negligible contribution in the supermicrometer range;
- (iv) highest mass concentration in the SWM19 season, but was comparable to the SWM18 season; ~~and~~
- (v) ~~WCWT~~ maps showed the most localized sources as compared to the other species examined (Fig. 11).

Maleate concentrations have been reported for other regions as follows: 7 – 75 ng m⁻³ (Rondônia, Brazil; PM_{2.5}; Decesari et al. (2006)), 2.21 – 37.2 ng m⁻³ (Hong Kong; PM_{2.5}; Ho et al. (2006)), 4.9 – 9.2 ng m⁻³ (New England, USA; 0.4 – 10 µm; Ziemba et al. (2011)), 0.04 – 3.8 ng m⁻³ (remote marine; TSP; Kawamura and Sakaguchi (1999)), and 0.04 – 0.83 ng m⁻³ (Arctic; TSP; Kawamura et al. (2010)). The values reported for this study region tended to be higher (0–119.19 ng m⁻³), which is unsurprising as vehicular emissions are so prominent in the Metro Manila region (Alas et al., 2018; Kecorius et al., 2017).

The average seasonal size distributions for maleate appeared to be uni-modal with peaks between 0.32 – 0.56 µm and 0.56 – 1.0 µm (Fig. 9). The absence of a supermicrometer peak, in contrast to most other species, indicates that it had less diverse sources and was derived from combustion emissions without being adsorbed onto supermicrometer particles like the other species investigated. The association of maleate with the waste processing source factor in Table 2 can be explained partly by the burning and recycling of electronic waste (Cruz et al., 2019; Gullett et al., 2007; Iijima et al., 2007). The Pabroa et al. (2011) study reported that there are few licensed operators for battery recycling, but there are numerous unregulated melters frequently melting metal and discarding the waste.

Seasonal ~~WCWT~~ maps for maleate (Fig. S6) consistently showed hotspots around Luzon indicative of local emissions. Maleate concentrations for the SWM18 (~~198.68 ± 154.89~~ ng m⁻³) and SWM19 (~~19.44 ± 34.04~~ ng m⁻³) were significantly higher than the other seasons (Transitional: ~~3.84 ± 4.23~~ ng m⁻³; NEM: ~~1.765 ± 3.765~~ ng m⁻³), and this could likely be due to increased traffic emissions because of gridlock due to intense rainfall. It should be noted that the Ateneo de Manila campus has student break periods in March, April, May, and December (Hilario et al., 2020a); those months pertain to the NEM season, which could lead to lower combustion emissions from vehicles (e.g., maleate and phthalate). Although the SWM season is associated with enhanced precipitation over Metro Manila, lower boundary layer height and appreciable RH values could counteract wet scavenging to some degree by promoting aqueous processing of aerosol (Hilario et al., 2020a). Furthermore, maleate's largely submicrometer size distribution (Fig. 9) may reduce the efficiency of wet scavenging (Greenfield, 1957).

5.5 Oxalate

Oxalate was shown to have the following traits:

- (i) influenced somewhat uniformly by combustion (32.9 %) and crustal (31.2 %) sources, followed by biomass burning (25.4 %), and waste processing (10.5 %);
- (ii) only organic acid to correlate with combustion tracers (V, Ni);
- (iii) pronounced presence in both the sub- and supermicrometer size ranges;
- (iv) highest mass concentrations in the Transitional period; ~~and~~
- (v) had contributions from the southwest, east/northeast, and locally.

Oxalate concentrations in this study ($148.59 \pm 94.26 \text{ ng m}^{-3}$) were surprisingly low for such a polluted megacity with strong regional sources. For context, concentrations in a few other regions are as follows: $1.14 \text{ } \mu\text{g m}^{-3}$ in Sao Paulo, Brazil (Souza et al., 1999); $0.27 - 1.35 \text{ } \mu\text{g m}^{-3}$ in Tokyo, Japan (Kawamura and Ikushima, 2002; Sempéré and Kawamura, 1994); $0.49 \text{ } \mu\text{g m}^{-3}$ in Los Angeles, California (Kawamura et al., 1985); $220 - 300 \text{ ng m}^{-3}$ in Nanjing, China (Yang et al., 2005); $75 - 210 \text{ ng m}^{-3}$ for multiple sites in Europe (Hungary, Belgium, Finland) (Maenhaut et al., 2011); $12.3 - 33.7 \text{ ng m}^{-3}$ in Cape San Juan, Puerto Rico (Jusino-Atresino et al., 2016); $20 - 400 \text{ ng m}^{-3}$ in rural/urban Finland (Kerminen et al., 2000); and $1 - 42 \text{ ng m}^{-3}$ around the Atlantic Ocean/Antarctic (Virkkula et al., 2006).

The average size distributions for oxalate appeared bi-modal for each individual season with modes between $0.32 - 0.56 \text{ } \mu\text{m}$ and $0.56 - 1.0 \text{ } \mu\text{m}$ for the submicrometer range and a separate mode between $1.8 - 3.2 \text{ } \mu\text{m}$ for the supermicrometer range (Fig. 10). A unique aspect for oxalate was its consistency in having a bi-modal profile each season with the supermicrometer mode always between $1.8 - 3.2 \text{ } \mu\text{m}$. Note that the modes discussed here represent the most pronounced ones but others could have been present too reflecting other sources. Submicrometer oxalate likely originated from secondary production from both biogenic and anthropogenic precursor emissions, and potentially from primary emissions (i.e., combustion/biomass burning) (i.e., Decesari et al., 2006; Falkovich et al., 2005; Golly et al., 2019; Kundu et al., 2010; Wang et al., 2010). Of all the six species studied, oxalate was best correlated with SO_4^{2-} ($r = 0.69$; Table S6), especially in the submicrometer range ($r = 0.72$; Table 3), which is consistent with their common production mechanism via aqueous processing (Sorooshian et al., 2006; Yu et al., 2005). Additionally, high concentrations of oxalate in the Transitional period indicate that photo-oxidation was an important process for oxalate formation since the Transitional period had low rain and high solar radiation. The prominent supermicrometer presence was likely due to adsorption onto supermicrometer particles. Past work by Sullivan and Prather (2007) reported the following with regard to oxalate's behavior in coarse particles of relevance to this study: (i) oxalic acid was predominately associated with mineral dust and to a lesser degree with aged sea salt; (ii) even though most of the total mass was sea salt, there was more oxalate per mass of mineral dust than sea salt; (iii) Asian dust particles are more alkaline as opposed to sea salt and therefore act as better sinks for dicarboxylic acids than sea salt; and (iv) it is feasible that a large fraction of supermicrometer dicarboxylic acid mass in remote marine air is associated with mineral dust and not sea salt. The PMF results from the present study indicate that oxalate was much more influenced by crustal sources (31.2 %) versus sea salt (0 %), similar to phthalate,

adipate, and succinate (Table 2). Reinforcing the relationship between oxalate and dust is the significant correlation between oxalate and both Al ($r = 0.59$) and Ti (0.29) in the supermicrometer range.

WCWT results for oxalate (Fig. S7) showed high concentrations around Luzon for all seasons, with the caveat that the SWM18 exhibited high concentrations coming from the southwest, which has already been linked to biomass burning emissions. The difference in oxalate levels between the SWM18 ($1787.86 \pm 139.41 \text{ ng m}^{-3}$) and SWM19 ($110.21 \pm 62.06 \text{ ng m}^{-3}$) seasons is largely due to the enhanced contribution of biomass burning in the former season since oxalate is abundant in fire emissions (Falkovich et al., 2005; Mardi et al., 2018; Narukawa et al., 1999).

5.6 MSA

Previous sections revealed the following characteristics for MSA:

- (i) influenced most by combustion (57.4 %), followed by biomass burning (41.2 %), waste processing (1.4 %), and then crustal sources (0.1 %);
- (ii) significantly correlated with succinate, oxalate, phthalate, and SO_4^{2-} ;
- (iii) similar to maleate, primarily consisted of a submicrometer mass size distribution peak with only minor contributions from the supermicrometer mode;
- (iv) concentration was highest during the SWM18 season; and
- (v) had concentrations dominated by sources from the southwest.

Concentrations of MSA in this study were surprisingly low for a site so close to marine and anthropogenic sources ($0.10 - 23.23 \text{ ng m}^{-3}$). For context, MSA concentrations in other regions are as follows: $30-60 \text{ ng m}^{-3}$ in Nanjing, China (Yang et al., 2005); $29 - 79 \text{ ng m}^{-3}$ for multiple sites in Europe (Hungary, Belgium, Finland) (Maenhaut et al., 2011); $2.33 - 3.33 \text{ ng m}^{-3}$ in Cape San Juan, Puerto Rico (Jusino-Atresino et al., 2016); $5 - 115 \text{ ng m}^{-3}$ in rural/urban Finland (Kerminen et al., 2000); $2.8 - 20 \text{ ng m}^{-3}$ around the Atlantic Ocean/Antarctic (Virkkula et al., 2006); $\sim 7 \text{ ng m}^{-3}$ in Tucson, Arizona and $\sim 101 \text{ ng m}^{-3}$ Marina, California (Sorooshian et al., 2015); $29 - 66 \text{ ng m}^{-3}$ over the China Sea (Gao et al., 1996); $13 - 59 \text{ ng m}^{-3}$ at various coastal and island sites over the North Pacific Ocean (Arimoto et al., 1996); and $34 \pm 33 \text{ ng m}^{-3}$ over Houston, Texas (Sorooshian et al., 2007b).

The average size distributions for MSA appeared uni-modal with the peak size being between $0.32 - 0.56 \mu\text{m}$ (Fig. 11). The consistent mass size distribution for MSA in all seasons, similar to maleate, could be due to some combination of limited sources and production pathways. Surprisingly, MSA showed no association to the sea salt source factor (Table 2) even though it would be expected given that DMS is co-emitted from the ocean with sea salt. Instead, combustion and biomass burning sources were more significant, which is consistent with some past studies linking MSA to anthropogenic sources (Yuan et al., 2004) and biomass burning (Sorooshian et al., 2015). WCWT results for MSA (Fig. S8) showed high concentrations coming

from the southwest during the SWM18 and SWM19 seasons, and from the east-northeast during the NEM and Transitional period.

6. Conclusions

This work used a 16-month long dataset of size-resolved aerosol composition to investigate the nature of five organic acids (oxalate, succinate, adipate, maleate, and phthalate) and MSA in the polluted Metro Manila region in the Philippines. Selected results are as follows in order of the three major questions posed at the end of Sect. 1.

- Organic acids and MSA contribute only a small fraction to the total gravimetric aerosol mass in Metro Manila (0.80 ± 0.66 %). The combined contribution of these six species was similar between the sub- and supermicrometer range (0.78 % and 0.84 %, respectively). After accounting for water-soluble ions and elements, and black carbon, there still was an unresolved mass fraction amounting to 33.74 % across all sizes, and 17.78 % and 69.10 % for sub- and supermicrometer sizes, respectively. Therefore, future work is still warranted to identify what the missing fraction is comprised of, which is speculated to be water-insoluble organics and elements.
- Oxalate was the most abundant of the six species accounting for 69.1 – 87.3 % of the total combined mass of the six species depending on the season. However, the bulk concentrations of oxalate were unusually low (1498.59 ± 94.26 ng m⁻³) for such a polluted area in contrast to other populated regions. Concentrations of the other five species were much lower than oxalate, with mean levels for the entire study period being less than 10 ng m⁻³. In particular, MSA exhibited the lowest mean concentration (5.40 ± 5.23 ng m⁻³). It is unclear exactly as to the reason for the low concentrations of the examined species in light of the diverse marine and anthropogenic sources in the region. The role of wet scavenging, especially in the SWM seasons, will be the subject of future research.
- The six species exhibited different behavior seasonally, both in terms of relative concentration and mass size distribution. The SWM18 season was uniquely different than the SWM19 season, owing to more biomass burning emissions transported from the southwest that yielded enhanced levels for most species in the submicrometer range, especially succinate, MSA, oxalate, and phthalate. Enhanced precipitation in the SWM seasons also was coincident with more influence from localized emissions leading to enhanced levels in the sub- and supermicrometer ranges depending on the species. The NEM season was characterized by generally lower concentrations of most species as air was predominantly transported from the northeast with reduced influence of anthropogenic and biomass burning emissions. Phthalate was enhanced in the supermicrometer range during the NEM season due to presumed adsorption to Asian dust and to a lesser extent sea salt. The Transitional season was characterized by having strong influence from localized emissions for all six species, which promoted especially high concentrations for phthalate and oxalate in both the sub- and supermicrometer ranges.

- All species exhibited a prominent submicrometer peak that likely stemmed largely from secondary formation from both anthropogenic and biogenic precursor emissions and was especially prominent during the SWM18 season due to extensive biomass burning influence. Biomass burning was an especially important source for succinate, phthalate, MSA, oxalate, and adipate. All six species exhibited relatively low association with sea salt particles; this was particularly interesting for MSA, which was instead better related to combustion and biomass burning emissions. In contrast to sea salt, most species were linked to crustal emissions as evident from peaks in the coarse mode during periods of dust influence. Oxalate, adipate, phthalate, and succinate in particular preferentially partitioned to dust rather than sea salt, potentially due to their affinity for alkaline particle types. Oxalate was best correlated with sulfate, especially in the submicrometer mode, explained by their common production via aqueous processing, which is common in the study region owing to high humidity levels year-round.

The results of this study point to the importance of size-resolved measurements of organic and sulfonic acids as this extensive dataset revealed important changes in mass size distributions between species and for different seasons. The data point to the partitioning of these species to coarse aerosol types and the potentially significant impact of precipitation on either the removal or enhancement of species' mass size distribution modes; these topics warrant additional research to put on firmer ground the sensitivity of these species to source regions, transport pathway, and wet scavenging effects. More research is warranted to investigate the remaining fraction of the unresolved mass (approximately one third of the gravimetric mass) that is not accounted for by black carbon and the water-soluble constituents speciated in this work. This is especially important for the supermicrometer range. Lastly, the current results point to the question as to what drives the affinity of individual species towards the coarse mode for different aerosol types (e.g., dust, sea salt), and how common this is for other regions.

Data availability

Size-resolved aerosol data collected at Manila Observatory are described in Stahl et al. (2020a) and archived on figshare (Stahl et al., 2020b) as well as on the NASA data repository at DOI:10.5067/Suborbital/CAMP2EX2018/DATA001.

Author contribution

MTC, MOC, JBS, RAB, ABM, CS, and AS designed the experiment. All coauthors carried out various aspects of the data collection. MTC, RAB, CS, and AS conducted analysis and interpretation of the data. CS and AS prepared the manuscript with contributions from the coauthors.

Competing interests

The authors declare that they have no conflict of interest.

Acknowledgements

The authors acknowledge support from NASA grant 80NSSC18K0148 in support of the NASA CAMP²Ex project. R. A. Braun acknowledges support from the ARCS Foundation. Cruz acknowledges support from the Philippine Department of Science and Technology's ASTHRD Program. A. B. MacDonald acknowledges support from the Mexican National Council for Science and Technology (CONACYT). We acknowledge Agilent Technologies for their support and Shane Snyder's laboratories for ICP-QQQ data.

References

- Adam, M. G., Chiang, A. W. J., and Balasubramanian, R.: Insights into characteristics of light absorbing carbonaceous aerosols over an urban location in Southeast Asia, *Environ Pollut*, 257, 113425, 10.1016/j.envpol.2019.113425, 2020.
- Agarwal, R., Shukla, K., Kumar, S., Aggarwal, S. G., and Kawamura, K.: Chemical composition of waste burning organic aerosols at landfill and urban sites in Delhi, *Atmos Pollut Res*, 11, 554-565, 10.1016/j.apr.2019.12.004, 2020.
- Akasaka, I., Morishima, W., and Mikami, T.: Seasonal march and its spatial difference of rainfall in the Philippines, *Int J Climatol*, 27, 715-725, 10.1002/joc.1428, 2007.
- Alas, H. D., Müller, T., Birmili, W., Kecorius, S., Cambaliza, M. O., Simpas, J. B. B., Cayetano, M., Weinhold, K., Vallar, E., Galvez, M. C., and Wiedensohler, A.: Spatial Characterization of Black Carbon Mass Concentration in the Atmosphere of a Southeast Asian Megacity: An Air Quality Case Study for Metro Manila, Philippines, *Aerosol Air Qual Res*, 18, 2301-2317, 10.4209/aaqr.2017.08.0281, 2018.
- Allen, A. G., Nemitz, E., Shi, J. P., Harrison, R. M., and Greenwood, J. C.: Size distributions of trace metals in atmospheric aerosols in the United Kingdom, *Atmos Environ*, 35, 4581-4591, 10.1016/s1352-2310(01)00190-x, 2001.
- Allen, H. C., Laux, J. M., Vogt, R., Finlayson-Pitts, B. J., and Hemminger, J. C.: Water-Induced Reorganization of Ultrathin Nitrate Films on NaCl: Implications for the Tropospheric Chemistry of Sea Salt Particles, *J Phys Chem*, 100, 6371-6375, 10.1021/jp953675a, 1996.
- Andreae, M. O.: Soot carbon and excess fine potassium: long-range transport of combustion-derived aerosols, *Science*, 220, 1148-1151, 10.1126/science.220.4602.1148, 1983.
- Andreae, M. O., and Crutzen, P. J.: Atmospheric Aerosols: Biogeochemical Sources and Role in Atmospheric Chemistry, *Science*, 276, 1052-1058, 10.1126/science.276.5315.1052, 1997.
- Arimoto, R., Duce, R. A., Savoie, D. L., Prospero, J. M., Talbot, R., Cullen, J. D., Tomza, U., Lewis, N. F., and Ray, B. J.: Relationships among aerosol constituents from Asia and the North Pacific during PEM-West A, *J Geophys Res-Atmos*, 101, 2011-2023, 10.1029/95jd01071, 1996.
- Artaxo, P., Gerab, F., Yamasoe, M. A., and Martins, J. V.: Fine mode aerosol composition at three long-term atmospheric monitoring sites in the Amazon Basin, *J Geophys Res*, 99, 22857-22868, 10.1029/94jd01023, 1994.
- Asmi, E., Frey, A., Virkkula, A., Ehn, M., Manninen, H. E., Timonen, H., Tolonen-Kivimäki, O., Aurela, M., Hillamo, R., and Kulmala, M.: Hygroscopicity and chemical composition of

835 Antarctic sub-micrometre aerosol particles and observations of new particle formation, *Atmos*
 836 *Chem Phys*, 10, 4253-4271, 10.5194/acp-10-4253-2010, 2010.
 837 Atwood, S. A., Reid, J. S., Kreidenweis, S. M., Blake, D. R., Jonsson, H. H., Lagrosas, N. D.,
 838 Xian, P., Reid, E. A., Sessions, W. R., and Simpas, J. B.: Size-resolved aerosol and cloud
 839 condensation nuclei (CCN) properties in the remote marine South China Sea – Part 1:
 840 Observations and source classification, *Atmos Chem Phys*, 17, 1105-1123, 10.5194/acp-17-
 841 1105-2017, 2017.
 842 AzadiAghdam, M., Braun, R. A., Edwards, E.-L., Bañaga, P. A., Cruz, M. T., Betito, G.,
 843 Cambaliza, M. O., Dadashazar, H., Lorenzo, G. R., Ma, L., MacDonald, A. B., Nguyen, P.,
 844 Simpas, J. B., Stahl, C., and Sorooshian, A.: On the nature of sea salt aerosol at a coastal
 845 megacity: Insights from Manila, Philippines in Southeast Asia, *Atmos Environ*, 216, 116922,
 846 10.1016/j.atmosenv.2019.116922, 2019.
 847 Baboukas, E. D., Kanakidou, M., and Mihalopoulos, N.: Carboxylic acids in gas and particulate
 848 phase above the Atlantic Ocean, *J Geophys Res-Atmos*, 105, 14459-14471,
 849 10.1029/1999jd900977, 2000.
 850 Bagtasa, G., Cayetano, M. G., and Yuan, C.-S.: Seasonal variation and chemical characterization
 851 of PM_{2.5} in northwestern Philippines, *Atmos Chem Phys*, 18, 4965-4980, 10.5194/acp-18-4965-
 852 2018, 2018.
 853 Bagtasa, G., Cayetano, M. G., Yuan, C.-S., Uchino, O., Sakai, T., Izumi, T., Morino, I., Nagai,
 854 T., Macatangay, R. C., and Velazco, V. A.: Long-range transport of aerosols from East and
 855 Southeast Asia to northern Philippines and its direct radiative forcing effect, *Atmos Environ*,
 856 218, 117007, 10.1016/j.atmosenv.2019.117007, 2019.
 857 Bagtasa, G., and Yuan, C.-S.: Influence of local meteorology on the chemical characteristics of
 858 fine particulates in Metropolitan Manila in the Philippines, *Atmos Pollut Res*, 11, 1359-1369,
 859 10.1016/j.apr.2020.05.013, 2020.
 860 Bañares, E. N., Narisma, G. T. T., Simpas, J. B. B., Cruz, F. A. T., Lorenzo, G. R. H.,
 861 Cambaliza, M. O., and Coronel, R. C.: Diurnal characterization of localized convective rain
 862 events in urban Metro Manila, Philippines, *AGUFM*, 2018, A11J-2367, 2018.
 863 Barbaro, E., Padoan, S., Kirchgeorg, T., Zangrando, R., Toscano, G., Barbante, C., and
 864 Gambaro, A.: Particle size distribution of inorganic and organic ions in coastal and inland
 865 Antarctic aerosol, *Environ Sci Pollut Res Int*, 24, 2724-2733, 10.1007/s11356-016-8042-x, 2017.
 866 Bardouki, H., Berresheim, H., Vrekoussis, M., Sciare, J., Kouvarakis, G., Oikonomou, K.,
 867 Schneider, J., and Mihalopoulos, N.: Gaseous (DMS, MSA, SO₂, H₂SO₄ and DMSO) and
 868 particulate (sulfate and methanesulfonate) sulfur species over the northeastern coast of Crete,
 869 *Atmos Chem Phys*, 3, 1871-1886, 10.5194/acp-3-1871-2003, 2003a.
 870 Bardouki, H., Liakakou, H., Economou, C., Sciare, J., Smolík, J., Ždímal, V., Eleftheriadis, K.,
 871 Lazaridis, M., Dye, C., and Mihalopoulos, N.: Chemical composition of size-resolved
 872 atmospheric aerosols in the eastern Mediterranean during summer and winter, *Atmos Environ*,
 873 37, 195-208, 10.1016/s1352-2310(02)00859-2, 2003b.
 874 Bates, T. S., Lamb, B. K., Guenther, A., Dignon, J., and Stoiber, R. E.: Sulfur emissions to the
 875 atmosphere from natural sources, *J Atmos Chem*, 14, 315-337, 10.1007/bf00115242, 2004.
 876 Bautista, A. T., Pabroa, P. C. B., Santos, F. L., Racho, J. M. D., and Quirit, L. L.: Carbonaceous
 877 particulate matter characterization in an urban and a rural site in the Philippines, *Atmos Pollut*
 878 *Res*, 5, 245-252, 10.5094/apr.2014.030, 2014.
 879 Beaver, M. R., Garland, R. M., Hasenkopf, C. A., Baynard, T., Ravishankara, A. R., and Tolbert,
 880 M. A.: A laboratory investigation of the relative humidity dependence of light extinction by

organic compounds from lignin combustion, *Environ Res Lett*, 3, 045003, 10.1088/1748-9326/3/4/045003, 2008.

Berresheim, H.: Biogenic sulfur emissions from the Subantarctic and Antarctic Oceans, *J Geophys Res*, 92, 13245-13262, 10.1029/JD092iD11p13245, 1987.

Bikkina, S., Kawamura, K., Miyazaki, Y., and Fu, P.: High abundances of oxalic, azelaic, and glyoxylic acids and methylglyoxal in the open ocean with high biological activity: Implication for secondary OA formation from isoprene, *Geophys Res Lett*, 41, 3649-3657, 10.1002/2014gl059913, 2014.

Biona, J. B., Mejia, A., Tacderas, M., Cruz, N. D., Dematera, K., and Romero, J.: Alternative Technologies for the Philippine Utility Jeepney A COST-BENEFIT STUDY, 2017.

Blando, J. D., and Turpin, B. J.: Secondary organic aerosol formation in cloud and fog droplets: a literature evaluation of plausibility, *Atmos Environ*, 34, 1623-1632, 10.1016/s1352-2310(99)00392-1, 2000.

Braun, R. A., Aghdam, M. A., Bañaga, P. A., Betito, G., Cambaliza, M. O., Cruz, M. T., Lorenzo, G. R., MacDonald, A. B., Simpas, J. B., Stahl, C., and Sorooshian, A.: Long-range aerosol transport and impacts on size-resolved aerosol composition in Metro Manila, Philippines, *Atmos Chem Phys*, 20, 2387-2405, 10.5194/acp-20-2387-2020, 2020.

Brown, S. G., Eberly, S., Paatero, P., and Norris, G. A.: Methods for estimating uncertainty in PMF solutions: examples with ambient air and water quality data and guidance on reporting PMF results, *Sci Total Environ*, 518-519, 626-635, 10.1016/j.scitotenv.2015.01.022, 2015.

Cai, C., Marsh, A., Zhang, Y. H., and Reid, J. P.: Group Contribution Approach To Predict the Refractive Index of Pure Organic Components in Ambient Organic Aerosol, *Environ Sci Technol*, 51, 9683-9690, 10.1021/acs.est.7b01756, 2017.

Carlton, A. G., Turpin, B. J., Lim, H.-J., Altieri, K. E., and Seitzinger, S.: Link between isoprene and secondary organic aerosol (SOA): Pyruvic acid oxidation yields low volatility organic acids in clouds, *Geophys Res Lett*, 33, 10.1029/2005gl025374, 2006.

Chebbi, A., and Carlier, P.: Carboxylic acids in the troposphere, occurrence, sources, and sinks: A review, *Atmos Environ*, 30, 4233-4249, 10.1016/1352-2310(96)00102-1, 1996.

Chow, J. C., Watson, J. G., Kuhns, H., Etyemezian, V., Lowenthal, D. H., Crow, D., Kohl, S. D., Engelbrecht, J. P., and Green, M. C.: Source profiles for industrial, mobile, and area sources in the Big Bend Regional Aerosol Visibility and Observational study, *Chemosphere*, 54, 185-208, 10.1016/j.chemosphere.2003.07.004, 2004.

Claeys, M., Vermeylen, R., Yasmeen, F., Gómez-González, Y., Chi, X., Maenhaut, W., Mészáros, T., and Salma, I.: Chemical characterisation of humic-like substances from urban, rural and tropical biomass burning environments using liquid chromatography with UV/vis photodiode array detection and electrospray ionisation mass spectrometry, *Environ Chem*, 9, 273-284, 10.1071/en11163, 2012.

Cohen, D. D., Stelcer, E., Santos, F. L., Prior, M., Thompson, C., and Pabroa, P. C. B.: Fingerprinting and source apportionment of fine particle pollution in Manila by IBA and PMF techniques: A 7-year study, *X-Ray Spectrom*, 38, 18-25, 10.1002/xrs.1112, 2009.

Crosbie, E., Sorooshian, A., Monfared, N. A., Shingler, T., and Esmaili, O.: A multi-year aerosol characterization for the greater Tehran area using satellite, surface, and modeling data, *Atmosphere*, 5, 178-197, 10.3390/atmos5020178, 2014.

Cruz, F. T., Narisma, G. T., Villafuerte, M. Q., Cheng Chua, K. U., and Olaguera, L. M.: A climatological analysis of the southwest monsoon rainfall in the Philippines, *Atmos Res*, 122, 609-616, 10.1016/j.atmosres.2012.06.010, 2013.

927 Cruz, M. T., Bañaga, P. A., Betito, G., Braun, R. A., Stahl, C., Aghdam, M. A., Cambaliza, M.
 928 O., Dadashazar, H., Hilario, M. R., Lorenzo, G. R., Ma, L., MacDonald, A. B., Pabroa, P. C.,
 929 Yee, J. R., Simpas, J. B., and Sorooshian, A.: Size-resolved composition and morphology of
 930 particulate matter during the southwest monsoon in Metro Manila, Philippines, *Atmos Chem*
 931 *Phys*, 19, 10675-10696, 10.5194/acp-19-10675-2019, 2019.
 932 Dasgupta, P. K., Campbell, S. W., Al-Horr, R. S., Ullah, S. M. R., Li, J., Amalfitano, C., and
 933 Poor, N. D.: Conversion of sea salt aerosol to NaNO₃ and the production of HCl: Analysis of
 934 temporal behavior of aerosol chloride/nitrate and gaseous HCl/HNO₃ concentrations with AIM,
 935 *Atmos Environ*, 41, 4242-4257, 10.1016/j.atmosenv.2006.09.054, 2007.
 936 Davis, D., Chen, G., Kasibhatla, P., Jefferson, A., Tanner, D., Eisele, F., Lenschow, D., Neff,
 937 W., and Berresheim, H.: DMS oxidation in the Antarctic marine boundary layer: Comparison of
 938 model simulations and held observations of DMS, DMSO, DMSO₂, H₂SO₄(g), MSA(g), and
 939 MSA(p), *J Geophys Res-Atmos*, 103, 1657-1678, 10.1029/97jd03452, 1998.
 940 Dawson, M. L., Varner, M. E., Perraud, V., Ezell, M. J., Gerber, R. B., and Finlayson-Pitts, B. J.:
 941 Simplified mechanism for new particle formation from methanesulfonic acid, amines, and water
 942 via experiments and ab initio calculations, *Proc Natl Acad Sci U S A*, 109, 18719-18724,
 943 10.1073/pnas.1211878109, 2012.
 944 De Bruyn, W. J., Shorter, J. A., Davidovits, P., Worsnop, D. R., Zahniser, M. S., and Kolb, C. E.:
 945 Uptake of gas phase sulfur species methanesulfonic acid, dimethylsulfoxide, and dimethyl
 946 sulfone by aqueous surfaces, *J Geophys Res*, 99, 16927-16932, 10.1029/94jd00684, 1994.
 947 Decesari, S., Fuzzi, S., Facchini, M. C., Mircea, M., Emblico, L., Cavalli, F., Maenhaut, W., Chi,
 948 X., Schkolnik, G., Falkovich, A., Rudich, Y., Claeys, M., Pashynska, V., Vas, G., Kourtshev, I.,
 949 Vermeylen, R., Hoffer, A., Andreae, M. O., Tagliavini, E., Moretti, F., and Artaxo, P.:
 950 Characterization of the organic composition of aerosols from Rondônia, Brazil, during the LBA-
 951 SMOCC 2002 experiment and its representation through model compounds, *Atmos Chem Phys*,
 952 6, 375-402, 10.5194/acp-6-375-2006, 2006.
 953 Deshmukh, D. K., Kawamura, K., Lazaar, M., Kunwar, B., and Boreddy, S. K. R.: Dicarboxylic
 954 acids, oxoacids, benzoic acid, α -dicarbonyls, WSOC, OC, and ions in spring aerosols from
 955 Okinawa Island in the western North Pacific Rim: size distributions and formation processes,
 956 *Atmos Chem Phys*, 16, 5263-5282, 10.5194/acp-16-5263-2016, 2016.
 957 Dimitriou, K.: The dependence of PM size distribution from meteorology and local-regional
 958 contributions, in Valencia (Spain)-A CWT model approach, *Aerosol Air Qual Res*, 15, 1979-
 959 1989, 10.4209/aaqr.2015.03.0162, 2015.
 960 Dimitriou, K., Remoundaki, E., Mantas, E., and Kassomenos, P.: Spatial distribution of source
 961 areas of PM_{2.5} by Concentration Weighted Trajectory (CWT) model applied in PM_{2.5}
 962 concentration and composition data, *Atmos Environ*, 116, 138-145,
 963 10.1016/j.atmosenv.2015.06.021, 2015.
 964 Ding, X., Wang, X., Xie, Z., Zhang, Z., and Sun, L.: Impacts of Siberian biomass burning on
 965 organic aerosols over the North Pacific Ocean and the Arctic: primary and secondary organic
 966 tracers, *Environ Sci Technol*, 47, 3149-3157, 10.1021/es3037093, 2013.
 967 Ding, X. X., Kong, L. D., Du, C. T., Zhanzakova, A., Fu, H. B., Tang, X. F., Wang, L., Yang,
 968 X., Chen, J. M., and Cheng, T. T.: Characteristics of size-resolved atmospheric inorganic and
 969 carbonaceous aerosols in urban Shanghai, *Atmos Environ*, 167, 625-641,
 970 10.1016/j.atmosenv.2017.08.043, 2017.

971 Drozd, G., Woo, J., Häkkinen, S. A. K., Nenes, A., and McNeill, V. F.: Inorganic salts interact
 972 with oxalic acid in submicron particles to form material with low hygroscopicity and volatility,
 973 *Atmos Chem Phys*, 14, 5205-5215, 10.5194/acp-14-5205-2014, 2014.
 974 Duarte, R., Matos, J. T. V., Paula, A. S., Lopes, S. P., Pereira, G., Vasconcellos, P., Gioda, A.,
 975 Carreira, R., Silva, A. M. S., Duarte, A. C., Smichowski, P., Rojas, N., and Sanchez-Ccoyllo, O.:
 976 Structural signatures of water-soluble organic aerosols in contrasting environments in South
 977 America and Western Europe, *Environ Pollut*, 227, 513-525, 10.1016/j.envpol.2017.05.011,
 978 2017.
 979 Echalar, F., Gaudichet, A., Cachier, H., and Artaxo, P.: Aerosol emissions by tropical forest and
 980 savanna biomass burning: Characteristic trace elements and fluxes, *Geophys Res Lett*, 22, 3039-
 981 3042, 10.1029/95gl03170, 1995.
 982 Ervens, B., Feingold, G., Clegg, S. L., and Kreidenweis, S. M.: A modeling study of aqueous
 983 production of dicarboxylic acids: 2. Implications for cloud microphysics, *J Geophys Res*, 109,
 984 10.1029/2004jd004575, 2004.
 985 Ervens, B., Sorooshian, A., Lim, Y. B., and Turpin, B. J.: Key parameters controlling OH-
 986 initiated formation of secondary organic aerosol in the aqueous phase (aqSOA), *J Geophys Res-
 987 Atmos*, 119, 3997-4016, 10.1002/2013jd021021, 2014.
 988 Ervens, B.: Progress and Problems in Modeling Chemical Processing in Cloud Droplets and Wet
 989 Aerosol Particles, in: *Multiphase Environmental Chemistry in the Atmosphere*, ACS Symposium
 990 Series, ACS Publications, 327-345, 2018.
 991 Falkovich, A. H., Schkolnik, G., Ganor, E., and Rudich, Y.: Adsorption of organic compounds
 992 pertinent to urban environments onto mineral dust particles, *J Geophys Res*, 109,
 993 10.1029/2003jd003919, 2004.
 994 Falkovich, A. H., Graber, E. R., Schkolnik, G., Rudich, Y., Maenhaut, W., and Artaxo, P.: Low
 995 molecular weight organic acids in aerosol particles from Rondônia, Brazil, during the biomass-
 996 burning, transition and wet periods, *Atmos Chem Phys*, 5, 781-797, 10.5194/acp-5-781-2005,
 997 2005.
 998 Fine, P. M., Chakrabarti, B., Krudysz, M., Schauer, J. J., and Sioutas, C.: Diurnal variations of
 999 individual organic compound constituents of ultrafine and accumulation mode particulate matter
 1000 in the Los Angeles Basin, *Environ Sci Technol*, 38, 1296-1304, 10.1021/es0348389, 2004.
 1001 Fitzgerald, J. W.: Marine aerosols: A review, *Atmos Environ A-Gen*, 25, 533-545,
 1002 10.1016/0960-1686(91)90050-h, 1991.
 1003 Fossum, K. N., Ovadnevaite, J., Ceburnis, D., Dall'Osto, M., Marullo, S., Bellacicco, M., Simo,
 1004 R., Liu, D., Flynn, M., Zuend, A., and O'Dowd, C.: Summertime Primary and Secondary
 1005 Contributions to Southern Ocean Cloud Condensation Nuclei, *Sci Rep*, 8, 13844,
 1006 10.1038/s41598-018-32047-4, 2018.
 1007 Freedman, M. A., Hasenkopf, C. A., Beaver, M. R., and Tolbert, M. A.: Optical properties of
 1008 internally mixed aerosol particles composed of dicarboxylic acids and ammonium sulfate, *J Phys
 1009 Chem A*, 113, 13584-13592, 10.1021/jp906240y, 2009.
 1010 Fu, P. Q., Kawamura, K., Chen, J., Li, J., Sun, Y. L., Liu, Y., Tachibana, E., Aggarwal, S. G.,
 1011 Okuzawa, K., Tanimoto, H., Kanaya, Y., and Wang, Z. F.: Diurnal variations of organic
 1012 molecular tracers and stable carbon isotopic composition in atmospheric aerosols over Mt. Tai in
 1013 the North China Plain: an influence of biomass burning, *Atmos Chem Phys*, 12, 8359-8375,
 1014 10.5194/acp-12-8359-2012, 2012.
 1015 Gao, S., Hegg, D. A., Hobbs, P. V., Kirchstetter, T. W., Magi, B. I., and Sadilek, M.: Water-
 1016 soluble organic components in aerosols associated with savanna fires in southern Africa:

1017 Identification, evolution, and distribution, *J Geophys Res-Atmos*, 108, 10.1029/2002jd002324,
 1018 2003.
 1019 Gao, Y., Arimoto, R., Duce, R. A., Chen, L. Q., Zhou, M. Y., and Gu, D. Y.: Atmospheric non-
 1020 sea-salt sulfate, nitrate and methanesulfonate over the China Sea, *J Geophys Res-Atmos*, 101,
 1021 12601-12611, 10.1029/96jd00866, 1996.
 1022 Ge, C., Wang, J., Reid, J. S., Posselt, D. J., Xian, P., and Hyer, E.: Mesoscale modeling of smoke
 1023 transport from equatorial Southeast Asian Maritime Continent to the Philippines: First
 1024 comparison of ensemble analysis with in situ observations, *J Geophys Res-Atmos*, 122, 5380-
 1025 5398, 10.1002/2016jd026241, 2017.
 1026 Gelencsér, and Varga: Evaluation of the atmospheric significance of multiphase reactions in
 1027 atmospheric secondary organic aerosol formation, *Atmos Chem Phys*, 5, 2823-2831,
 1028 10.5194/acp-5-2823-2005, 2005.
 1029 Golly, B., Waked, A., Weber, S., Samake, A., Jacob, V., Conil, S., Rangognio, J., Chrétien, E.,
 1030 Vagnot, M. P., Robic, P. Y., Besombes, J. L., and Jaffrezo, J. L.: Organic markers and OC source
 1031 apportionment for seasonal variations of PM_{2.5} at 5 rural sites in France, *Atmos Environ*, 198,
 1032 142-157, 10.1016/j.atmosenv.2018.10.027, 2019.
 1033 Gondwe, M., Krol, M., Klaassen, W., Gieskes, W., and de Baar, H.: Comparison of modeled
 1034 versus measured MSA:nss SO₄=ratios: A global analysis, *Global Biogeochem Cy*, 18,
 1035 10.1029/2003gb002144, 2004.
 1036 Graham, B., Mayol-Bracero, O. L., Guyon, P., Roberts, G. C., Decesari, S., Facchini, M. C.,
 1037 Artaxo, P., Maenhaut, W., Koll, P., and Andreae, M. O.: Water-soluble organic compounds in
 1038 biomass burning aerosols over Amazonia I. Characterization by NMR and GC-MS, *J Geophys*
 1039 *Res*, 107, LBA 14-11-LBA 14-16, 10.1029/2001jd000336, 2002.
 1040 Greenfield, S. M.: Rain scavenging of radioactive particulate matter from the atmosphere, *J*
 1041 *Meteorol*, 14, 115-125, 10.1175/1520-0469(1957)0142.0.CO, 1957.
 1042 Grosjean, D., Van Cauwenberghe, K., Schmid, J. P., Kelley, P. E., and Pitts, J. N.: Identification
 1043 of C₃-C₁₀ aliphatic dicarboxylic acids in airborne particulate matter, *Environ Sci Technol*, 12,
 1044 313-317, 10.1021/es60139a005, 1978.
 1045 Gullett, B. K., Linak, W. P., Touati, A., Wasson, S. J., Gatica, S., and King, C. J.:
 1046 Characterization of air emissions and residual ash from open burning of electronic wastes during
 1047 simulated rudimentary recycling operations, *J Mater Cycles Waste*, 9, 69-79, 10.1007/s10163-
 1048 006-0161-x, 2007.
 1049 Hanson, D. R.: Mass accommodation of H₂SO₄ and CH₃SO₃H on water-sulfuric acid solutions
 1050 from 6% to 97% RH, *J Phys Chem A*, 109, 6919-6927, 10.1021/jp0510443, 2005.
 1051 Harrison, R. M., Beddows, D. C., and Dall'Osto, M.: PMF analysis of wide-range particle size
 1052 spectra collected on a major highway, *Environ Sci Technol*, 45, 5522-5528, 10.1021/es2006622,
 1053 2011.
 1054 Hatakeyama, S., Ohno, M., Weng, J., Takagi, H., and Akimoto, H.: Mechanism for the formation
 1055 of gaseous and particulate products from ozone-cycloalkene reactions in air, *Environ Sci*
 1056 *Technol*, 21, 52-57, 10.1021/es00155a005, 1987.
 1057 Hilario, M. R. A., Cruz, M. T., Bañaga, P. A., Betito, G., Braun, R. A., Stahl, C., Cambaliza, M.
 1058 O., Lorenzo, G. R., MacDonald, A. B., AzadiAghdam, M., Pabroa, P. C., Yee, J. R., Simpas, J.
 1059 B., and Sorooshian, A.: Characterizing weekly cycles of particulate matter in a coastal megacity:
 1060 The importance of a seasonal, size-resolved, and chemically-speciated analysis, *J Geophys Res-*
 1061 *Atmos*, 125, 10.1029/2020JD032614, 2020a.

1062 Hilario, M. R. A., Cruz, M. T., Cambaliza, M. O. L., Reid, J. S., Xian, P., Simpas, J. B.,
 1063 Lagrosas, N. D., Uy, S. N. Y., Cliff, S., and Zhao, Y.: Investigating size-segregated sources of
 1064 elemental composition of particulate matter in the South China Sea during the 2011 Vasco
 1065 cruise, *Atmos Chem Phys*, 20, 1255-1276, 10.5194/acp-20-1255-2020, 2020b.
 1066 Ho, K. F., Lee, S. C., Cao, J. J., Kawamura, K., Watanabe, T., Cheng, Y., and Chow, J. C.:
 1067 Dicarboxylic acids, ketocarboxylic acids and dicarbonyls in the urban roadside area of Hong
 1068 Kong, *Atmos Environ*, 40, 3030-3040, 10.1016/j.atmosenv.2005.11.069, 2006.
 1069 Hodshire, A. L., Campuzano-Jost, P., Kodros, J. K., Croft, B., Nault, B. A., Schroder, J. C.,
 1070 Jimenez, J. L., and Pierce, J. R.: The potential role of methanesulfonic acid (MSA) in aerosol
 1071 formation and growth and the associated radiative forcings, *Atmos Chem Phys*, 19, 3137-3160,
 1072 10.5194/acp-19-3137-2019, 2019.
 1073 Hoffmann, E. H., Tilgner, A., Schrodner, R., Brauer, P., Wolke, R., and Herrmann, H.: An
 1074 advanced modeling study on the impacts and atmospheric implications of multiphase dimethyl
 1075 sulfide chemistry, *Proc Natl Acad Sci U S A*, 113, 11776-11781, 10.1073/pnas.1606320113,
 1076 2016.
 1077 Hoffmann, E. H., Tilgner, A., Vogelsberg, U., Wolke, R., and Herrmann, H.: Near-Explicit
 1078 Multiphase Modeling of Halogen Chemistry in a Mixed Urban and Maritime Coastal Area, *ACS*
 1079 *Earth and Space Chem*, 3, 2452-2471, 10.1021/acsearthspacechem.9b00184, 2019.
 1080 Hopke, P. K., Cohen, D. D., Begum, B. A., Biswas, S. K., Ni, B., Pandit, G. G., Santoso, M.,
 1081 Chung, Y.-S., Rahman, S. A., Hamzah, M. S., Davy, P., Markwitz, A., Waheed, S., Siddique, N.,
 1082 Santos, F. L., Pabroa, P. C. B., Seneviratne, M. C. S., Wimolwattanapun, W., Bunprapob, S.,
 1083 Vuong, T. B., and Markowicz, A.: Urban air quality in the Asian region, *Sci Total Environ*, 409,
 1084 4140, 10.1016/j.scitotenv.2011.06.028, 2011.
 1085 Hsu, S. C., Liu, S. C., Huang, Y. T., Chou, C. C., Lung, S. C., Liu, T. H., Tu, J. Y., and Tsai, F.:
 1086 Long-range southeastward transport of Asian biomass pollution: Signature detected by aerosol
 1087 potassium in northern Taiwan, *J Geophys Res-Atmos*, 114, 10.1029/2009JD011725, 2009.
 1088 Hsu, Y.-K., Holsen, T. M., and Hopke, P. K.: Comparison of hybrid receptor models to locate
 1089 PCB sources in Chicago, *Atmos Environ*, 37, 545-562, 10.1016/S1352-2310(02)00886-5, 2003.
 1090 Iijima, A., Sato, K., Yano, K., Tago, H., Kato, M., Kimura, H., and Furuta, N.: Particle size and
 1091 composition distribution analysis of automotive brake abrasion dusts for the evaluation of
 1092 antimony sources of airborne particulate matter, *Atmos Environ*, 41, 4908-4919,
 1093 10.1016/j.atmosenv.2007.02.005, 2007.
 1094 Jusino-Atresino, R., Anderson, J., and Gao, Y.: Ionic and elemental composition of PM_{2.5}
 1095 aerosols over the Caribbean Sea in the Tropical Atlantic, *J Atmos Chem*, 73, 427-457,
 1096 10.1007/s10874-016-9337-5, 2016.
 1097 Kautzman, K. E., Surratt, J. D., Chan, M. N., Chan, A. W., Hersey, S. P., Chhabra, P. S.,
 1098 Dalleska, N. F., Wennberg, P. O., Flagan, R. C., and Seinfeld, J. H.: Chemical composition of
 1099 gas- and aerosol-phase products from the photooxidation of naphthalene, *J Phys Chem A*, 114,
 1100 913-934, 10.1021/jp908530s, 2010.
 1101 Kavouras, I. G., and Stephanou, E. G.: Particle size distribution of organic primary and
 1102 secondary aerosol constituents in urban, background marine, and forest atmosphere, *J Geophys*
 1103 *Res*, 107, 10.1029/2000jd000278, 2002.
 1104 Kawamura, K., Ng, L. L., and Kaplan, I. R.: Determination of organic acids (C₁-C₁₀) in the
 1105 atmosphere, motor exhausts, and engine oils, *Environ Sci Technol*, 19, 1082-1086,
 1106 10.1021/es00141a010, 1985.

1107 Kawamura, K., and Kaplan, I. R.: Motor exhaust emissions as a primary source for dicarboxylic
 1108 acids in Los Angeles ambient air, *Environ Sci Technol*, 21, 105-110, 10.1021/es00155a014,
 1109 1987.
 1110 Kawamura, K., and Sakaguchi, F.: Molecular distributions of water soluble dicarboxylic acids in
 1111 marine aerosols over the Pacific Ocean including tropics, *J Geophys Res-Atmos*, 104, 3501-
 1112 3509, 10.1029/1998jd100041, 1999.
 1113 Kawamura, K., and Ikushima, K.: Seasonal changes in the distribution of dicarboxylic acids in
 1114 the urban atmosphere, *Environ Sci Technol*, 27, 2227-2235, 10.1021/es00047a033, 2002.
 1115 Kawamura, K., and Yasui, O.: Diurnal changes in the distribution of dicarboxylic acids,
 1116 ketocarboxylic acids and dicarbonyls in the urban Tokyo atmosphere, *Atmos Environ*, 39, 1945-
 1117 1960, 10.1016/j.atmosenv.2004.12.014, 2005.
 1118 Kawamura, K., Kasukabe, H., and Barrie, L. A.: Secondary formation of water-soluble organic
 1119 acids and α -dicarbonyls and their contributions to total carbon and water-soluble organic carbon:
 1120 Photochemical aging of organic aerosols in the Arctic spring, *J Geophys Res*, 115,
 1121 10.1029/2010jd014299, 2010.
 1122 Kawamura, K., Tachibana, E., Okuzawa, K., Aggarwal, S. G., Kanaya, Y., and Wang, Z. F.:
 1123 High abundances of water-soluble dicarboxylic acids, ketocarboxylic acids and α -dicarbonyls in
 1124 the mountaintop aerosols over the North China Plain during wheat burning season, *Atmos Chem*
 1125 *Phys*, 13, 8285-8302, 10.5194/acp-13-8285-2013, 2013.
 1126 Kawamura, K., and Bikkina, S.: A review of dicarboxylic acids and related compounds in
 1127 atmospheric aerosols: Molecular distributions, sources and transformation, *Atmos Res*, 170, 140-
 1128 160, 10.1016/j.atmosres.2015.11.018, 2016.
 1129 Kecorius, S., Madueño, L., Vallar, E., Alas, H., Betito, G., Birmili, W., Cambaliza, M. O.,
 1130 Catipay, G., Gonzaga-Cayetano, M., Galvez, M. C., Lorenzo, G., Müller, T., Simpas, J. B.,
 1131 Tamayo, E. G., and Wiedensohler, A.: Aerosol particle mixing state, refractory particle number
 1132 size distributions and emission factors in a polluted urban environment: Case study of Metro
 1133 Manila, Philippines, *Atmos Environ*, 170, 169-183, 10.1016/j.atmosenv.2017.09.037, 2017.
 1134 Kerminen, V.-M., Teinilä, K., Hillamo, R., and Mäkelä, T.: Size-segregated chemistry of
 1135 particulate dicarboxylic acids in the Arctic atmosphere, *Atmos Environ*, 33, 2089-2100,
 1136 10.1016/s1352-2310(98)00350-1, 1999.
 1137 Kerminen, V.-M., Ojanen, C., Pakkanen, T., Hillamo, R., Aurela, M., and Meriläinen, J.: Low-
 1138 Molecular-Weight Dicarboxylic Acids in an Urban and Rural Atmosphere, *J Aerosol Sci*, 31,
 1139 349-362, 10.1016/s0021-8502(99)00063-4, 2000.
 1140 Kerminen, V.-M., Aurela, M., Hillamo, R. E., and Virkkula, A.: Formation of particulate MSA:
 1141 deductions from size distribution measurements in the Finnish Arctic, *Tellus B*, 49, 159-171,
 1142 10.3402/tellusb.v49i2.15959, 2017.
 1143 Kim Oanh, N. T., Upadhyay, N., Zhuang, Y. H., Hao, Z. P., Murthy, D. V. S., Lestari, P.,
 1144 Villarin, J. T., Chengchua, K., Co, H. X., and Dung, N. T.: Particulate air pollution in six Asian
 1145 cities: Spatial and temporal distributions, and associated sources, *Atmos Environ*, 40, 3367-3380,
 1146 10.1016/j.atmosenv.2006.01.050, 2006.
 1147 Kleindienst, T. E., Jaoui, M., Lewandowski, M., Offenberg, J. H., and Docherty, K. S.: The
 1148 formation of SOA and chemical tracer compounds from the photooxidation of naphthalene and
 1149 its methyl analogs in the presence and absence of nitrogen oxides, *Atmos Chem Phys*, 12, 8711-
 1150 8726, 10.5194/acp-12-8711-2012, 2012.

1151 Kobayashi, H., Matsunaga, T., Hoyano, A., Aoki, M., Komori, D., and Boonyawat, S.: Satellite
 1152 estimation of photosynthetically active radiation in Southeast Asia: Impacts of smoke and cloud
 1153 cover, *J Geophys Res-Atmos*, 109, 10.1029/2003jd003807, 2004.
 1154 Kondo, Y., Matsui, H., Moteki, N., Sahu, L., Takegawa, N., Kajino, M., Zhao, Y., Cubison, M.
 1155 J., Jimenez, J. L., Vay, S., Diskin, G. S., Anderson, B., Wisthaler, A., Mikoviny, T., Fuelberg, H.
 1156 E., Blake, D. R., Huey, G., Weinheimer, A. J., Knapp, D. J., and Brune, W. H.: Emissions of
 1157 black carbon, organic, and inorganic aerosols from biomass burning in North America and Asia
 1158 in 2008, *J Geophys Res*, 116, 10.1029/2010jd015152, 2011.
 1159 Kumar, S., Aggarwal, S. G., Gupta, P. K., and Kawamura, K.: Investigation of the tracers for
 1160 plastic-enriched waste burning aerosols, *Atmos Environ*, 108, 49-58,
 1161 10.1016/j.atmosenv.2015.02.066, 2015.
 1162 Kundu, S., Kawamura, K., Andreae, T. W., Hoffer, A., and Andreae, M. O.: Molecular
 1163 distributions of dicarboxylic acids, ketocarboxylic acids and α -dicarbonyls in biomass
 1164 burning aerosols: implications for photochemical production and degradation in smoke layers,
 1165 *Atmos Chem Phys*, 10, 2209-2225, 10.5194/acp-10-2209-2010, 2010.
 1166 Kunwar, B., Kawamura, K., Fujiwara, S., Fu, P., Miyazaki, Y., and Pokhrel, A.: Dicarboxylic
 1167 acids, oxocarboxylic acids and α -dicarbonyls in atmospheric aerosols from Mt. Fuji, Japan:
 1168 Implication for primary emission versus secondary formation, *Atmos Res*, 221, 58-71,
 1169 10.1016/j.atmosres.2019.01.021, 2019.
 1170 Li, J., Wang, G., Zhang, Q., Li, J., Wu, C., Jiang, W., Zhu, T., and Zeng, L.: Molecular
 1171 characteristics and diurnal variations of organic aerosols at a rural site in the North China Plain
 1172 with implications for the influence of regional biomass burning, *Atmos Chem Phys*, 19, 10481-
 1173 10496, 10.5194/acp-19-10481-2019, 2019.
 1174 Limbeck, A., Puxbaum, H., Otter, L., and Scholes, M. C.: Semivolatile behavior of dicarboxylic
 1175 acids and other polar organic species at a rural background site (Nylsvley, RSA), *Atmos*
 1176 *Environ*, 35, 1853-1862, 10.1016/s1352-2310(00)00497-0, 2001.
 1177 Linak, W. P., Miller, C. A., and Wendt, J. O.: Comparison of particle size distributions and
 1178 elemental partitioning from the combustion of pulverized coal and residual fuel oil, *J Air Waste*
 1179 *Manag Assoc*, 50, 1532-1544, 10.1080/10473289.2000.10464171, 2000.
 1180 Liu, Y., Minofar, B., Desyaterik, Y., Dames, E., Zhu, Z., Cain, J. P., Hopkins, R. J., Gilles, M.
 1181 K., Wang, H., Jungwirth, P., and Laskin, A.: Internal structure, hygroscopic and reactive
 1182 properties of mixed sodium methanesulfonate-sodium chloride particles, *Phys Chem Chem Phys*,
 1183 13, 11846-11857, 10.1039/c1cp20444k, 2011.
 1184 Ma, L., Dadashazar, H., Braun, R. A., MacDonald, A. B., Aghdam, M. A., Maudlin, L. C., and
 1185 Sorooshian, A.: Size-resolved characteristics of water-soluble particulate elements in a coastal
 1186 area: Source identification, influence of wildfires, and diurnal variability, *Atmos Environ*, 206,
 1187 72-84, 10.1016/j.atmosenv.2019.02.045, 2019.
 1188 Madueño, L., Kecorius, S., Birmili, W., Müller, T., Simpas, J., Vallar, E., Galvez, M. C.,
 1189 Cayetano, M., and Wiedensohler, A.: Aerosol Particle and Black Carbon Emission Factors of
 1190 Vehicular Fleet in Manila, Philippines, *Atmosphere*, 10, 603, 10.3390/atmos10100603, 2019.
 1191 Maenhaut, W., Wang, W., and Chi, X.: Semivolatile behaviour and filter sampling artifacts for
 1192 dicarboxylic acids during summer campaigns at three forested sites in Europe, *Boreal Environ*
 1193 *Res*, 16, 273-287, 2011.
 1194 Mahowald, N., Jickells, T. D., Baker, A. R., Artaxo, P., Benitez-Nelson, C. R., Bergametti, G.,
 1195 Bond, T. C., Chen, Y., Cohen, D. D., Herut, B., Kubilay, N., Losno, R., Luo, C., Maenhaut, W.,
 1196 McGee, K. A., Okin, G. S., Siefert, R. L., and Tsukuda, S.: Global distribution of atmospheric

phosphorus sources, concentrations and deposition rates, and anthropogenic impacts, *Global Biogeochem Cy*, 22, 10.1029/2008gb003240, 2008.

Malm, W. C., Sisler, J. F., Huffman, D., Eldred, R. A., and Cahill, T. A.: Spatial and seasonal trends in particle concentration and optical extinction in the United States, *J Geophys Res-Atmos*, 99, 1347-1370, 10.1029/93jd02916, 1994.

Mardi, A. H., Dadashazar, H., MacDonald, A. B., Braun, R. A., Crosbie, E., Xian, P., Thorsen, T. J., Coggon, M. M., Fenn, M. A., Ferrare, R. A., Hair, J. W., Woods, R. K., Jonsson, H. H., Flagan, R. C., Seinfeld, J. H., and Sorooshian, A.: Biomass Burning Plumes in the Vicinity of the California Coast: Airborne Characterization of Physicochemical Properties, Heating Rates, and Spatiotemporal Features, *J Geophys Res-Atmos*, 123, 13,560-513,582, 10.1029/2018jd029134, 2018.

Marple, V., Olson, B., Romy, F., Hudak, G., Geerts, S. M., and Lundgren, D.: Second Generation Micro-Orifice Uniform Deposit Impactor, 120 MOUDI-II: Design, Evaluation, and Application to Long-Term Ambient Sampling, *Aerosol Sci. Tech.*, 48, 427-433, 10.1080/02786826.2014.884274, 2014.

Marsh, A., Miles, R. E. H., Rovelli, G., Cowling, A. G., Nandy, L., Dutcher, C. S., and Reid, J. P.: Influence of organic compound functionality on aerosol hygroscopicity: dicarboxylic acids, alkyl-substituents, sugars and amino acids, *Atmos Chem Phys*, 17, 5583-5599, 10.5194/acp-17-5583-2017, 2017.

Marsh, A., Rovelli, G., Miles, R. E. H., and Reid, J. P.: Complexity of Measuring and Representing the Hygroscopicity of Mixed Component Aerosol, *J Phys Chem A*, 123, 1648-1660, 10.1021/acs.jpca.8b11623, 2019.

Matsumoto, J., Olaguera, L. M. P., Nguyen-Le, D., Kubota, H., and Villafuerte, M. Q.: Climatological seasonal changes of wind and rainfall in the Philippines, *Int J Climatol*, 10.1002/joc.6492, 2020.

Maudlin, L. C., Wang, Z., Jonsson, H. H., and Sorooshian, A.: Impact of wildfires on size-resolved aerosol composition at a coastal California site, *Atmos Environ*, 119, 59-68, 10.1016/j.atmosenv.2015.08.039, 2015.

McGinty, S. M., Kapala, M. K., and Niedziela, R. F.: Mid-infrared complex refractive indices for oleic acid and optical properties of model oleic acid/water aerosols, *Phys Chem Chem Phys*, 11, 7998-8004, 10.1039/b905371a, 2009.

Mochida, M., Umemoto, N., Kawamura, K., and Uematsu, M.: Bimodal size distribution of C2-C4dicarboxylic acids in the marine aerosols, *Geophys Res Lett*, 30, 10.1029/2003gl017451, 2003.

Mooibroek, D., Schaap, M., Weijers, E. P., and Hoogerbrugge, R.: Source apportionment and spatial variability of PM2.5 using measurements at five sites in the Netherlands, *Atmos Environ*, 45, 4180-4191, 10.1016/j.atmosenv.2011.05.017, 2011.

Mora, M., Braun, R. A., Shingler, T., and Sorooshian, A.: Analysis of remotely sensed and surface data of aerosols and meteorology for the Mexico Megalopolis Area between 2003 and 2015, *J Geophys Res Atmos*, 122, 8705-8723, 10.1002/2017JD026739, 2017.

Myhre, C. E. L., and Nielsen, C. J.: Optical properties in the UV and visible spectral region of organic acids relevant to tropospheric aerosols, *Atmos Chem Phys*, 4, 1759-1769, 10.5194/acp-4-1759-2004, 2004.

Narukawa, M., Kawamura, K., Takeuchi, N., and Nakajima, T.: Distribution of dicarboxylic acids and carbon isotopic compositions in aerosols from 1997 Indonesian forest fires, *Geophys Res Lett*, 26, 3101-3104, 10.1029/1999gl010810, 1999.

1243 Neusüss, C., Pelzing, M., Plewka, A., and Herrmann, H.: A new analytical approach for size-
 1244 resolved speciation of organic compounds in atmospheric aerosol particles: Methods and first
 1245 results, *J Geophys Res-Atmos*, 105, 4513-4527, 10.1029/1999jd901038, 2000.
 1246 Nguyen, D. L., Kawamura, K., Ono, K., Ram, S. S., Engling, G., Lee, C.-T., Lin, N.-H., Chang,
 1247 S.-C., Chuang, M.-T., and Hsiao, T.-C.: Comprehensive PM_{2.5} organic molecular composition
 1248 and stable carbon isotope ratios at Sonla, Vietnam: Fingerprint of biomass burning components,
 1249 *Aerosol Air Qual Res*, 16, 2618-2634, 10.4209/aaqr.2015.07.0459 2016.
 1250 Norton, R. B., Roberts, J. M., and Huebert, B. J.: Tropospheric oxalate, *Geophys Res Lett*, 10,
 1251 517-520, 10.1029/GL010i007p00517, 1983.
 1252 Ovadnevaite, J., Ceburnis, D., Leinert, S., Dall'Osto, M., Canagaratna, M., O'Doherty, S.,
 1253 Berresheim, H., and O'Dowd, C.: Submicron NE Atlantic marine aerosol chemical composition
 1254 and abundance: Seasonal trends and air mass categorization, *J Geophys Res-Atmos*, 119, 11,850-
 1255 811,863, 10.1002/2013jd021330, 2014.
 1256 Paatero, P., and Tapper, U.: Positive matrix factorization: A non-negative factor model with
 1257 optimal utilization of error estimates of data values, *Environmetrics*, 5, 111-126, 1994.
 1258 Pabroa, P. C. B., Santos, F. L., Morco, R. P., Racho, J. M. D., Bautista Vii, A. T., and Bucal, C.
 1259 G. D.: Receptor modeling studies for the characterization of air particulate lead pollution sources
 1260 in Valenzuela sampling site (Philippines), *Atmos Pollut Res*, 2, 213-218, 10.5094/apr.2011.027,
 1261 2011.
 1262 PAGASA: Onset of the rainy season: <http://bagong.pagasa.dost.gov.ph/press-release/29#>, 2018a.
 1263 PAGASA: Termination of the southwest monsoon: [http://bagong.pagasa.dost.gov.ph/press-](http://bagong.pagasa.dost.gov.ph/press-release/30)
 1264 [release/30](http://bagong.pagasa.dost.gov.ph/press-release/30), 2018b.
 1265 PAGASA: Onset of the northeast monsoon: <http://bagong.pagasa.dost.gov.ph/press-release/32>,
 1266 2018c.
 1267 PAGASA: Transition to northeast monsoon: <http://bagong.pagasa.dost.gov.ph/press-release/56>,
 1268 2019a.
 1269 PAGASA: Onset of the rainy season: <http://bagong.pagasa.dost.gov.ph/press-release/50>, 2019b.
 1270 Peng, C., and Chan, C. K.: The water cycles of water-soluble organic salts of atmospheric
 1271 importance, *Atmos Environ*, 35, 1183-1192, 10.1016/s1352-2310(00)00426-x, 2001.
 1272 Peng, C., Jing, B., Guo, Y. C., Zhang, Y. H., and Ge, M. F.: Hygroscopic Behavior of
 1273 Multicomponent Aerosols Involving NaCl and Dicarboxylic Acids, *J Phys Chem A*, 120, 1029-
 1274 1038, 10.1021/acs.jpca.5b09373, 2016.
 1275 Pereira, W. E., Rostad, C. E., Taylor, H. E., and Klein, J. M.: Characterization of organic
 1276 contaminants in environmental samples associated with Mount St. Helens 1980 volcanic
 1277 eruption, *Environ Sci Technol*, 16, 387-396, 10.1021/es00101a005, 1982.
 1278 Prabhakar, G., Sorooshian, A., Toffol, E., Arellano, A. F., and Betterton, E. A.: Spatiotemporal
 1279 Distribution of Airborne Particulate Metals and Metalloids in a Populated Arid Region, *Atmos*
 1280 *Environ*, 92, 339-347, 10.1016/j.atmosenv.2014.04.044, 2014.
 1281 Pratt, K. A., Murphy, S. M., Subramanian, R., DeMott, P. J., Kok, G. L., Campos, T., Rogers, D.
 1282 C., Prenni, A. J., Heymsfield, A. J., Seinfeld, J. H., and Prather, K. A.: Flight-based chemical
 1283 characterization of biomass burning aerosols within two prescribed burn smoke plumes, *Atmos*
 1284 *Chem Phys*, 11, 12549-12565, 10.5194/acp-11-12549-2011, 2011.
 1285 Prenni, A. J., DeMott, P. J., Kreidenweis, S. M., Sherman, D. E., Russell, L. M., and Ming, Y.:
 1286 The Effects of Low Molecular Weight Dicarboxylic Acids on Cloud Formation, *J Phys Chem A*,
 1287 105, 11240-11248, 10.1021/jp012427d, 2001.

1288 PSA: Highlights of the Philippine population 2015 census of population:
 1289 <https://psa.gov.ph/content/highlights-philippine-population-2015-census-population>, access:
 1290 January 7, 2016.
 1291 Ramachandran, S., and Rajesh, T. A.: Black carbon aerosol mass concentrations over
 1292 Ahmedabad, an urban location in western India: Comparison with urban sites in Asia, Europe,
 1293 Canada, and the United States, *J Geophys Res*, 112, 10.1029/2006jd007488, 2007.
 1294 Ran, L., Deng, Z. Z., Wang, P. C., and Xia, X. A.: Black carbon and wavelength-dependent
 1295 aerosol absorption in the North China Plain based on two-year aethalometer measurements,
 1296 *Atmos Environ*, 142, 132-144, 10.1016/j.atmosenv.2016.07.014, 2016.
 1297 Reff, A., Eberly, S. I., and Bhawe, P. V.: Receptor modeling of ambient particulate matter data
 1298 using positive matrix factorization: review of existing methods, *J Air Waste Manag Assoc*, 57,
 1299 146-154, 10.1080/10473289.2007.10465319, 2007.
 1300 Reid, J. S., Hobbs, P. V., Ferek, R. J., Blake, D. R., Martins, J. V., Dunlap, M. R., and Liousse,
 1301 C.: Physical, chemical, and optical properties of regional hazes dominated by smoke in Brazil, *J*
 1302 *Geophys Res-Atmos*, 103, 32059-32080, 10.1029/98jd00458, 1998.
 1303 Reid, J. S., Koppmann, R., Eck, T. F., and Eleuterio, D. P.: A review of biomass burning
 1304 emissions part II: intensive physical properties of biomass burning particles, *Atmos Chem Phys*,
 1305 5, 799-825, 10.5194/acp-5-799-2005, 2005.
 1306 Reid, J. S., Hyer, E. J., Johnson, R. S., Holben, B. N., Yokelson, R. J., Zhang, J., Campbell, J. R.,
 1307 Christopher, S. A., Di Girolamo, L., Giglio, L., Holz, R. E., Kearney, C., Miettinen, J., Reid, E.
 1308 A., Turk, F. J., Wang, J., Xian, P., Zhao, G., Balasubramanian, R., Chew, B. N., Janjai, S.,
 1309 Lagrosas, N., Lestari, P., Lin, N.-H., Mahmud, M., Nguyen, A. X., Norris, B., Oanh, N. T. K.,
 1310 Oo, M., Salinas, S. V., Welton, E. J., and Liew, S. C.: Observing and understanding the
 1311 Southeast Asian aerosol system by remote sensing: An initial review and analysis for the Seven
 1312 Southeast Asian Studies (7SEAS) program, *Atmos Res*, 122, 403-468,
 1313 10.1016/j.atmosres.2012.06.005, 2013.
 1314 Reid, J. S., Xian, P., Holben, B. N., Hyer, E. J., Reid, E. A., Salinas, S. V., Zhang, J., Campbell,
 1315 J. R., Chew, B. N., Holz, R. E., Kuciauskas, A. P., Lagrosas, N., Posselt, D. J., Sampson, C. R.,
 1316 Walker, A. L., Welton, E. J., and Zhang, C.: Aerosol meteorology of the Maritime Continent for
 1317 the 2012 7SEAS southwest monsoon intensive study – Part 1: regional-scale phenomena, *Atmos*
 1318 *Chem Phys*, 16, 14041-14056, 10.5194/acp-16-14041-2016, 2016.
 1319 Rogge, W. F., Mazurek, M. A., Hildemann, L. M., Cass, G. R., and Simoneit, B. R. T.:
 1320 Quantification of urban organic aerosols at a molecular level: Identification, abundance and
 1321 seasonal variation, *Atmos Environ A-Gen*, 27, 1309-1330, 10.1016/0960-1686(93)90257-y,
 1322 1993.
 1323 Rolph, G., Stein, A., and Stunder, B.: Real-time Environmental Applications and Display
 1324 sYstem: READY, *Environ Modell Softw*, 95, 210-228, 10.1016/j.envsoft.2017.06.025, 2017.
 1325 Rose, C., Chaumerliac, N., Deguillaume, L., Perroux, H., Mouchel-Vallon, C., Leriche, M.,
 1326 Patryl, L., and Armand, P.: Modeling the partitioning of organic chemical species in cloud
 1327 phases with CLEPS (1.1), *Atmos Chem Phys*, 18, 2225-2242, 10.5194/acp-18-2225-2018, 2018.
 1328 Russell, L. M., Maria, S. F., and Myneni, S. C. B.: Mapping organic coatings on atmospheric
 1329 particles, *Geophys Res Lett*, 29, 26-21-26-24, 10.1029/2002gl014874, 2002.
 1330 Saltzman, E. S., Savoie, D. L., Zika, R. G., and Prospero, J. M.: Methane sulfonic acid in the
 1331 marine atmosphere, *J Geophys Res-Oceans*, 88, 10897-10902, 10.1029/JC088iC15p10897, 1983.
 1332 Sareen, N., Carlton, A. G., Surratt, J. D., Gold, A., Lee, B., Lopez-Hilfiker, F. D., Mohr, C.,
 1333 Thornton, J. A., Zhang, Z., Lim, Y. B., and Turpin, B. J.: Identifying precursors and aqueous

1334 organic aerosol formation pathways during the SOAS campaign, *Atmos Chem Phys*, 16, 14409-
 1335 14420, 10.5194/acp-16-14409-2016, 2016.
 1336 Saxena, P., and Hildemann, L. M.: Water-soluble organics in atmospheric particles: A critical
 1337 review of the literature and application of thermodynamics to identify candidate compounds, *J*
 1338 *Atmos Chem*, 24, 57-109, 10.1007/bf00053823, 1996.
 1339 Schlosser, J. S., Braun, R. A., Bradley, T., Dadashazar, H., MacDonald, A. B., Aldhaif, A. A.,
 1340 Aghdam, M. A., Mardi, A. H., Xian, P., and Sorooshian, A.: Analysis of aerosol composition
 1341 data for western United States wildfires between 2005 and 2015: Dust emissions, chloride
 1342 depletion, and most enhanced aerosol constituents, *J Geophys Res-Atmos*, 122, 8951-8966,
 1343 2017.
 1344 Seinfeld, J. H., and Pandis, S. N.: *Atmospheric chemistry and physics*, 3rd ed., Wiley-
 1345 Interscience, New York, 2016.
 1346 Sempéré, R., and Kawamura, K.: Comparative distributions of dicarboxylic acids and related
 1347 polar compounds in snow, rain and aerosols from urban atmosphere, *Atmos Environ*, 28, 449-
 1348 459, 10.1016/1352-2310(94)90123-6, 1994.
 1349 Simoneit, B. R., Medeiros, P. M., and Didyk, B. M.: Combustion products of plastics as
 1350 indicators for refuse burning in the atmosphere, *Environ Sci Technol*, 39, 6961-6970,
 1351 10.1021/es050767x, 2005.
 1352 Simpas, J., Lorenzo, G., and Cruz, M.: Monitoring Particulate Matter Levels and Composition
 1353 for Source Apportionment Study in Metro Manila, Philippines, in: *Improving Air Quality in*
 1354 *Asian Developing Countries: Compilation of Research Findings*, edited by: Kim Oanh, N. T.,
 1355 239-261, 2014.
 1356 Singh, M., Jaques, P. A., and Sioutas, C.: Size distribution and diurnal characteristics of particle-
 1357 bound metals in source and receptor sites of the Los Angeles Basin, *Atmos Environ*, 36, 1675-
 1358 1689, 10.1016/s1352-2310(02)00166-8, 2002.
 1359 Skyllakou, K., Fountoukis, C., Charalampidis, P., and Pandis, S. N.: Volatility-resolved source
 1360 apportionment of primary and secondary organic aerosol over Europe, *Atmos Environ*, 167, 1-
 1361 10, 10.1016/j.atmosenv.2017.08.005, 2017.
 1362 Song, J., Zhao, Y., Zhang, Y., Fu, P., Zheng, L., Yuan, Q., Wang, S., Huang, X., Xu, W., Cao,
 1363 Z., Gromov, S., and Lai, S.: Influence of biomass burning on atmospheric aerosols over the
 1364 western South China Sea: Insights from ions, carbonaceous fractions and stable carbon isotope
 1365 ratios, *Environ Pollut*, 242, 1800-1809, 10.1016/j.envpol.2018.07.088, 2018.
 1366 Sorooshian, A., Varutbangkul, V., Brechtel, F. J., Ervens, B., Feingold, G., Bahreini, R.,
 1367 Murphy, S. M., Holloway, J. S., Atlas, E. L., Buzorius, G., Jonsson, H., Flagan, R. C., and
 1368 Seinfeld, J. H.: Oxalic acid in clear and cloudy atmospheres: Analysis of data from International
 1369 Consortium for Atmospheric Research on Transport and Transformation 2004, *J Geophys Res-*
 1370 *Atmos*, 111, 10.1029/2005jd006880, 2006.
 1371 Sorooshian, A., Lu, M. L., Brechtel, F. J., Jonsson, H., Feingold, G., Flagan, R. C., and Seinfeld,
 1372 J. H.: On the source of organic acid aerosol layers above clouds, *Environ Sci Technol*, 41, 4647-
 1373 4654, 10.1021/es0630442, 2007a.
 1374 Sorooshian, A., Ng, N. L., Chan, A. W. H., Feingold, G., Flagan, R. C., and Seinfeld, J. H.:
 1375 Particulate organic acids and overall water-soluble aerosol composition measurements from the
 1376 2006 Gulf of Mexico Atmospheric Composition and Climate Study (GoMACCS), *J Geophys*
 1377 *Res-Atmos*, 112, 10.1029/2007jd008537, 2007b.
 1378 Sorooshian, A., Hersey, S., Brechtel, F. J., Corless, A., Flagan, R. C., and Seinfeld, J. H.: Rapid,
 1379 Size-Resolved Aerosol Hygroscopic Growth Measurements: Differential Aerosol Sizing and

1380 Hygroscopicity Spectrometer Probe (DASH-SP), *Aerosol Sci. Tech.*, 42, 445-464,
 1381 10.1080/02786820802178506, 2008.
 1382 Sorooshian, A., Padró, L. T., Nenes, A., Feingold, G., McComiskey, A., Hersey, S. P., Gates, H.,
 1383 Jonsson, H. H., Miller, S. D., Stephens, G. L., Flagan, R. C., and Seinfeld, J. H.: On the link
 1384 between ocean biota emissions, aerosol, and maritime clouds: Airborne, ground, and satellite
 1385 measurements off the coast of California, *Global Biogeochem Cy*, 23, 10.1029/2009gb003464,
 1386 2009.
 1387 Sorooshian, A., Murphy, S. M., Hersey, S., Bahreini, R., Jonsson, H., Flagan, R. C., and
 1388 Seinfeld, J. H.: Constraining the contribution of organic acids and AMSm/z44 to the organic
 1389 aerosol budget: On the importance of meteorology, aerosol hygroscopicity, and region, *Geophys*
 1390 *Res Lett*, 37, 10.1029/2010gl044951, 2010.
 1391 Sorooshian, A., Wonaschutz, A., Jarjour, E. G., Hashimoto, B. I., Schichtel, B. A., and Betterton,
 1392 E. A.: An aerosol climatology for a rapidly growing arid region (southern Arizona): Major
 1393 aerosol species and remotely sensed aerosol properties, *J Geophys Res Atmos*, 116, 16,
 1394 10.1029/2011JD016197, 2011.
 1395 Sorooshian, A., Crosbie, E., Maudlin, L. C., Youn, J. S., Wang, Z., Shingler, T., Ortega, A. M.,
 1396 Hersey, S., and Woods, R. K.: Surface and Airborne Measurements of Organosulfur and
 1397 Methanesulfonate Over the Western United States and Coastal Areas, *J Geophys Res Atmos*,
 1398 120, 8535-8548, 10.1002/2015JD023822, 2015.
 1399 Souza, S. R., Vasconcellos, P., and Carvalho, L. R.: Low molecular weight carboxylic acids in
 1400 an urban atmosphere: Winter measurements in Sao Paulo City, Brazil, *Atmos Environ*, 33, 2563-
 1401 2574, 10.1016/s1352-2310(98)00383-5, 1999.
 1402 Stahl, C., Cruz, M. T., Banaga, P. A., Betito, G., Braun, R. A., Aghdam, M. A., Cambaliza, M.
 1403 O., Lorenzo, G. R., MacDonald, A. B., Pabroa, P. C., Yee, J. R., Simpas, J. B., and Sorooshian,
 1404 A.: An annual time series of weekly size-resolved aerosol properties in the megacity of Metro
 1405 Manila, Philippines, *Sci Data*, 7, 128, 10.1038/s41597-020-0466-y, 2020a.
 1406 Stahl, C., Cruz, M. T., Banaga, P. A., Betito, G., Braun, R. A., Aghdam, M. A., Cambaliza, M.
 1407 O., Lorenzo, G. R., MacDonald, A. B., Pabroa, P. C., Yee, J. R., Simpas, J. B., and Sorooshian,
 1408 A.: An annual time series of weekly size-resolved aerosol properties in the megacity of Metro
 1409 Manila, Philippines, figshare, <https://doi.org/10.6084/m9.figshare.11861859>, 2020b
 1410 Stein, A. F., Draxler, R. R., Rolph, G. D., Stunder, B. J. B., Cohen, M. D., and Ngan, F.:
 1411 NOAA's HYSPLIT Atmospheric Transport and Dispersion Modeling System, *B Am Meteorol*
 1412 *Soc*, 96, 2059-2077, 10.1175/bams-d-14-00110.1, 2015.
 1413 Streets, D. G., Carmichael, G. R., and Arndt, R. L.: Sulfur dioxide emissions and sulfur
 1414 deposition from international shipping in Asian waters, *Atmos Environ*, 31, 1573-1582,
 1415 10.1016/s1352-2310(96)00204-x, 1997.
 1416 Streets, D. G., Guttikunda, S. K., and Carmichael, G. R.: The growing contribution of sulfur
 1417 emissions from ships in Asian waters, 1988–1995, *Atmos Environ*, 34, 4425-4439,
 1418 10.1016/s1352-2310(00)00175-8, 2000.
 1419 Sullivan, R. C., and Prather, K. A.: Investigations of the diurnal cycle and mixing state of oxalic
 1420 acid in individual particles in Asian aerosol outflow, *Environ Sci Technol*, 41, 8062-8069,
 1421 10.1021/es071134g, 2007.
 1422 Sun, Y., Wang, Z., Dong, H., Yang, T., Li, J., Pan, X., Chen, P., and Jayne, J. T.:
 1423 Characterization of summer organic and inorganic aerosols in Beijing, China with an Aerosol
 1424 Chemical Speciation Monitor, *Atmos Environ*, 51, 250-259, 10.1016/j.atmosenv.2012.01.013,
 1425 2012.

1426 Takahashi, K., Nansai, K., Tohno, S., Nishizawa, M., Kurokawa, J.-i., and Ohara, T.:
 1427 Production-based emissions, consumption-based emissions and consumption-based health
 1428 impacts of PM_{2.5} carbonaceous aerosols in Asia, *Atmos Environ*, 97, 406-415,
 1429 10.1016/j.atmosenv.2014.04.028, 2014.
 1430 Tang, M., Guo, L., Bai, Y., Huang, R.-J., Wu, Z., Wang, Z., Zhang, G., Ding, X., Hu, M., and
 1431 Wang, X.: Impacts of methanesulfonate on the cloud condensation nucleation activity of sea salt
 1432 aerosol, *Atmos Environ*, 201, 13-17, 10.1016/j.atmosenv.2018.12.034, 2019.
 1433 Tang, M. J., Whitehead, J., Davidson, N. M., Pope, F. D., Alfarra, M. R., McFiggans, G., and
 1434 Kalberer, M.: Cloud condensation nucleation activities of calcium carbonate and its atmospheric
 1435 ageing products, *Phys Chem Chem Phys*, 17, 32194-32203, 10.1039/c5cp03795f, 2015.
 1436 Thepnuan, D., Chantara, S., Lee, C. T., Lin, N. H., and Tsai, Y. I.: Molecular markers for
 1437 biomass burning associated with the characterization of PM_{2.5} and component sources during
 1438 dry season haze episodes in Upper South East Asia, *Sci Total Environ*, 658, 708-722,
 1439 10.1016/j.scitotenv.2018.12.201, 2019.
 1440 Tsai, Y. I., Kuo, S.-C., Young, L.-H., Hsieh, L.-Y., and Chen, P.-T.: Atmospheric dry plus wet
 1441 deposition and wet-only deposition of dicarboxylic acids and inorganic compounds in a coastal
 1442 suburban environment, *Atmos Environ*, 89, 696-706, 10.1016/j.atmosenv.2014.03.013, 2014.
 1443 van Drooge, B. L., and Grimalt, J. O.: Particle size-resolved source apportionment of primary
 1444 and secondary organic tracer compounds at urban and rural locations in Spain, *Atmos Chem*
 1445 *Phys*, 15, 7735-7752, 10.5194/acp-15-7735-2015, 2015.
 1446 van Pinxteren, M., Fiedler, B., van Pinxteren, D., Iinuma, Y., Körtzinger, A., and Herrmann, H.:
 1447 Chemical characterization of sub-micrometer aerosol particles in the tropical Atlantic Ocean:
 1448 marine and biomass burning influences, *J Atmos Chem*, 72, 105-125, 10.1007/s10874-015-9307-
 1449 3, 2015.
 1450 Vasconcellos, P. C., Souza, D. Z., Sanchez-Ccoyllo, O., Bustillos, J. O., Lee, H., Santos, F. C.,
 1451 Nascimento, K. H., Araujo, M. P., Saarnio, K., Teinila, K., and Hillamo, R.: Determination of
 1452 anthropogenic and biogenic compounds on atmospheric aerosol collected in urban, biomass
 1453 burning and forest areas in Sao Paulo, Brazil, *Sci Total Environ*, 408, 5836-5844,
 1454 10.1016/j.scitotenv.2010.08.012, 2010.
 1455 Virkkula, A., Teinilä, K., Hillamo, R., Kerminen, V. M., Saarikoski, S., Aurela, M., Viidanoja,
 1456 J., Paatero, J., Koponen, I. K., and Kulmala, M.: Chemical composition of boundary layer
 1457 aerosol over the Atlantic Ocean and at an Antarctic site, *Atmos Chem Phys*, 6, 3407-3421,
 1458 10.5194/acp-6-3407-2006, 2006.
 1459 Wang, G., Xie, M., Hu, S., Gao, S., Tachibana, E., and Kawamura, K.: Dicarboxylic acids,
 1460 metals and isotopic compositions of C and N in atmospheric aerosols from inland China:
 1461 implications for dust and coal burning emission and secondary aerosol formation, *Atmos Chem*
 1462 *Phys*, 10, 6087-6096, 10.5194/acp-10-6087-2010, 2010.
 1463 Wang, G., Chen, C., Li, J., Zhou, B., Xie, M., Hu, S., Kawamura, K., and Chen, Y.: Molecular
 1464 composition and size distribution of sugars, sugar-alcohols and carboxylic acids in airborne
 1465 particles during a severe urban haze event caused by wheat straw burning, *Atmos Environ*, 45,
 1466 2473-2479, 10.1016/j.atmosenv.2011.02.045, 2011.
 1467 Wang, G., Kawamura, K., Cheng, C., Li, J., Cao, J., Zhang, R., Zhang, T., Liu, S., and Zhao, Z.:
 1468 Molecular distribution and stable carbon isotopic composition of dicarboxylic acids,
 1469 ketocarboxylic acids, and alpha-dicarbonyls in size-resolved atmospheric particles from Xi'an
 1470 City, China, *Environ Sci Technol*, 46, 4783-4791, 10.1021/es204322c, 2012.

Wang, G., Kawamura, K., Xie, M., Hu, S., Li, J., Zhou, B., Cao, J., and An, Z.: Selected water-soluble organic compounds found in size-resolved aerosols collected from urban, mountain and marine atmospheres over East Asia, *Tellus B*, 63, 371-381, 10.1111/j.1600-0889.2011.00536.x, 2017.

Wang, J., Ge, C., Yang, Z., Hyer, E. J., Reid, J. S., Chew, B.-N., Mahmud, M., Zhang, Y., and Zhang, M.: Mesoscale modeling of smoke transport over the Southeast Asian Maritime Continent: Interplay of sea breeze, trade wind, typhoon, and topography, *Atmos Res*, 122, 486-503, 10.1016/j.atmosres.2012.05.009, 2013.

Wang, Y. Q., Zhang, X. Y., and Draxler, R. R.: TrajStat: GIS-based software that uses various trajectory statistical analysis methods to identify potential sources from long-term air pollution measurement data, *Environ Modell Softw*, 24, 938-939, 10.1016/j.envsoft.2009.01.004, 2009.

Warneck, P.: Multi-Phase Chemistry of C2 and C3 Organic Compounds in the Marine Atmosphere, *J Atmos Chem*, 51, 119-159, 10.1007/s10874-005-5984-7, 2005.

Wasson, S. J., Linak, W. P., Gullett, B. K., King, C. J., Touati, A., Huggins, F. E., Chen, Y., Shah, N., and Huffman, G. P.: Emissions of chromium, copper, arsenic, and PCDDs/Fs from open burning of CCA-treated wood, *Environ Sci Technol*, 39, 8865-8876, 10.1021/es050891g, 2005.

Wonaschuetz, A., Sorooshian, A., Ervens, B., Chuang, P. Y., Feingold, G., Murphy, S. M., de Gouw, J., Warneke, C., and Jonsson, H. H.: Aerosol and gas re-distribution by shallow cumulus clouds: An investigation using airborne measurements, *J Geophys Res-Atmos*, 117, 10.1029/2012jd018089, 2012.

Wonaschütz, A., Hersey, S. P., Sorooshian, A., Craven, J. S., Metcalf, A. R., Flagan, R. C., and Seinfeld, J. H.: Impact of a large wildfire on water-soluble organic aerosol in a major urban area: the 2009 Station Fire in Los Angeles County, *Atmos Chem Phys*, 11, 8257-8270, 10.5194/acp-11-8257-2011, 2011.

Xian, P., Reid, J. S., Atwood, S. A., Johnson, R. S., Hyer, E. J., Westphal, D. L., and Sessions, W.: Smoke aerosol transport patterns over the Maritime Continent, *Atmos Res*, 122, 469-485, 10.1016/j.atmosres.2012.05.006, 2013.

Xu, J., Tian, Y., Cheng, C., Wang, C., Lin, Q., Li, M., Wang, X., and Shi, G.: Characteristics and source apportionment of ambient single particles in Tianjin, China: The close association between oxalic acid and biomass burning, *Atmos Res*, 237, 104843, 10.1016/j.atmosres.2020.104843, 2020.

Xue, H., Khalizov, A. F., Wang, L., Zheng, J., and Zhang, R.: Effects of dicarboxylic acid coating on the optical properties of soot, *Phys Chem Chem Phys*, 11, 7869-7875, 10.1039/b904129j, 2009.

Yamasoe, M. A., Artaxo, P., Miguel, A. H., and Allen, A. G.: Chemical composition of aerosol particles from direct emissions of vegetation fires in the Amazon Basin: water-soluble species and trace elements, *Atmos Environ*, 34, 1641-1653, 10.1016/s1352-2310(99)00329-5, 2000.

Yang, H., Yu, J. Z., Ho, S. S. H., Xu, J., Wu, W.-S., Wan, C. H., Wang, X., Wang, X., and Wang, L.: The chemical composition of inorganic and carbonaceous materials in PM_{2.5} in Nanjing, China, *Atmos Environ*, 39, 3735-3749, 10.1016/j.atmosenv.2005.03.010, 2005.

Yao, X., Fang, M., and Chan, C. K.: Size distributions and formation of dicarboxylic acids in atmospheric particles, *Atmos Environ*, 36, 2099-2107, 10.1016/s1352-2310(02)00230-3, 2002.

Yao, X., Lau, A. P. S., Fang, M., Chan, C. K., and Hu, M.: Size distributions and formation of ionic species in atmospheric particulate pollutants in Beijing, China: 2—dicarboxylic acids, *Atmos Environ*, 37, 3001-3007, 10.1016/s1352-2310(03)00256-5, 2003.

1517 Youn, J. S., Wang, Z., Wonaschutz, A., Arellano, A., Betterton, E. A., and Sorooshian, A.:
 1518 Evidence of aqueous secondary organic aerosol formation from biogenic emissions in the North
 1519 American Sonoran Desert, *Geophys Res Lett*, 40, 3468-3472, 10.1002/grl.50644, 2013.
 1520 Yu, J. Z., Huang, X.-F., Xu, J., and Hu, M.: When Aerosol Sulfate Goes Up, So Does
 1521 Oxalate: Implication for the Formation Mechanisms of Oxalate, *Environ Sci Technol*, 39, 128-
 1522 133, 10.1021/es049559f, 2005.
 1523 Yuan, H., Wang, Y., and Zhuang, G.: MSA in Beijing aerosol, *Chinese Sci Bull*, 49, 1020-1025,
 1524 10.1007/bf03184031, 2004.
 1525 Zeng, G., Kelley, J., Kish, J. D., and Liu, Y.: Temperature-dependent deliquescent and
 1526 efflorescent properties of methanesulfonate sodium studied by ATR-FTIR spectroscopy, *J Phys*
 1527 *Chem A*, 118, 583-591, 10.1021/jp405896y, 2014.
 1528 Ziemba, L. D., Griffin, R. J., Whitlow, S., and Talbot, R. W.: Characterization of water-soluble
 1529 organic aerosol in coastal New England: Implications of variations in size distribution, *Atmos*
 1530 *Environ*, 45, 7319-7329, 10.1016/j.atmosenv.2011.08.022, 2011.
 1531

1532 **Table 1:** Seasonal concentrations (ng m⁻³) of organic acids and MSA for all (0.056 – 18 µm), submicrometer (0.056 – 1 µm), and
 1533 supermicrometer (1 – 18 µm) sizes measured in Metro Manila from July 2018 to October 2019. n = number of sets.

Size/Species		All (n = 54)		SWM18 (n = 11)		Transitional (n = 3)		NEM (n = 27)		SWM19 (n = 13)	
		Range	Mean (SD)	Range	Mean (SD)	Range	Mean (SD)	Range	Mean (SD)	Range	Mean (SD)
All: 0.056 - 18 μm	Phthalate	0 - 67.02	9 (14)	1.97 - 67.02	17 (25)	17.36 - 45.30	27 (16)	0 - 14.72	4.8 (4.4)	0-25.03	5.7 (7.4)
	Adipate	0 - 43.83	7.6 (9.4)	0 - 20.18	9.1 (8.8)	0.24 - 19.56	8 (10)	0 - 13.00	4.2 (3.8)	0 - 43.83	13 (15)
	Succinate	0 - 116.28	10 (22)	0 - 116.28	22 (43)	0 - 14.31	7.6 (7.2)	0 - 62.83	7 (14)	0 - 20.14	4.7 (7.4)
	Maleate	0 - 119.19	10 (20)	2.56 - 58.39	19 (15)	0.19 - 8.45	3.8 (4.2)	0 - 14.42	1.7 (3.7)	2.30 - 119.19	19 (34)
	Oxalate	37.67 - 472.82	149 (94)	49.83 - 472.82	178 (139)	179.42 - 365.10	252 (99)	51.62 - 421.82	144 (76)	37.67 - 214.62	110 (62)
	MSA	0.10 - 23.33	5.4 (5.2)	2.77 - 23.33	10.0 (6.6)	0.16 - 16.14	5.6 (9.2)	0.10 - 7.45	3.1 (2.0)	0.84 - 17.52	6.3 (5.4)
0.056 - 1 μm	Phthalate	0 - 64.53	6 (13)	0.51 - 64.53	15 (24)	9.14 - 39.62	20 (17)	0 - 9.38	1.6 (2.5)	0 - 8.51	2.7 (3.1)
	Adipate	0 - 31.57	4.3 (5.8)	0 - 15.94	6.1 (6.3)	0 - 10.99	5.5 (5.5)	0 - 10.64	2.5 (3.2)	0 - 31.57	6.1 (8.8)
	Succinate	0 - 108.47	7 (20)	0 - 108.47	19 (39)	0 - 13.54	7.3 (6.8)	0 - 52.42	4 (10)	0 - 15.68	4.3 (6.6)
	Maleate	0 - 108.65	9 (18)	2.56 - 57.73	18 (15)	0.19 - 8.45	3.8 (4.2)	0 - 14.42	1.6 (3.6)	2.30 - 108.65	18 (31)
	Oxalate	16.21 - 318.49	93 (62)	29.96 - 256.72	108 (75)	96.84 - 250.78	166 (78)	26.11 - 318.49	91 (58)	16.21 - 151.79	70 (40)
	MSA	0 - 21.32	5.0 (4.9)	2.41 - 21.32	9.3 (6.2)	0.08 - 15.58	5.3 (8.9)	0 - 7.45	2.9 (2.1)	0.84 - 16.22	5.7 (5.1)
1-18 μm	Phthalate	0 - 16.52	3.1 (3.3)	0 - 4.07	2.0 (1.7)	5.43 - 9.03	6.7 (2.0)	0 - 9.42	3.2 (2.6)	0 - 16.52	3.0 (5.0)
	Adipate	0 - 26.00	3.3 (4.9)	0 - 7.87	3.0 (3.2)	0 - 8.56	2.9 (4.9)	0 - 8.07	1.7 (2.2)	0 - 26.00	7.1 (8.0)
	Succinate	0 - 21.18	2.2 (4.5)	0 - 16.02	3.1 (4.9)	0 - 0.77	0.3 (0.4)	0 - 21.18	2.9 (5.4)	0 - 5.33	0.4 (1.5)
	Maleate	0 - 10.54	0.4 (1.5)	0 - 2.30	0.3 (0.7)	0	0	0 - 0.45	0.02 (0.09)	0 - 10.54	1.2 (2.9)
	Oxalate	6.27 - 216.10	55 (39)	19.87 - 216.10	70 (67)	62.90 - 114.32	87 (26)	18.51 - 104.88	53 (23)	6.27 - 103.58	41 (29)
	MSA	0 - 2.00	0.4 (0.5)	0 - 2.00	0.8 (0.6)	0 - 0.56	0.2 (0.3)	0 - 1.58	0.2 (0.4)	0 - 1.93	0.6 (0.6)

1534

1535 **Table 2:** Contributions of the five positive matrix factorization (PMF) source factors to each
 1536 individual organic acid and MSA.

	Combustion	Biomass Burning	Crustal	Sea Salt	Waste Processing
Phthalate	27.4 %	49.5 %	13.3 %	9.9 %	0 %
Adipate	32.9 %	26.4 %	35.9 %	4.7 %	0 %
Succinate	0 %	90.3 %	9.7 %	0 %	0 %
Maleate	69.7 %	0 %	0.2 %	0 %	30.1 %
Oxalate	32.9 %	25.4 %	31.2 %	0 %	10.5 %
MSA	57.4 %	41.2 %	0.1 %	0 %	1.4 %

1537

1538

1539 **Table 3:** Pearson's correlation matrices (r values) of water-soluble species for submicrometer
1540 (0.056 – 1.0 µm) and supermicrometer (1.0 – 18 µm) sizes. Blank boxes indicate p-values
1541 exceeding 0.05 and thus deemed to be statistically insignificant. Ad – adipate, Su – succinate,
1542 Ma – maleate, Ox – oxalate, Ph – phthalate. A similar correlation matrix for the full size range
1543 (0.056 – 18 µm) is in Table S6.

< 1 μm																				
Al	1.00																			
Ti		1.00																		
K	0.91		1.00																	
Rb	0.44		0.48	1.00																
V		0.28		0.36	1.00															
Ni		0.47		0.40	0.89	1.00														
As							1.00													
Cd					0.64	0.68		1.00												
Pb	0.41		0.32	0.27	0.28	0.40		0.42	1.00											
Na										1.00										
Cl	0.90		0.99	0.39					0.30		1.00									
NO3	0.76		0.82	0.28							0.84	1.00								
SO4				0.42	0.48	0.40							1.00							
MSA				0.39									0.60	1.00						
Ad															1.00					
Su		0.31		0.67									0.45	0.67	0.33	1.00				
Ma															0.32		1.00			
Ox		0.35		0.70	0.47	0.53							0.72	0.47		0.69		1.00		
Ph		0.37		0.53									0.39	0.67	0.45	0.82		0.57	1.00	
	Al	Ti	K	Rb	V	Ni	As	Cd	Pb	Na	Cl	NO3	SO4	MSA	Ad	Su	Ma	Ox	Ph	

> 1 μm																				
Al	1.00																			
Ti	0.56	1.00																		
K			1.00																	
Rb	0.62		0.48	1.00																
V		0.40		0.31	1.00															
Ni		0.30				1.00														
As		0.37			0.33		1.00													
Cd					0.66	0.41	0.34	1.00												
Pb	0.43	0.45		0.36	0.51	0.45		0.65	1.00											
Na	0.49	0.42								1.00										
Cl	0.45	0.48								0.90	1.00									
NO3	0.38			0.32	0.41					0.64	0.30	1.00								
SO4	0.39		0.81	0.64						0.37	0.29	0.36	1.00							
MSA										0.32				1.00						
Ad															1.00					
Su	0.39			0.28						0.30						1.00				
Ma															0.57		1.00			
Ox	0.59	0.29		0.48						0.45		0.59	0.35			0.45		1.00		
Ph		0.29									0.34				0.30				1.00	
	Al	Ti	K	Rb	V	Ni	As	Cd	Pb	Na	Cl	NO3	SO4	MSA	Ad	Su	Ma	Ox	Ph	

1544

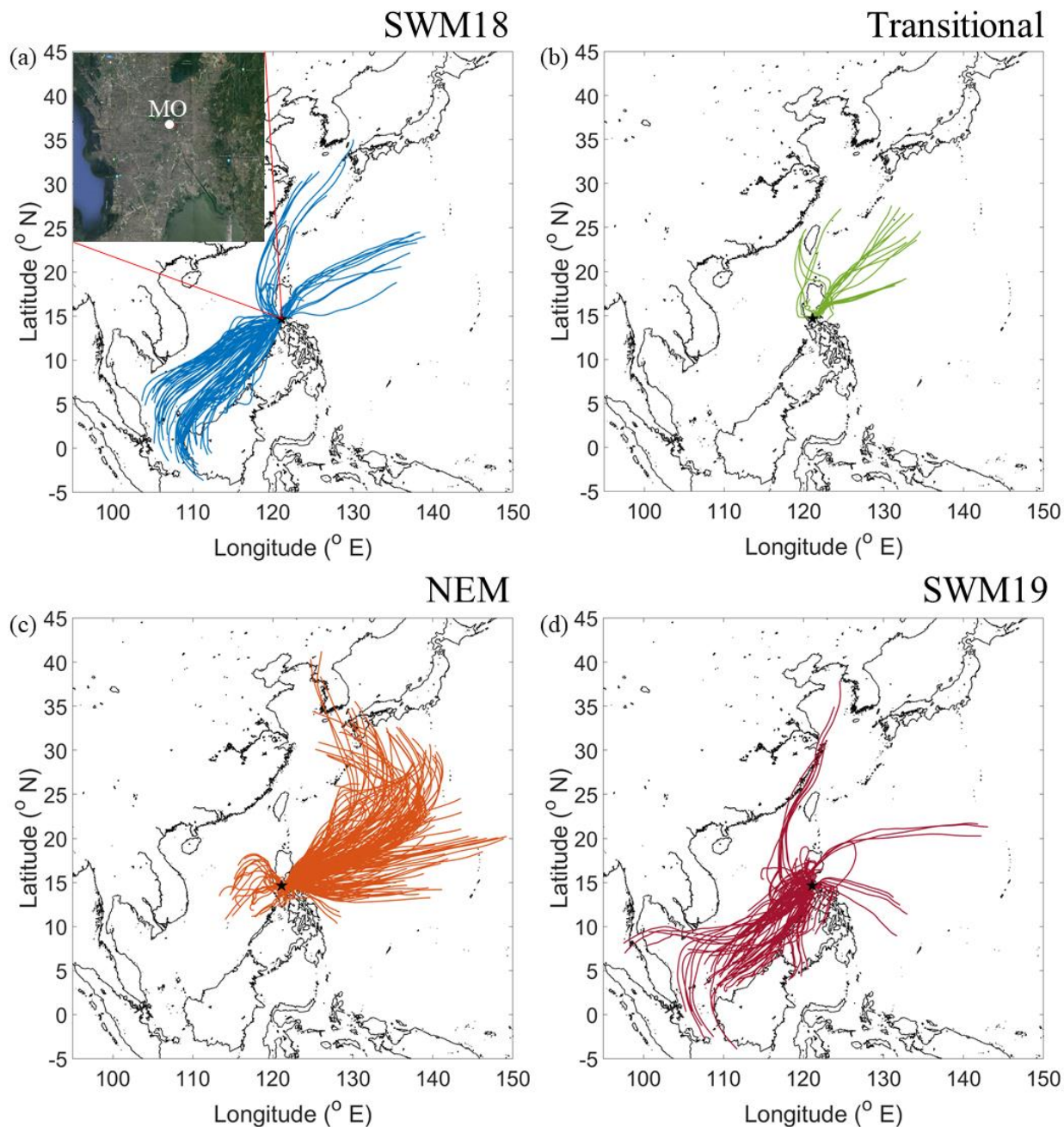


Figure 1: HYSPLIT back-trajectories for four seasons: (a) 2018 southwest monsoon (SWM18), (b) ~~transitional~~ Transitional period (~~Trans~~), (c) northeast monsoon (NEM), and (d) 2019 southwest monsoon (SWM19). Results shown are based on 72-hour back-trajectories collected every 6 h during sampling periods. The top left corner of panel (a) zooms in on Metro Manila with Manila Observatory (MO) marked. The black star in each panel represents the sampling site. Map data: © Google Earth, Maxar Technologies, CNES/Airbus, Data SIO, NOAA, U.S. Navy, NGA, GEBCO.

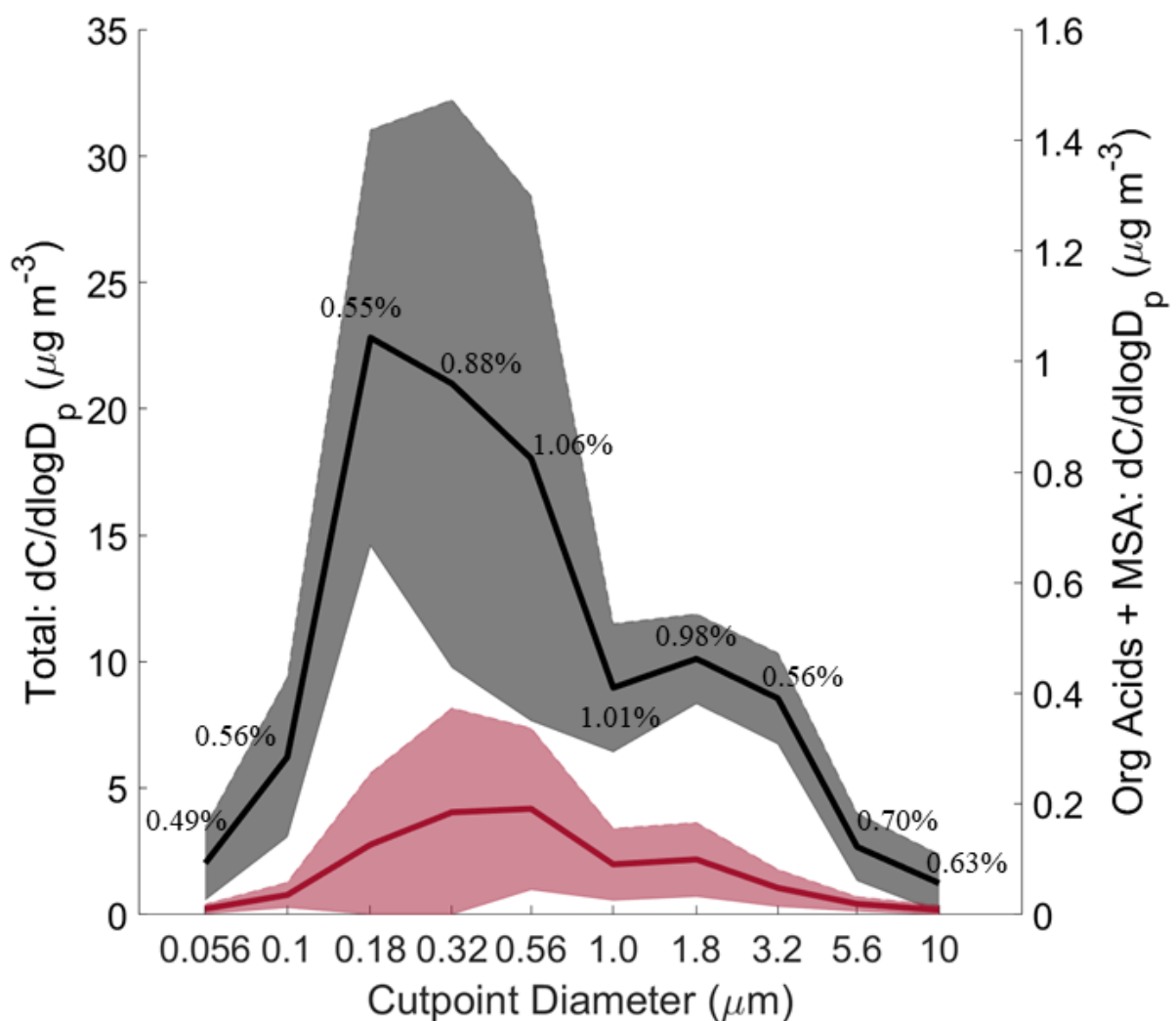


Figure 2: Size-resolved comparison of total mass versus the sum of measured organic acids and MSA. The black curve represents total mass and the red curve represents the summed organic acids and MSA. Solid lines are the averages and shaded areas are one standard deviation. These plots were made based on data from the 11 MOUDI chemical sets with accompanying gravimetric measurements. The average percent contribution of the organic acids and MSA to total mass is provided for each size bin. Refer to Fig. S1 for the seasonally-resolved version of this figure.

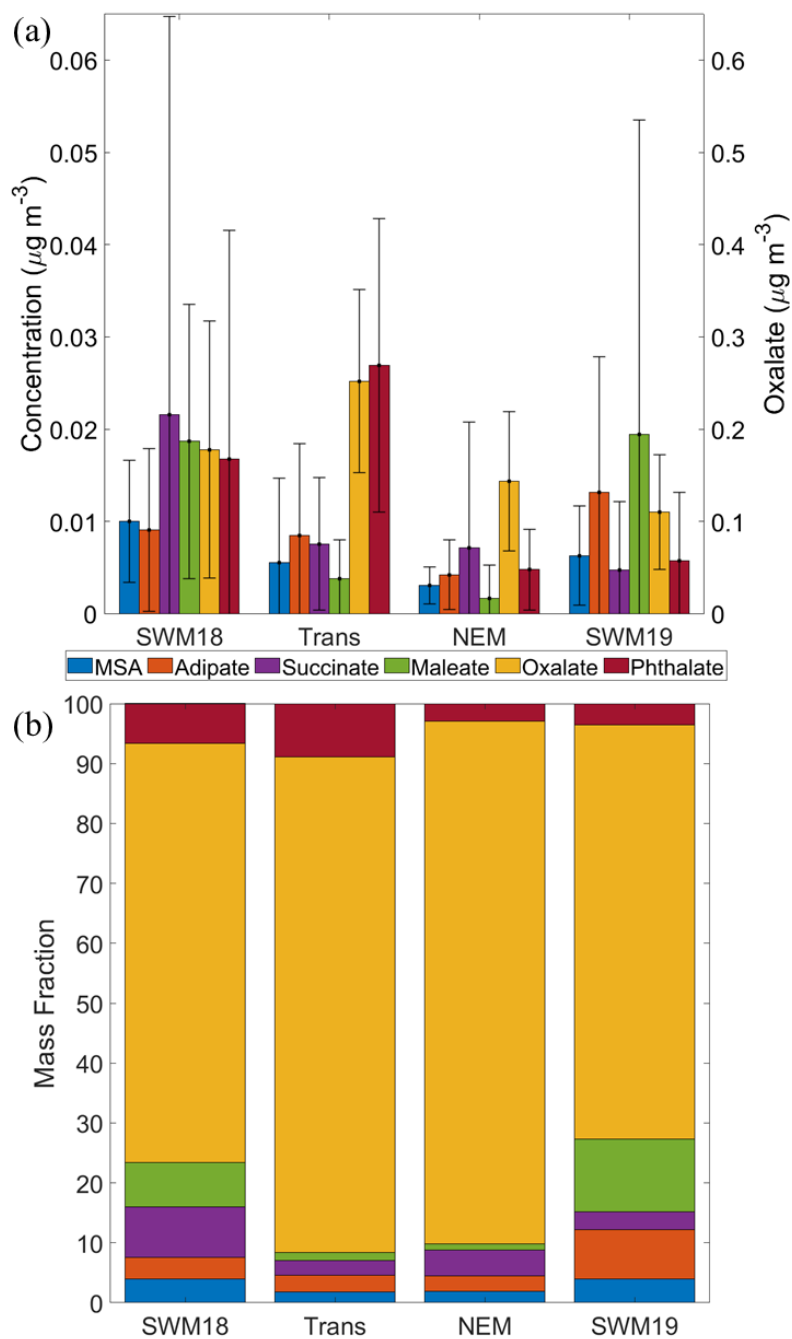


Figure 3: (a) Average concentrations (0.056 – 18 μm) for (left y-axis) MSA, adipate, succinate, maleate, and phthalate, in addition to (right y-axis) oxalate. Black bars represent one standard deviation. (b) Percentage relative mass abundance of organic acids and MSA separated based on season.

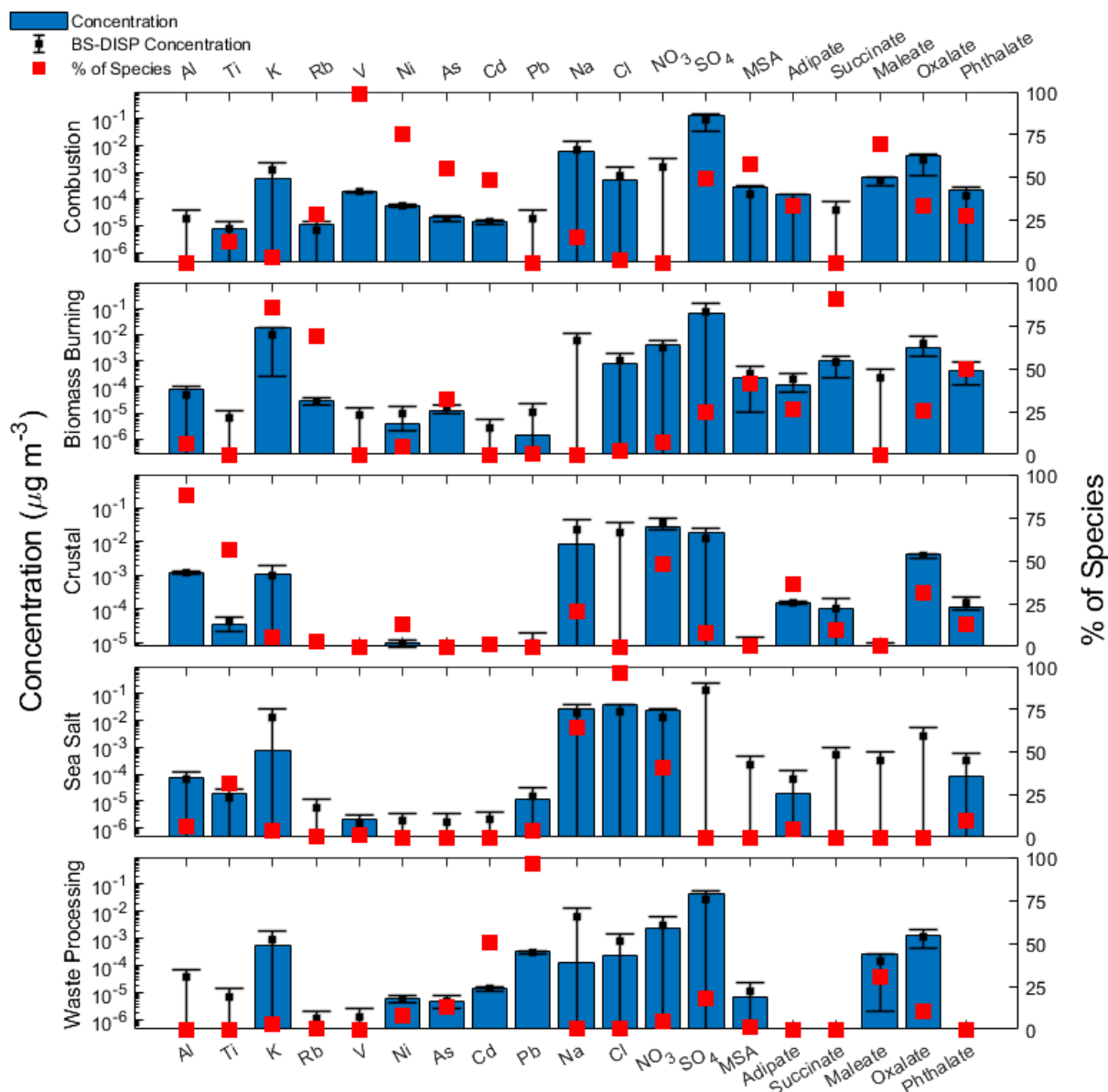


Figure 4: Source factor profiles from positive matrix factorization (PMF) analysis. Blue bars represent the mass concentration contributed to the respective factor, red filled squares represent the percentage of total species associated with that source factor, and black squares with error bars represent the average, 5th, and 95th percentiles of bootstrapping with displacement (BS-DISP) values.

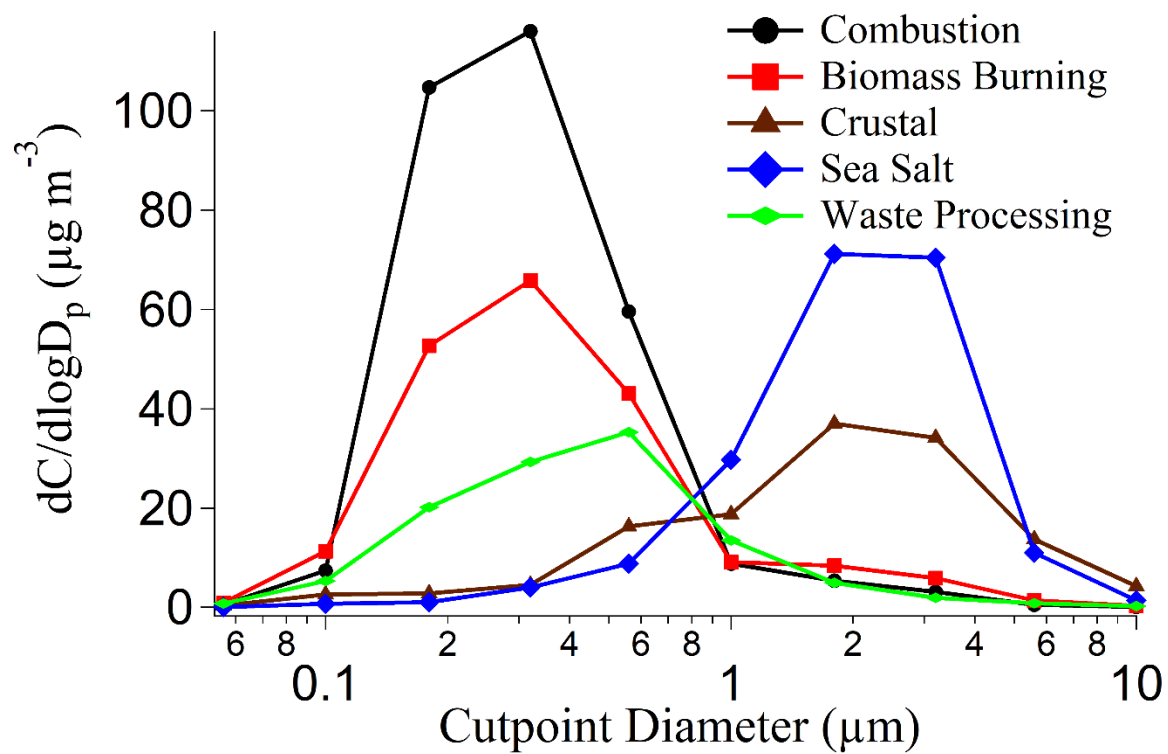


Figure 5: Reconstructed mass size distributions of positive matrix factorization (PMF) factors.

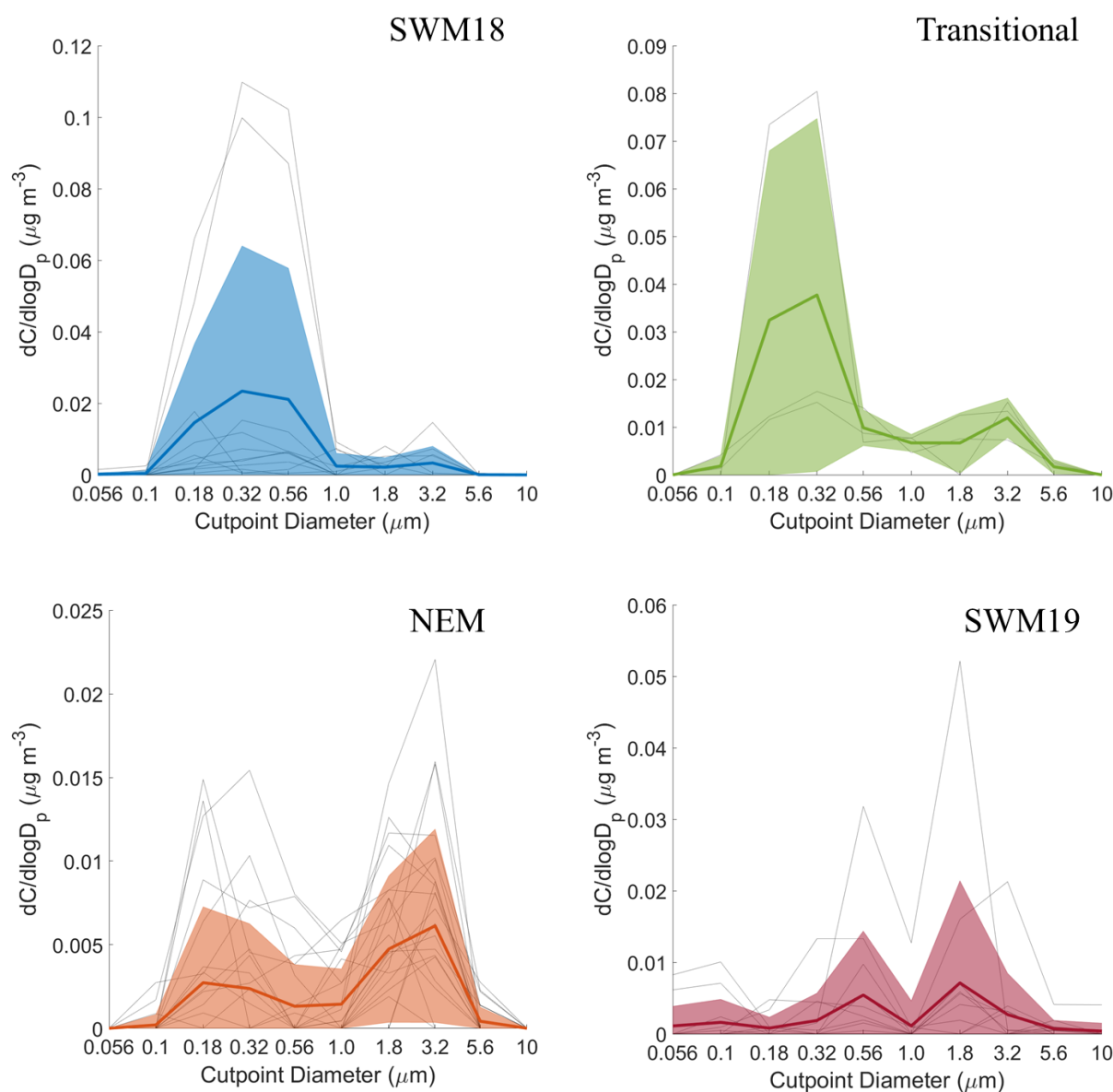


Figure 6: Seasonal size distributions of phthalate. Gray lines represent individual sets, dark colored lines are the average of all seasonal distributions, and transparent colored areas represent one standard deviation. Note that the range of concentrations presented on the y-axis for each season varies.

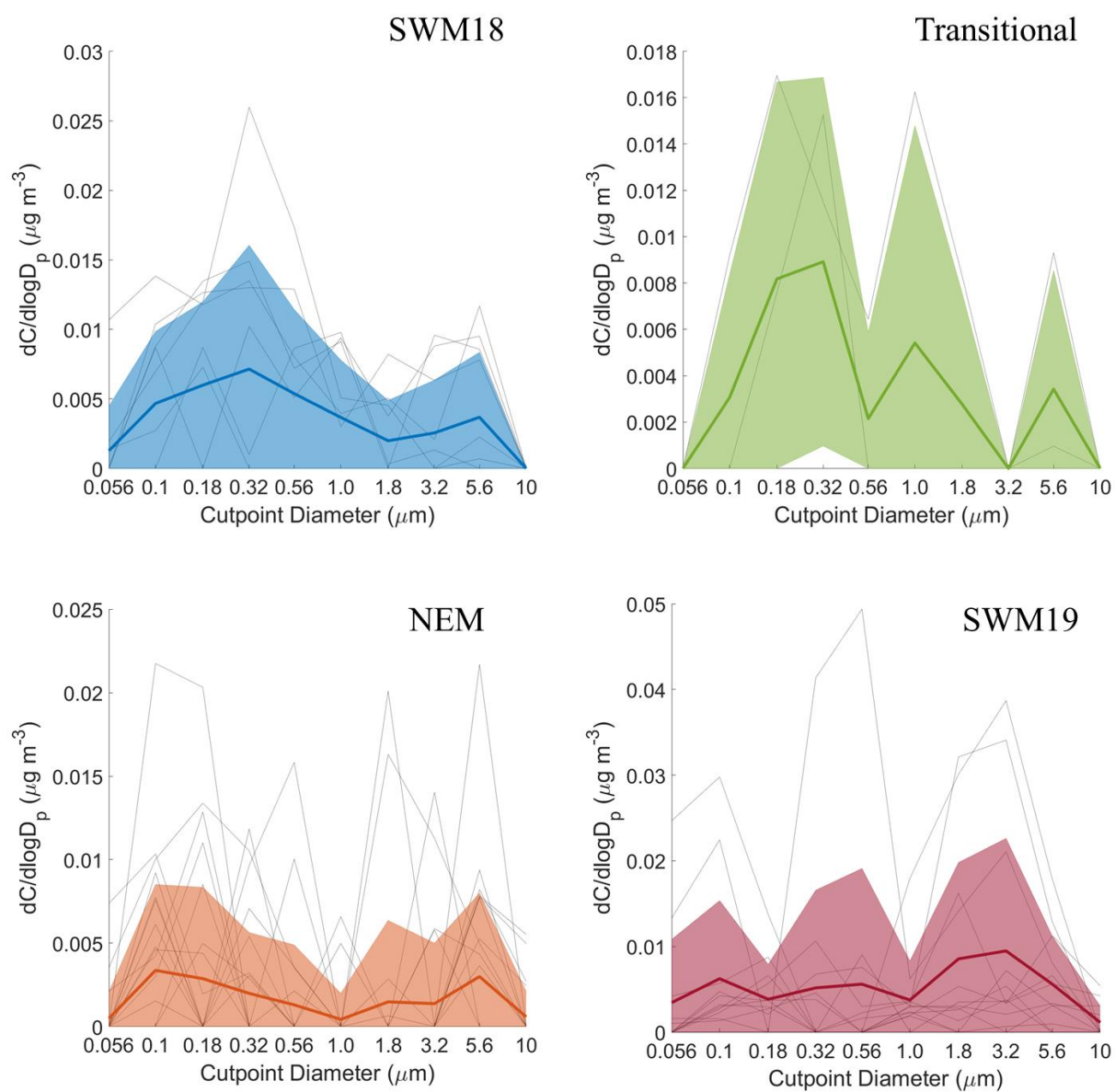


Figure 7: Same as Fig. 6 but for adipate.

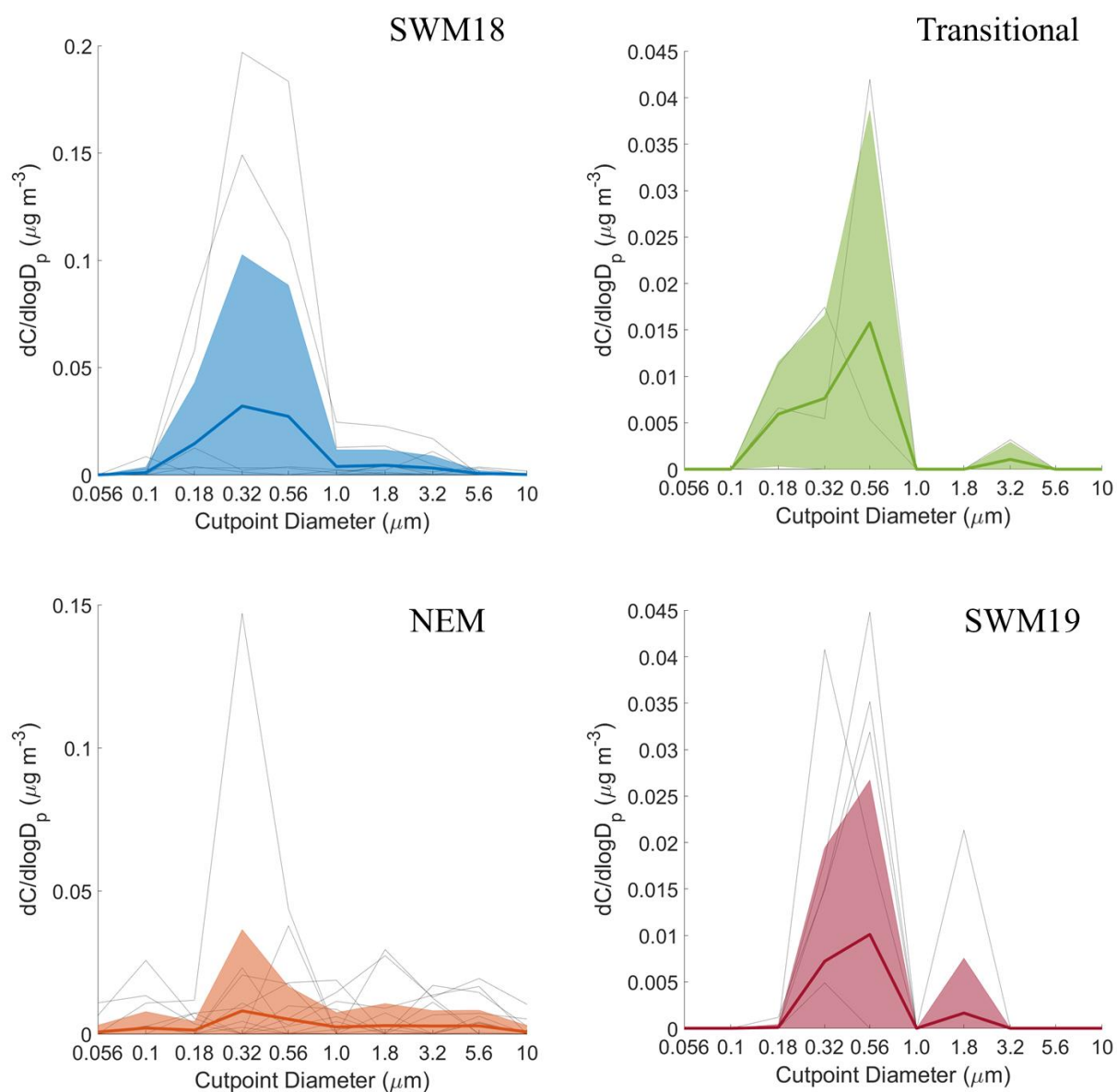


Figure 8: Same as Fig. 6 but for succinate.

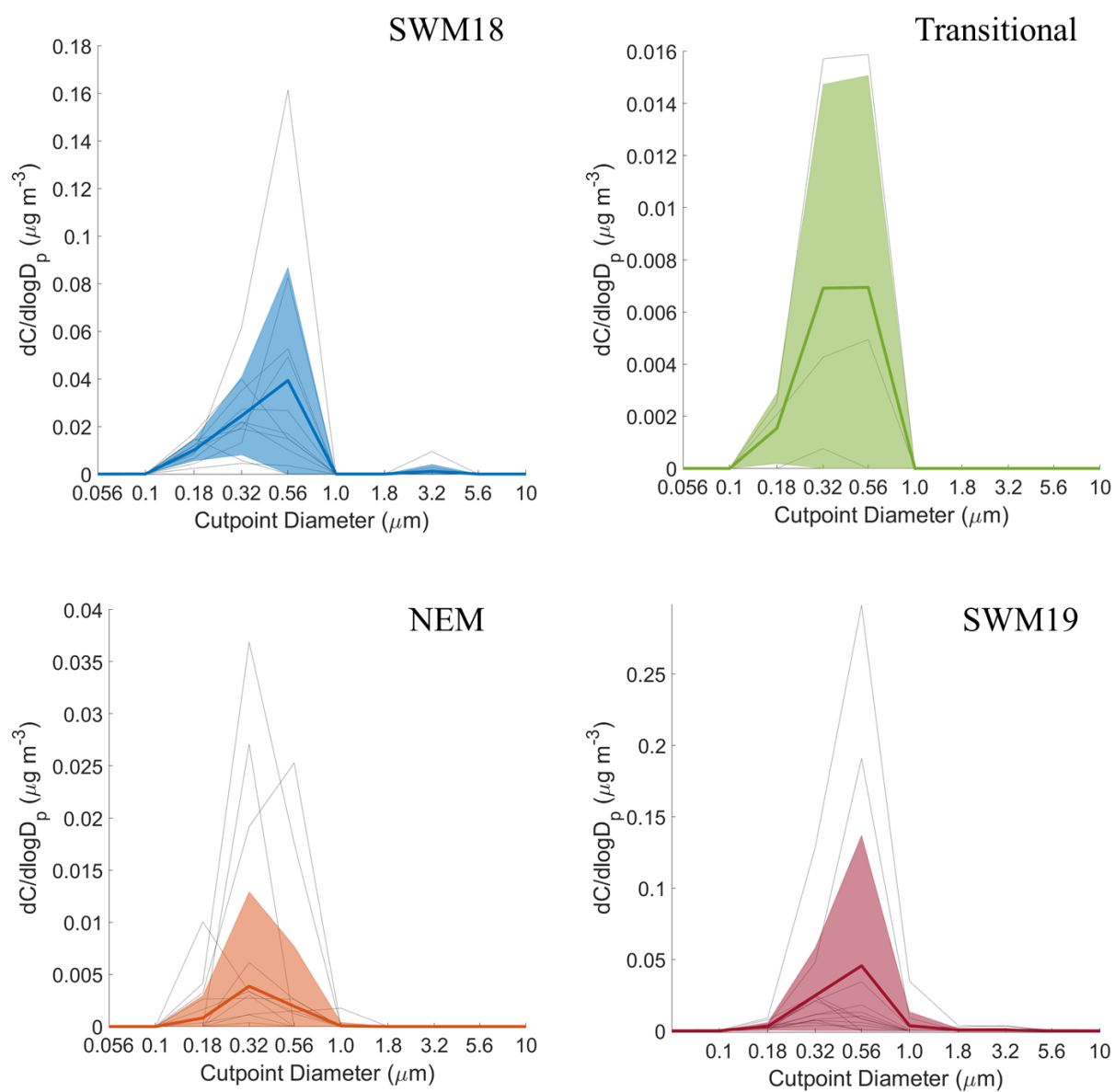


Figure 9: Same as Fig. 6 but for maleate.

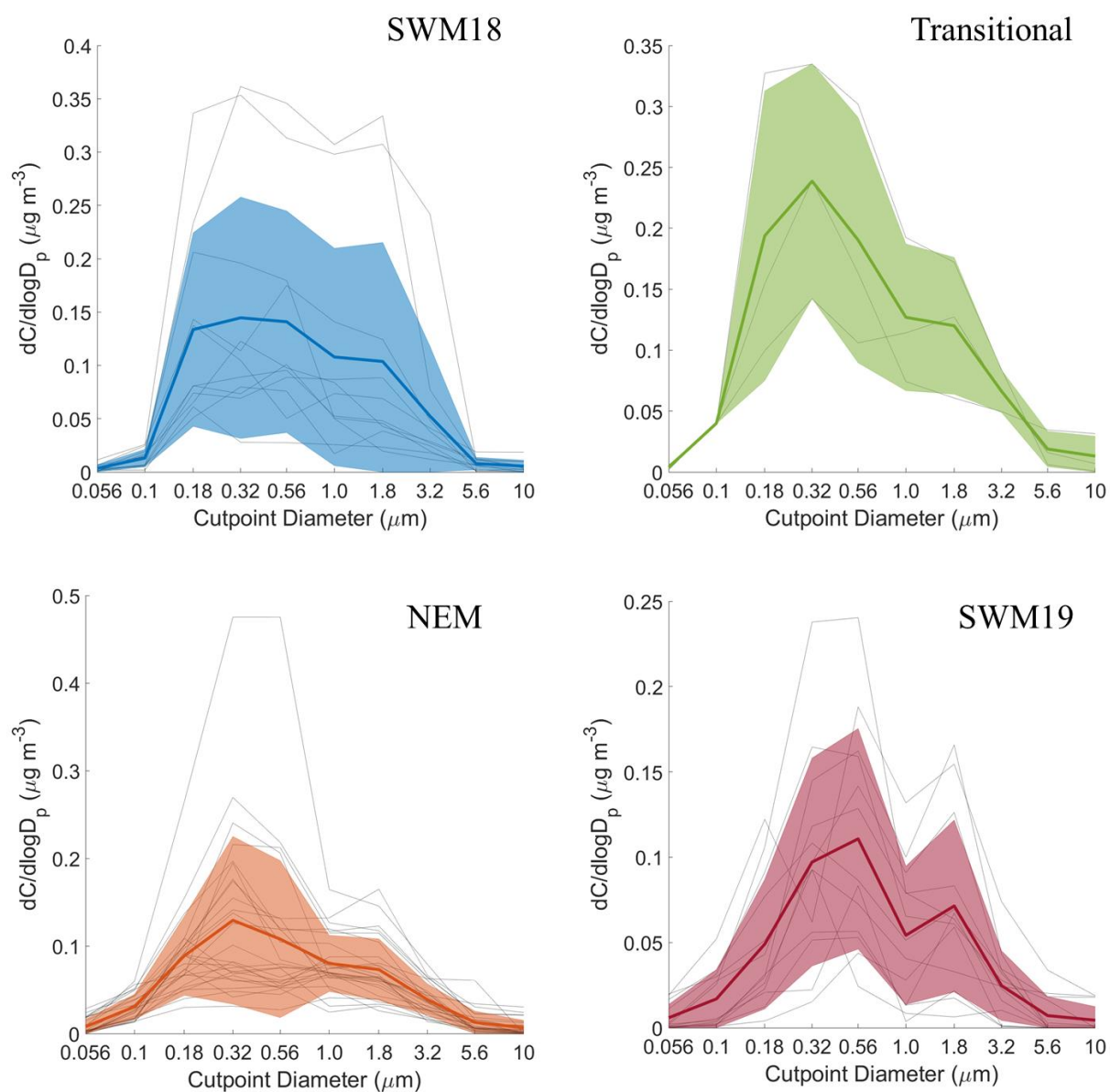


Figure 10: Same as Fig. 6 but for oxalate.

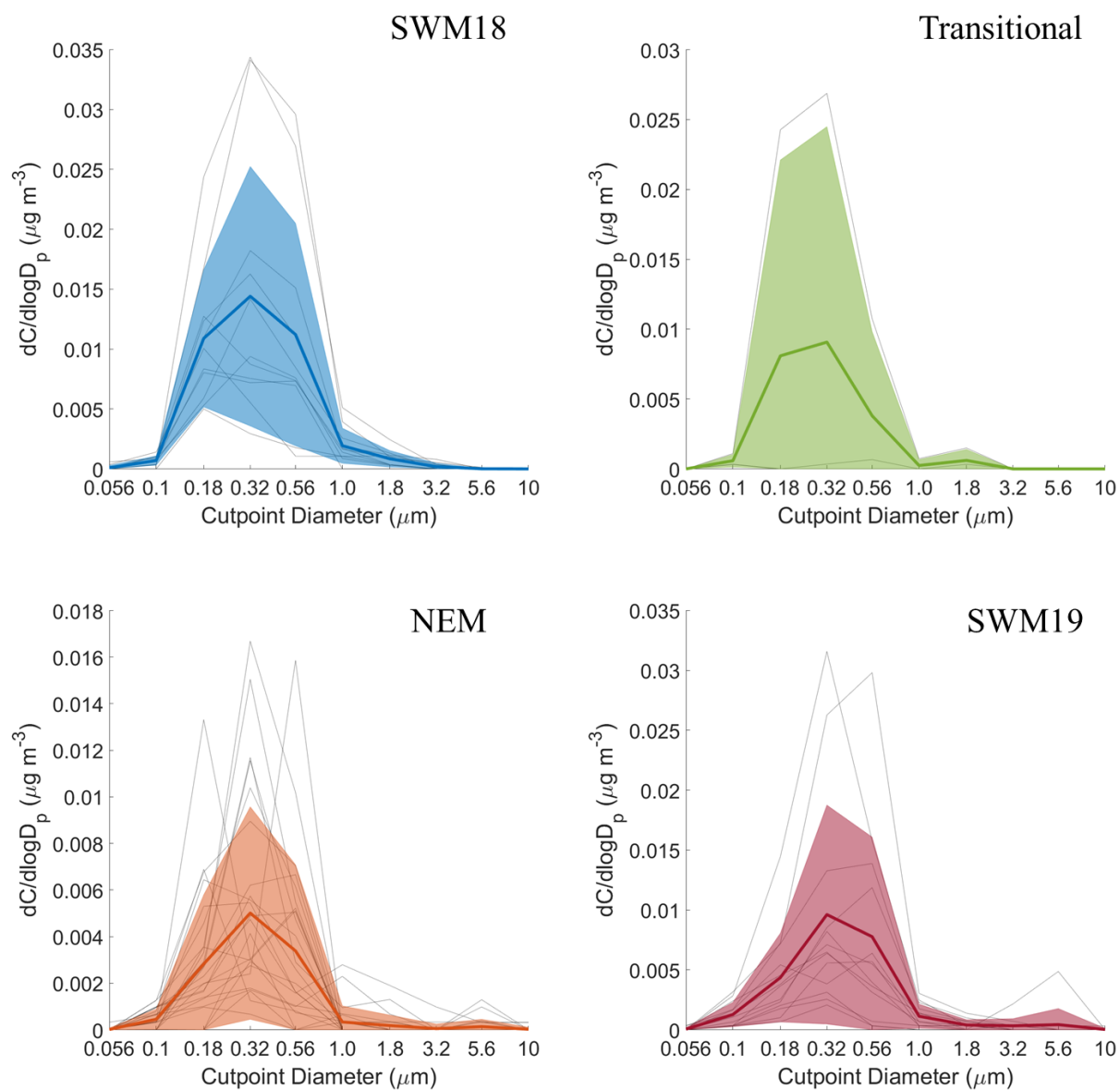


Figure 11: Same as Fig. 6 but for MSA.

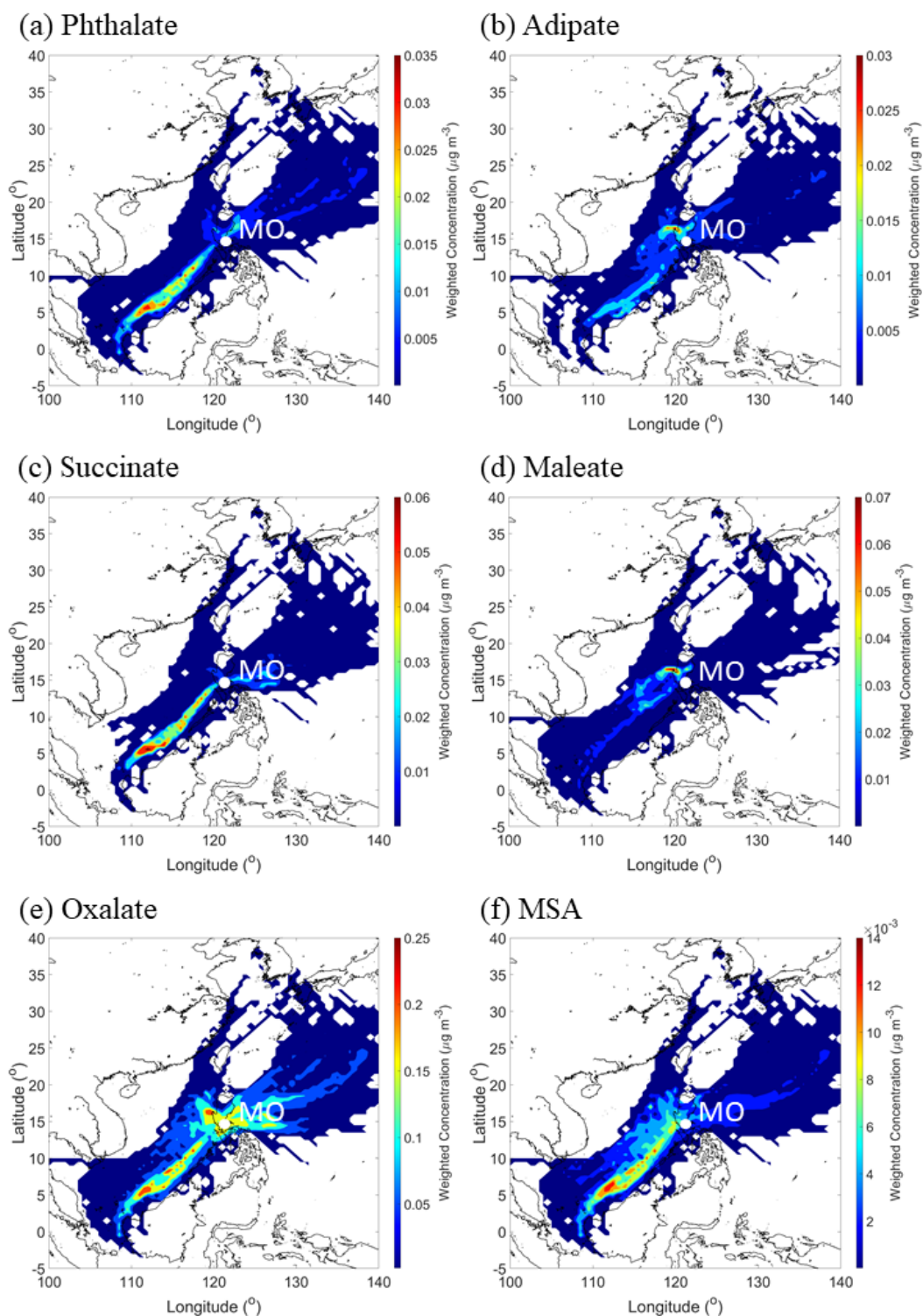


Figure 12: WCWT maps of (a-e) individual organic acids and (f) MSA over the entire sampling period. These results are based on all MOUDI sizes (0.056 – 18 μm). Maps showing the seasonal results for each organic acid and MSA are shown in the Supplement (Figs. S3 – S8).